



Max Planck Institute
for Chemical Ecology



FRIEDRICH-SCHILLER-
UNIVERSITÄT
JENA

Generation and Application of an HPLC-Ion Mobility-MS Library for Plant and Insect Saccharide Analysis

Master's Thesis

Johanna Rettner

born on 08th February 1994 in Berlin

Erstgutachter: Dr. Daniel Giddings Vassão

Zweitgutachter: Prof. Dr. Christoph Steinbeck

Jena, 22nd October 2021

Acknowledgement

I wish to thank Dr. Daniel Giddings Vassão for the opportunity to work on this project, for supervising, reviewing and your confidence.

I want to thank Prof. Dr. Christoph Steinbeck for reviewing this thesis.

I want to thank Prof. Dr. Gershenzon for the opportunity to do my Master's Thesis in the Biochemistry department and the Max-Planck-Society for funding the time-TOF instrument.

For the scientific support and especially help with analytical questions and aphid rearing I want to thank Dr. Michael Reichelt, Dr. Michael Easson and Duc Tam Mai, respectively. I wish to thank Dr. Torsten Knauer, Dr. Rieta Gols and Bettina Raguschke for providing aphids and biological samples.

My grateful thanks are also extended to the Detox group for feeling less lost and to Piera Wiesinger being a sympathetic colleague and friend.

I want to thank my family and friends for encouraging words and providing child care in these challenging times.

And last, I want to thank everyone, who probably will not read this, but kept the world spinning and fights for a better one.

Zusammenfassung

Eine der bedeutsamsten Stoffklassen sind Kohlenhydrate. Als Photosyntheseprodukt und Stützsubstanz spielen sie im Pflanzenreich eine wichtige Rolle. In allen Lebewesen sind Kohlenhydrate in biologischen Signal- und Erkennungsprozessen involviert und sind häufig Grundnahrungsquelle und Energiespeicher. Sie sind aus Einfachzuckern zusammengesetzt und ergeben eine Vielzahl von Regio- und Stereoisomeren. Die Trennung dieser strukturell ähnlichen, gleichzeitig jedoch sehr diversen Isomere ist mit konventionellen analytischen Methoden nur bedingt möglich.

Vor 20 Jahren wurde die Ionen-Mobilitäts-Spektrometrie in Kombination mit herkömmlichen Verfahren erstmals angewendet, um Isomere aufzutrennen und Naturstoffe aufzuklären. Bei der *trapped ion mobility spectrometry* werden Ionen mit einem Stickstoffstrom durch ein entgegenwirkendes, graduell ansteigendes elektrisches Feld bewegt. Entsprechend der Ionen Mobilität ergibt sich eine Position, an der sich die auf das Ionen wirkenden Kräfte ausgleichen, dort werden Moleküle gleicher Mobilität gesammelt und so voneinander getrennt.

In der vorliegenden Arbeit wurden Methoden der Hochleistungsflüssigkeitschromatographie-Ionen-Mobilitäts-Massenspektrometrie (UHPLC-IM-MS) entwickelt und 47 Zuckerstandards gemessen. Die in dieser Arbeit erstellte Bibliothek beinhaltet Retentionszeiten zweier Säulen, das Masse-zu-Ladung-Verhältnis, sowie Mobilitäten einer Vielzahl von Addukt-Ionen in positiver und negativer Ionisierung. Durch Vergleich von Stereoisomeren, Anomeren und Konfigurationsisomeren konnten Zusammenhänge von Molekülstruktur und ihrer Mobilität erkannt werden. Die Tauglichkeit der erstellten Bibliothek wurde durch Analysen biologischer Proben bestätigt.

Blattläuse und andere Insekten ernähren sich von Pflanzensaft, einer hoch osmotischen Lösung mit ungünstigem Stickstoff-Kohlenstoff-Verhältnis. Der osmotische Haushalt wird durch Umformungen von Zuckern reguliert, die mit dem Honigtau ausgeschieden werden. Um diese Vorgänge zu untersuchen, wurde zum einen Pflanzensaft von *Zea mays* und der Honigtau von sich davon ernährenden Blattläusen *Rhopalosiphum padi* und *Sitobion avenae* verglichen. Durch die Ionen Mobilität konnten zwölf verschiedene Zucker aufgetrennt und identifiziert werden. Zum anderen wurden *Brevicoryne brassicae* Blattläuse in einem künstlichen Versuchsaufbau mit verschiedenen Zuckerkonzentrationen gefüttert. Saccharose war der einzig zugeetzte Zucker der Nahrung. Im Gegensatz wurden im ausgeschiedenen Honigtau 15 verschiedene Zucker nachgewiesen, die auf diverse regulatorische Umwandlungsprozesse zurückzuführen sind.

Abstract

Carbohydrates are a very abundant compound class in nature and significant in metabolic processes. They are major product of photosynthesis, and serve as structural components, crucial nutrition and energy storage.

Countless possible combinations of structures exist for complex carbohydrates, since these substances are composed of various monosaccharide building blocks connected together to form diverse regio- and stereoisomers. Separation of the vast number of isomeric structures poses a great challenge for established analytical tools. In the last decade, ion mobility was integrated into modern instrumentations allowing for the observation of structural and spatial information.

Among the different ion mobility strategies, trapped ion mobility spectrometry (TIMS) is a powerful technique, where ions are propelled through a gradually electric field by a nitrogen flow. According to their mobilities, the ions are trapped in a position where they are in equilibrium with a corresponding electric field strength, and thus accumulate and can be selectively released for MS analysis.

In this study, UHPLC-IM-MS methods were created to generate a three dimensional library of analytical data corresponding to 47 sugar standards, including retention times in two different columns, mass-to-charge ratios and ion mobility values of various ion species in positive and negative ionisation modes.

Comparison of different groups of isomers revealed relationships between mobility behaviours and structural composition, configuration or connection of saccharides. To demonstrate the utility of the generated saccharide library, it was applied on the analysis of biological samples of phloem sap and aphid honeydew. Aphids, as other phloem feeding insects, struggle with the high dietary osmotic pressure caused by an unfavourable nitrogen-to-carbon ratio and high carbohydrate concentrations. The metabolism of saccharides in the aphids *Rhopalosiphum padi* and *Sitobion avenae* was observed by analysis of their diet, *Zea mays* phloem sap, and their excreted honeydew, in which twelve different saccharides have been identified.

Additionally, in an artificial feeding experiment, the dietary sucrose level of *Brevicoryne brassicae* was controlled and the impact on honeydew production and composition observed. Sucrose was fed as the exclusive carbon source, and 15 different (oligo)saccharides were identified in honeydew arising from multiple types of sucrose transformation.

Contents

List of Figures	vi
List of Tables	vii
List of Abbreviations	viii
1. Introduction	1
1.1. Saccharides	1
1.1.1. Monosaccharides	1
1.1.2. Disaccharides	3
1.1.3. Oligo-, Polysaccharides and other Glycans	3
1.1.4. Plant and Insect Saccharides	4
1.2. Analytical Challenge	8
1.3. Ion Mobility Mass Spectrometry	9
1.3.1. Route through timsTOF	11
1.3.2. Transforming Mobility to Collision Cross Section	12
1.4. State of Knowledge on Glycan Analysis via IM-MS	14
1.5. Aim of this Work	16
2. Materials and Methods	19
2.1. Materials	19
2.1.1. Chemicals	19
2.1.2. Preparation of Standards	19
2.1.3. Aphid and Plant Species	19
2.1.4. Artificial Diet	20
2.1.5. Software	20
2.2. Methods	21
2.2.1. UHPLC Methods	21
2.2.2. Mass Spectrometry Analyses	22
2.2.3. timsTOF Calibration	23
2.2.4. Mobility Data Processing and CCS Determination	24
2.2.5. Quantitative Calibration and Analysis	24
2.3. Preparation of Biological Samples	25
2.3.1. Phloem Sap	25
2.3.2. Honeydew	26

3. Results	29
3.1. Method Development	29
3.2. Generation of CCS Library	30
3.3. CCS Patterns	35
3.4. Application of CCS Library to Natural Samples	40
3.4.1. Maize Phloem Sap and Honeydew	40
3.4.2. Sucrose Feeding Experiment	42
4. Discussion	49
4.1. Saccharide Identification in Plant and Insect Samples	49
4.1.1. Influence of Dietary Sucrose Content	51
4.1.2. Sucrose Modifications	53
4.2. Mobility and CCS Library	55
4.2.1. CCS Pattern	58
4.2.2. Comparison of CCS Values with Published Data	58
4.3. Quantification Method	60
4.4. Further Improvements and Application	61
5. Conclusion and Outlook	63
Literature	xi
A. Appendix	xxv
A.1. Saccharide Standards	xxv
A.1.1. InChiKey	xxv
A.1.2. Chemical Structures	xxvi
A.2. Material and Method Details	xxxix
A.2.1. Calibration	xxxv
A.2.2. R Code	xliv
A.3. Results	xlvi
A.3.1. Ion Mobility and CCS Library	xlvi
A.3.2. Application on Biological Samples	liv
Selbstständigkeitserklärung	lix

List of Figures

1.	Straight chain and ring configurations of monosaccharides	2
2.	Sugar regioisomers	4
3.	Simplified equation of photosynthesis	5
4.	TIMS tunnel	11
5.	Route through timsTOF	12
6.	Setup of the feeding assay	27
7.	Overlaid chromatograms of sugar standards	31
8.	Disaccharide isomers	32
9.	Chromatograms and mobilograms of selected isobaric disaccharides	33
10.	Chromatographic separation via two different columns	34
11.	Disaccharide discrimination via ion mobility	35
12.	Schematic ion mobilogram	36
13.	Plot of mobility as a function of m/z	37
14.	Mobility in dependence on composition	38
15.	Mobility in dependence on linkage	39
16.	Sugar composition of maize phloem sap and aphid honeydew	42
17.	Chromatographic separation of <i>Brevicoryne brassicae</i> honeydew	43
18.	Extracted ion mobility aids in compound identification	44
19.	Sugar composition of honeydew of <i>Brevicoryne brassicae</i>	46
20.	Concentration of fructose and glucose in dependence on dietary sucrose levels.	47
21.	High concentrations promoted dimer formation.	57
22.	Deviating peak areas	60
I.	Monosaccharides	xxvi
II.	Disaccharides I	xxvii
III.	Disaccharides II	xxviii
IV.	Trisaccharides	xxix
V.	Tetrasaccharides	xxx
VI.	Calibration curves I	xlii
VII.	Calibration curves II	xliii

List of Tables

1.	Available CCS databases of carbohydrates.	16
2.	Software	20
3.	Analytical methods.	21
4.	Chromatographic gradients.	22
5.	Retention time ranges of saccharide classes.	31
6.	Fitness of <i>Brevicoryne brassicae</i>	45
I.	List of all observed saccharide standards	xxv
II.	Supplier sugar standards	xxxii
III.	Supplier ingredients of artificial diet	xxxiii
IV.	Recipe artificial diet	xxxiii
V.	Parameters multi reaction monitoring	xxxiv
VI.	Script automated calibration	xxxv
VII.	Parameters automated calibration	xxxvi
VIII.	Constants for CCS calculation	xlvi
IX.	Ion mobility and CCS library	xlvii
X.	CCS values (literature)	lii
XI.	Saccharide composition of maize phloem sap I	liv
XII.	Saccharide composition of maize phloem sap II	liv
XIII.	Saccharide composition of maize phloem sap (dark) I	lv
XIV.	Saccharide composition of maize phloem sap (dark, graphite column) II	lvi
XV.	Saccharide composition of honeydew of maize feeding aphids I	lvii
XVI.	Saccharide composition of honeydew of maize feeding aphids II	lx
XVII.	Saccharide composition of honeydew of <i>Brevicoryne brassicae</i> I	lxiii
XVIII.	Saccharide composition of honeydew of <i>Brevicoryne brassicae</i> II	lxvi

List of Abbreviations

API	Atmospheric pressure ionisation cell
CCS	Collision cross section
CID	Collision induced dissociation
D	Dexter = right
DIMS	Differential ion mobility spectrometry
DP	Degree of polymerisation
DTIMS	Drift time ion mobility spectrometry
EFG	Electrical field gradient
EIC	Extracted ion chromatogram
EIM	Extracted ion mobilogram
ESI	Electrospray ionisation
FAIMS	Field asymmetric waveform ion mobility
fru	Fructose
gal	Galactose
glc	Glucose
HILIC	Hydrophilic interaction liquid chromatography
HPLC	High performance liquid chromatography
IM	Ion mobility
IMS	Ion mobility spectrometry
isCID	In source collision induced dissociation
L	Laevus = left
LC	Liquid chromatography
MRM	Multiple reaction monitoring
MS	Mass spectrometry
MS/MS	Tandem mass Spectrometry

MW	Molecular weight
m/z	Mass-to-charge ratio
NMR	Nuclear magnetic resonance
PAD	Pulse amperometric detection
PGC	Porous graphite carbon
RT	Retention time
SD	Standard deviation
TIMS	Trapped ion mobility spectrometry
TOF	Time-of-flight
TWIMS	Travelling wave ion mobility spectrometry
UHPLC	Ultra high performance liquid chromatography
QTOF	Quadrupole time-of-flight

1. Introduction

1.1. Saccharides

Saccharides in biochemistry are synonymous with the large class of carbohydrates. This compound class makes up more than 50% of the dry weight of the Earth's biomass, largely in green plants in the form of water-insoluble polymers and is accordingly the most abundant one in the biological world¹. Its most frequently found representatives are cellulose, being responsible for cell wall stabilisation and water conduction, and starch used for energy storage.

Saccharides consist of monosaccharide building blocks, with the basic brutto formula being $C_nH_{2n}O_n$, expressed in other terms $C_n(H_2O)_n$. This led Carl Schmidt in 1844 to the assumption that saccharides are in fact hydrated carbons, which offers the origin of the classification name carbohydrates². Nowadays, even more diverse carbohydrates are known, also including nitrogen, sulfur or phosphate (e.g. amino sugars)³.

Carbohydrates and glycoconjugates play important roles in development, growth and function of all living organisms. They are involved in maintenance of tissue structures, energy supply, metabolism, and part of signaling hormones and many other important biomolecules. RNA and DNA, for example, constitute of the highly specialized monosaccharides deoxyribose and ribose. Sugar chains of glycoproteins are responsible for protein folding, detection and activity^{1,4,5}.

Carbohydrates can be grouped based on their functional or technological properties such as sweetness or solubility. However, the more common classification is the number of present carbon atoms or their degree of polymerisation (DP)¹:

- 1) Monosaccharides (DP 1)
- 2) Disaccharides (DP 2)
- 3) Oligosaccharides (DP 3–9)
- 4) Polysaccharides (DP \geq 10).

1.1.1. Monosaccharides

Monosaccharides are the basic building blocks of all saccharides, however, even at this simple structural level, they are highly diverse. According to the number of their constituent carbon atoms, they are named bi-, tri-, tetr-, pent-, hex- or hep-

toses³. In nature, just pentoses and hexoses have a noteworthy contribution, with the best-known being glucose and fructose. In general, monosaccharides are straight-chained polyalcohols with ketone or aldehyde functionality, properly named ketose (e.g. fructose) or aldose (e.g. glucose) (Figure 1)^{1,6}.

Configuration

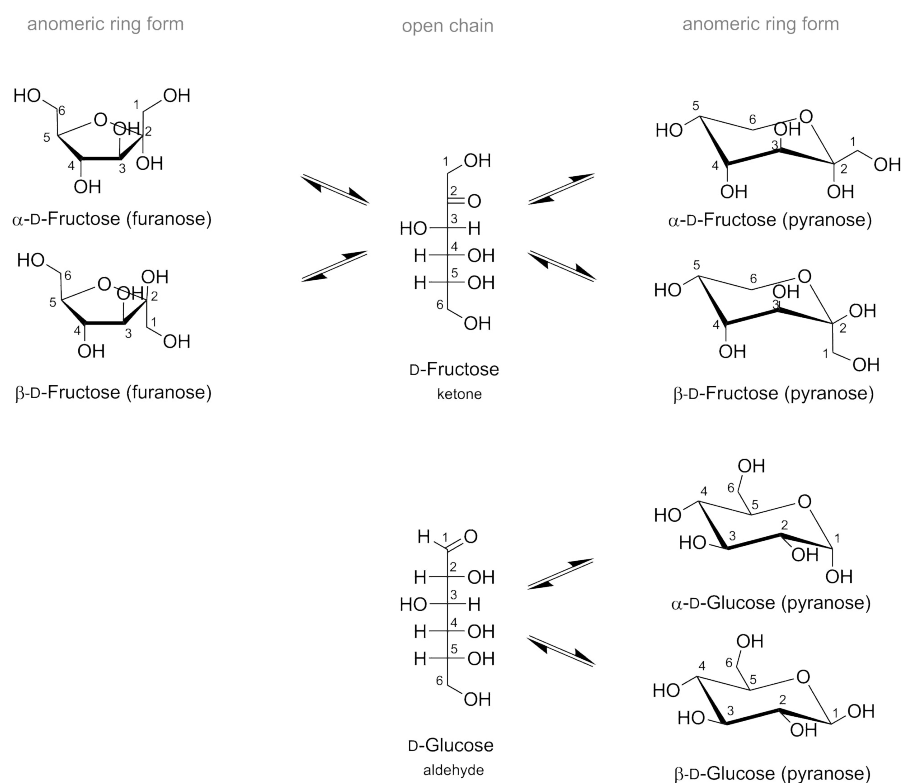


Figure 1: Straight chain and ring configurations of monosaccharides. Open chain form of the ketose fructose and aldose glucose are presented in Fischer projection. In solution, they equilibrate between the α - and β -ring anomers, the open chain forms are intermediates.

They have several stereogenic centres and a molecule consequently has 2^n stereoisomers. For example, glucose, an aldohexose, has four chiral centres and 16 different stereoisomers ($2^4 = 16$). In standard Fischer projection, the stereo centre furthest from the carbonyl group is decisive for the molecule being in *D*- (dexter=right) or *L*- (laevus=left) conformation. In general, *D*-saccharides are found naturally, with an exception being *L*-fucose¹. If not stated otherwise, the *D*-confirmation is assumed. Observed monosaccharides and alcohols are presented in the appendix (Figure I). By changing individual chiral centres of glucose many other natural sugars are gotten. Galactose and glucose only differ in the orientation of one hydroxyl group, they

are C-4 epimers. Galactose, glucose and fructose are of special interest being the building blocks of all exhibited di- and oligosaccharides (appendix Figure II).

The open-chain form often co-occurs with the cyclic conformation. Hereby, the hydroxyl group (-OH) bonded to C-5 attacks nucleophilic the aldehyde or ketone carbonyl group carbon (C=O) and forms a cyclic hemiacetal or hemiketal with a new C-O-C bond. The resultant anomeric carbon becomes a new chiral centre in α - or β -configuration. This reversible reaction forms energetic preferred rings with five or six atoms, which are called furanoses or pyranoses, respectively. In solution, the ring form equilibrates with the open-chain form as an intermediate structure (Figure 1)¹.

1.1.2. Disaccharides

The condensation of two monosaccharides forms a disaccharide, whereby a glycosidic linkage is formed between the anomeric carbon of the first and one hydroxyl group of the second monomer. Numerous possible hydroxyl groups of the second monosaccharide enable the formation of regioisomers. That means, the composing building blocks are equal, whereby the linkage position varies. For example, both sucrose and isomaltulose consist of one glucose and one fructose building block hooked together by an α -(1,2)- in the case of sucrose or rather an α -(1,6)-glycosidic linkage in the case of isomaltulose (Figure 2). The linkages influence properties as rates of digestion and absorption, where isomaltulose is more stable to enzymatic digestion by numerous sucrases⁷. Another example for substrate specific linkages are amylases targeting α -(1,4)-linkages, but not α -(1,6)-linkages⁸.

Saccharides can be classified as either reducing or non-reducing sugars (listed in appendix Table I). All monosaccharides can react as reducing substrate, except for monosaccharide alcohols. Moreover, di- and oligosaccharides having a free anomeric carbonyl group are reducing. They can convert into an aldehyde functionality, which further can become oxidised to carboxylic acid, to do so ketoses must first convert into aldoses by enolisation. In contrast, non-reducing saccharides have bonded anomeric carbons and thus cannot equilibrate to the open chain form acetals.

1.1.3. Oligo-, Polysaccharides and other Glycans

Oligo- and polysaccharides are formed by condensation of three or more monosaccharides. If more than ten monomers are polymerised, they are called polysaccharides. Sometimes three or more glycosidic bonds link with the same monosaccharide

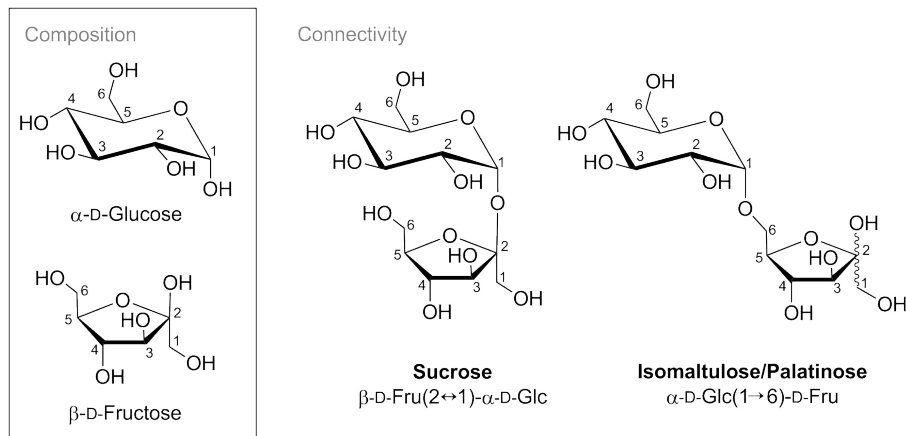


Figure 2: Sugar regioisomers. The connection of the two monosaccharides glucose and fructose by a glycosidic bond forms various regioisomeric disaccharides. The regioisomers sucrose (α -(1,2)-bond) and isomaltulose (α -(1,6)-bond) differ in their connectivity.

building block, which results in branched structures (e.g. amylopectin)⁷.

Polysaccharides often serve as energy reservoirs like starch in plants, consisting of amylose and amylopectin, or glycogen in animals. However, they may also serve as structural components of organisms. The most abundant polymers on earth are cellulose followed by chitin. Cellulose is a β -(1,4)-linked *D*-glucose polysaccharide found as primary component of cell walls in green plants. Analogous, chitin is a polymer of N-acetylglucosamine and component of fungi, arthropods, molluscs or fish. Saccharides may also conjugate with non carbohydrate groups like amino acids or lipids to form glycoproteins, glycopeptides or glycolipids⁵.

1.1.4. Plant and Insect Saccharides

Plants produce carbohydrates by photosynthesis. Taking aerial carbon dioxide and water through the roots, they produce oxygen and glyceraldehyde 3-phosphate. The phosphorylated triose is further transformed to glucose or other carbohydrates like sucrose. The required energy is obtained from sunlight captured in chloroplasts, the photosystem of green plants (Figure 3)¹. Surplus glucose is stored via polymerisation as a quickly accessible reservoir of energy - in plants as starch, in animals, fungi and bacteria as glycogen⁹.

A huge transport system of vascular bundles distributes sugars and other nutrients from the place of production or storage to where it is needed - from source to sink. The phloem sap is an 0.1-1.0 M aqueous solution of predominant sucrose, but also

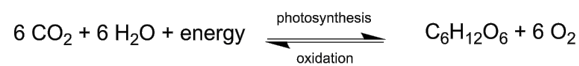


Figure 3: Simplified equation of photosynthesis. In the chloroplast of the plant, carbon dioxide reacts with water to form glucose and oxygen. The required energy is obtained from sunlight. In the reverse oxidative reaction, glucose is broken down and provides energy.

other non-reducing transport sugars and sugar alcohols like raffinose, stachyose or mannitol. In sieve tubes also amino acids, minerals, phytohormones and multitude of other substances are transported. The composition depends on the plant species, organs of the plant and many ecological and physiological conditions like season and plant developmental age¹⁰.

This nutritious composition is an attractive food for many plant sap feeding insects. Aphids and other insects of the order Hemiptera (the half-wings) specialized their feeding by inserting their stylets into the phloem and puncture the sieve tubes.

The nitrogenous concentration in sap is low compared to the carbohydrate level¹⁰. That means, hemipterans need to take up a lot of phloem sap to saturate their demand for nitrogen. Furthermore, phloem sap lacks certain essential amino acids, which the insect may overcome with the help of certain symbiotic bacteria¹¹.

With the need to ingest large volumes of phloem, and further the high sieve-tube turgor offering almost passive uptake of sap, comes the problem that the osmotic pressure of the plant sap is up to three times the body fluids of the insect themselves^{11,12,13}. Consequently, efficient osmoregulatory processes are needed.

Aphids ingest mainly sucrose, the predominant sugar in phloem sap. In the insect, sucrose is cleaved by a sucrase (α -glucosidase) into its constituents glucose and fructose. Fructose and to a lesser extent glucose is assimilated by the aphid's gut. Mono and disaccharides, but mainly glucose, are incorporated into oligosaccharides by transglycosylation enzymes^{13,14}. It is reported that the insects themselves are responsible for the enzymatic activities and not associated microbiota where antibiotic treated aphids showed the same behaviour in osmoregulation than untreated aphids¹⁵. Both treated and untreated aphids reduced the osmotic pressure of the gut content being osmotically equal to the insect's body fluids. The remained question, whether sucrase activity and transglycosylation is catalysed by the same enzyme or separate ones, was determined by purifying a protein with both activities^{13,14}. The transglycosylating α -glucosidase showed low activity in freeing glucose in the presence of excess sucrose due to the fact that glucose is linked to the substrate forming

oligosaccharides and is not released to the solution, whereby fructose is released and metabolised¹⁶. The synthesised oligosaccharides and other waste products are excreted via honeydew^{13,17}. Honeydew is a viscose, sugar-rich aqueous solution varying in composition dependent on many factors like aphid species, season, food source, symbiotic bacteria or gut enzymes^{17,18,19,20,21}.

All phloem feeders produce honeydew, common sugars present in most species of Hemiptera are fructose, glucose and sucrose. The predominant sugar in silverleaf whitefly *Bemisia tabaci* is the disaccharide trehalulose, but also the trisaccharide melezitose and tetrasaccharide stachyose have been reported^{22,23}. The whitefly *Bemisia argentifolia* shows significant levels of sorbitol and an unusual saccharide bemisiose^{24,25}.

In contrast, aphid honeydew is generally composed of the monosaccharides fructose and glucose, the disaccharides sucrose, trehalose and maltose, the trisaccharides melezitose, raffinose and erlose, also named fructomaltose, and further unspecified oligosaccharides^{18,21,26,27}. The composition of honeydew is species dependent by the fact that Völkl et al. observed four different aphid species feeding on the same plant and reported qualitative as well as quantitative differences in honeydew production²¹.

Galling aphids *Baizongia pistaciae*, *Geoica wertheimae*, *Forda formicaria* and *Forda marginata* excrete among other sugars fructose, glucose, trehalose and sucrose. Inositol and mannitol were detected under uncertainty in honeydew samples¹⁸. Furthermore, trehalose and raffinose were found in *Aphis asclepiadis* honeydew²⁷. A final comparison of the soybean aphid *Aphis glycines* and the tansy aphid *Metopeurum fuscoviride* makes the interspecies variations clear, with both aphids excreting fructose, glucose, sucrose and erlose, but the soybean aphid additionally excreting raffinose, whereby in contrast, the tansy aphid is producing trehalose, melezitose and maltose^{28,29,30}. The trisaccharide erlose was first identified in the aphid honeydew of *Aphis spiraecola* and mealybug *Pseudococcus citri* by hydrolysis via yeast invertase and colometrical identification of the fructose/maltose ratio³¹.

Besides the species dependent differences, external circumstances influence the honeydew composition even within a species, where fluctuations of honeydew are further caused by seasonal changes. Galling aphids feeding on their host plant in a natural habitat produced high levels of glucose with a peak in October. This can be due to the seasonal change of phloem sap composition of the host tree or due to temperature-dependent changes in the aphid's metabolism^{10,18,24}. As mentioned

previously, the phloem sap is not stable in its composition, it varies within plant species, light and water supply and even within the same plant¹⁰.

Therefore, it is obvious that also for aphids the 'output' changes, when the 'input' changes. This variation is highlighted in several studies, where the dependence on sucrose levels in diet in relation to honeydew composition were investigated by establishing artificial setups for feeding experiments to ensure stable conditions. It is consistently stated that a rising sucrose level raises the need of osmoregulation and therefore the oligosaccharide synthesis^{13,19,32}. If the diet exceeds a level of 10% sucrose, the aphid *Acyrtosiphon pisum* starts the oligosaccharide production with oligosaccharides being marginal in honeydew below this concentration^{15,17}. Whether the critical concentration of 10% is valid for all aphid species is not further investigated.

Another point to consider regarding the diet influencing the honeydew composition is the general food intake and age-specifications. The ingestion rate of aphids depends inversely on the sucrose level in the diet being that the higher the sucrose level, the less the food demand^{13,20}. However, a minimum sucrose level is required, because sucrose serves as an important phagostimulant for aphids³³. Moreover, ingestion and honeydew production are fundamentally dependent on the aphid development with nymphs progressing through four larval instars before becoming an adult aphid. The qualitative honeydew composition in all instars did not change remarkably in *M. fuscoviride*, besides xylose only being detected in the fourth instar and not in the other developmental stages²⁹. Whereas the amount of honeydew excretion is the lowest in the first two instars and the highest in the third one with approximately 550 µg/aphid per h.

To summarise, according to present literature the saccharide pattern is mostly dependent on the aphid species and the diet, whereby the dietary sucrose level has a large impact on oligosaccharide incidence being crucial for osmoregulation.

Aside from the physiological function reducing the gut osmolarity, honeydew also covers ecological functions. The sugar rich honeydew is taken up by birds and many insects such as honeybees, ants or wasps^{34,35,36}. Honey originating of honeydew collection contains higher rates of erlose and oligosaccharides than floral honey, thus saccharide profiling of honey can proof authenticity and origin^{34,37}.

Some aphids and ants live in mutualistic symbiosis, where ants are supplied with nutrients by aphid honeydew in exchange for ants provision of defense against aphid predators, parasitoids and fungal infections¹¹. For their symbiosis covenant, ants

prefer high honeydew emitters and aphids living in colonies^{21,30}. Besides quantitative effects, also the honeydew composition is a decisive factor for foraging activities of ants. In general, trisaccharides are preferred over disaccharides and monosaccharides^{21,38}. One of the most frequently observed aphid-specific trisaccharide is melezitose composed of glucose being α -(1,3)-bonded to sucrose. The production of melezitose is crucial for aphid osmoregulation and signals ant attendance, with the promise of plenty of sugar rich food. In contrast, another trisaccharide erlose was not attractive to ants^{30,39}. Some honeydew sugars promote the ant tending, but on reverse ants also have an impact on aphid honeydew³⁰. It is supposed that aphids adapt the honeydew quantity as well as quality regarding the presence of ants to optimise cost-benefit ratio³⁰.

This introduction into honeydew should help to overcome the outward first impression: 'Honeydew is just aphid poop'. Honeydew is a sugar rich excretion of aphids composed of variable levels of fructose, glucose, sucrose and various oligosaccharides like melezitose or raffinose. The production of oligosaccharides is essential for osmoregulation, as well as supporting the symbiosis with ants. In order to further understand the characteristics of honeydew and the ecological role, knowledge about its composition and dependencies become crucial. At the same time, an impasse is reached due to the limited analytical methods for saccharides.

1.2. Analytical Challenge

Saccharides consist of monosaccharide building blocks, which differ sometimes only in the stereochemistry at one single carbon atom. The connection of two or more results in disparate regioisomers. Moreover, the possibility for α - or β -anomers rises exponentially with the number of potential constituents. As an illustration, linking three monomers to form a trisaccharide, theoretically more than 1.13×10^7 different structures can be obtained³⁷. Most knowledge about honeydew composition was generated in the 80s via thin layer chromatography^{19,32,40,41}. Since then, numerous more differentiating analytical tools became available. To start, nuclear magnetic resonance (NMR) is widely used to elucidate the primary as well as three dimensional structures or conformation of carbohydrates. With regards to structural determination, NMR is unrivaled, however it requires rather large amounts of samples and has a relative detection limit of only 3-5%³⁷.

In contrast, mass spectrometry (MS) techniques are fast, accurate and allow the analysis of low amounts in complex mixtures. Moreover, the possibility for fragmen-

tation gives information about the single building blocks and their linkage, whereby the stereoisomeric discrimination still lacks using routinely MS methods⁴². Another separation technique is liquid chromatography, which is widely applied with or without coupling to MS. It allows the analyses of most configurational isomers in the restrictions of resolution limits, with the polarity of sugars impeding reversed-phase separation⁶. For example, Fischer and Shingleton (2001) analysed sugars in honeydew samples via HPLC with an electrochemical detector. Their repertoire encompassed 14 sugars, 7 sugars were identified in honeydew³⁰. Wool et al. (2005) detected more than 20 sugars in honeydew samples by anion HPLC with pulse amperometric detection (PAD), and an ultraviolet-visible absorbance detector. They managed to identify three sugars with certainty and three more tentatively¹⁸. Likewise, Shaaban et al. (2020) used HPLC with PAD, but equipped with an anion exchange column. With assistance of 17 sugar standards they identified 8 saccharides in aphid honeydew. The oligosaccharide peak of kestose could also represent nigerose and stachyose, because they did not separate completely⁴³. Hydrophilic interaction liquid chromatography (HILIC) coupled to a triple quadrupole MS (MS/MS) detector were used by Nguyen et al. (2020) to analyse seven sugars²⁷.

The literature about honeydew analysis shows a deficit in oligosaccharides ($DP \geq 4$) identification. The reports cover a limited and repetitive number of mono-, di- and trisaccharides. This might be traced to the limits of analytical methods for saccharides and shows the need for development of advanced techniques to handle the intricacy of saccharides. As a leading approach ion mobility-MS (IM-MS) gains ground in glycan analysis^{5,6,44}.

1.3. Ion Mobility Mass Spectrometry

To investigate saccharides it becomes necessary to add another dimension of analytical information to the common HPLC-MS/MS values. Additionally to retention time (RT) and mass-to-charge ratio (m/z), ion mobility offers information about size and shape of the analytes. But what is ion mobility and how is it applied in chemical analytics?

In essence, ion mobility utilises an electrical field which propels ions through an ion mobility cell filled with an inert gas. In dependence of their ion surface area and charge state, they interact differently with the gas and can be separated according to their mobility on a millisecond timescale⁶.

Historically we look back to the 1890s when ion mobility was mentioned by the

Cavendish lab in Cambridge University, USA⁴⁵. Fifteen years later the same lab first reported MS⁴⁶. The combination of ion mobility and MS took until the late 1960s, when Earl W. McDaniels coupled a low-field ion mobility drift cell to a sector mass spectrometer⁴⁷. In 1970 Cohen and Karasek forecasted the new analytical dimension offered by their published plasma chromatograph, as the IM-MS was called back then⁴⁸. The first IM-MS became commercially available in 2006^{49,50}. At present, various types of IM-MS exist. Roughly said, they differ considerable in the nature of the electrical field impelling the ions:

DTIMS (drift time ion mobility spectrometry) is the classical IM-MS. A homogeneous low electrical field ($10 - 100 \text{ V} \cdot \text{cm}^{-1}$) carries the ions through an inert gas filled tube⁵. The ions drift with a constant velocity and reach the detector in order of decreasing mobility. One advantage is that the drift times can be directly transformed into collision cross section values (CCS) by the Mason-Schamp-equation⁵ (chapter 1.3.2).

TWIMS (travelling wave ion mobility spectrometry) uses an electrical field just covering a small region. Travelling axially along the tube a wave is created pushing the ions forward bypassing the need for high drift voltages⁵. Standards with known CCS values are necessary for estimation, as they cannot be determined directly. But Giles et al. have proposed an alternative method which allows the direct calculation of CCS values from TWIMS⁵¹.

FAIMS (field asymmetric waveform ion mobility spectrometry) or DIMS (differential ion mobility spectrometry), in which the ions are introduced between two electrodes. A short period of high electrical field is followed by a longer period of low field of opposite polarity⁵. The fact that ion mobilities are dependent on electric field intensities is used to separate ions by their mobility differences in the altering field⁵². This method is targeted and only ions with certain mobility can exit the cell⁵.

TIMS (trapped ion mobility spectrometry) differentially traps the ions in an electrical field according to their ion mobility. The ions are pushed by a gas flow through an axial electrical field gradient (EFG) in the TIMS tunnel. At the point where the force of the electrical field matches the drift force the ions experience by the gas flow, the ions are held stationary and accumulate. Selectively lowering the electric force releases the trapped ions according to their mobility (Figure 4)⁵⁰.

To date, IM-MS finds diverse applications for distinction, identification and structural elucidation for a broad range of analysts such as supramolecular complexes,

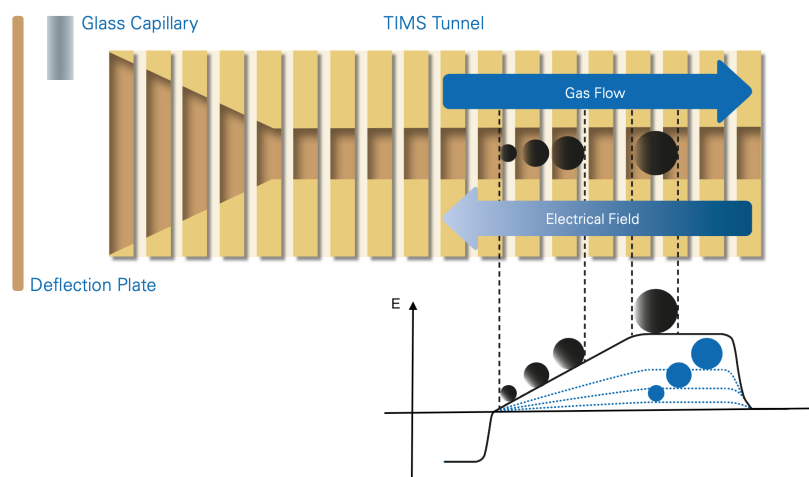


Figure 4: Schema of TIMS tunnel. Ions are propelled by a gas flow through the tunnel of the trapped ion mobility spectrometer (TIMS). An increasing electrical field traps the ions at the point where the opposing force matches the push of the gas flow. By reducing the electrical field, the ions are eluted stepwise according to their mobility. The scheme is adapted from timsTOF brochure provided by Bruker⁵⁰.

lipids, proteins, natural products and glycans⁵².

1.3.1. Route through timsTOF

In this study, TIMS was connected with a quadrupole time-of-flight (QTOF) mass spectrometer (MS) (Bruker Daltonics, Bremen, Germany), hereafter called timsTOF as it is the device name.

Following steps bring us to the multiple analytical dimensions required for insect saccharide analyses:

At first, an UHPLC is coupled to timsTOF, where the analyte mixture is injected into and separated according to their retention. The liquid sample solution enters the atmospheric pressure electrospray ionisation cell. There, it is converted into gas phase ions by electrospray ionisation (ESI) and dried by a gas flow. Then, the ions are transferred through a glass capillary to the entrance funnel. Here, the incoming ions are collected before the separation takes place in the second part of the TIMS tunnel. In the TIMS analyser region the electric field is uniform during the accumulation phase, whereas it is ramped in the separation period. In this second interval the isomers are propelled by a nitrogen stream and separated depending on their mobility in the non-uniform EFG. By decreasing the voltage, the ions are released

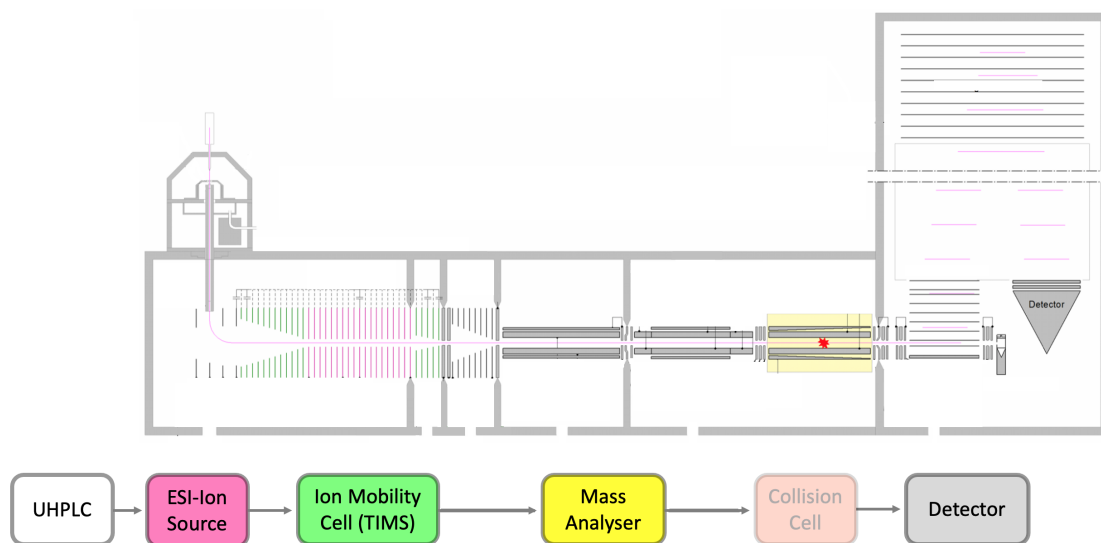


Figure 5: Route through timsTOF. The schema is adapted of the otof-Control user manual provided by Bruker⁵³.

at a characteristic elution voltage (V_e) according to their mobility. The released ions are focused in the hexapole before they are m/z selected in the quadrupole. Downstream, a collision cell enables collision induced dissociation (CID). After orthogonal acceleration, the ions are passing the flight tube and finally reach the detector. Using MS full scan mode for quantification the collision energy is kept low and no dissociation in the collision cell as well as no isolation in the quadrupole takes place in this method^{50,54}.

1.3.2. Transforming Mobility to Collision Cross Section

Ion mobility is plotted as mobility spectra and taken to calculate the instrument independent collision cross section (CCS). The relation of ion mobility and CCS is inverse, meaning large mobility values result in small CCS. For this reason, the instrument software reports mobility as an inverse reduced mobility $1/K_0$ ⁵⁵. The timsTOF instrument cannot determine ion mobility nor CCS directly. The mobility K is connected to the gas flow velocity v_g , elution voltage V_e of the isomer, ramp time t_{ramp} , the base voltage V_{out} and the electrical field \vec{E} . The reduced mobility K_0 is defined by

$$K_0 = \frac{v_g}{\bar{E}} = \frac{A}{V_e - V_{out}}, \quad (1)$$

where A is an instrumental calibration constant. The calibration is done with standards of known mobilities (chapter 2.2.3)⁵².

To enable a direct cross-instrumental comparison, an independent identification parameter becomes necessary. Actually, the conversion into ion's surface area as the rotationally-averaged ion-neutral CCS (Ω) in a specific drift gas is recommended⁵².

For empirical studies with TIMS, a static and relatively low electrical field can be approximated. In this limit, the Mason-Schamp equation can be used to calculate the experimental CCS values from mobility ($1/K_0$)^{5,52,56}:

$$CCS = 3/16 \sqrt{\frac{2\pi}{\mu k_B T} \frac{ze}{NK}} \quad (2)$$

$$= 3/16 \sqrt{\frac{2\pi}{\mu k_B T} \frac{ze}{N_0 K_0}} \quad (3)$$

$$\text{with } \mu = \frac{m_i \cdot m_g}{m_i + m_g}, \quad (4)$$

where μ is the reduced mass of the ion gas pair, m_i is the mass of the ion, m_g is the mass of the gas, k_B is the Boltzmann constant, T is the absolute Temperature in Kelvin, z is the integer charge state, e is the fundamental charge, N is the inert gas number density and N_0 the Loschmidt's number. Constants and units for each term used in equations (1-4) are listed in the appendix (Table VIII). They were chosen following recommendations of Gabelica et al.⁵².

Besides the experimental estimation, a theoretical calculation of CCS is possible. Therefore, the lowest energy conformation is determined through 3D simulation and then the cross section is obtained by *in silico* IM experiment⁵⁷.

To report CCS, the used nomenclature was introduced by the Barran group: Method type as a superscript and drift gas as subscript⁵⁸. Here as follows ^{TIMS}CCS_{N₂} as we obtained mobilities and CCS values using TIMS with nitrogen as inert gas in the mobility cell. All CCS are given in Å² (1 Å² = 0.01 nm²).

1.4. State of Knowledge on Glycan Analysis via IM-MS

As highlighted before, analysing carbohydrates is challenging. Saccharide isomers can be different in their composition (stereoisomers), connectivity (regioisomers) or configuration (anomers). Sometimes little structural differences affect the function of biomolecules⁵⁹. Differentiation of those isomers with identical mass reaches the limit of common MS. In the last two decades great advances in sugar analyses were achieved due to the integration of IM-MS techniques. The separation according to the analyte's size and shape offers orthogonal data. In this section the current state of knowledge on glycan analysis via IM-MS is outlined.

To date, IM-MS finds broad application starting with small intact molecules as monosaccharides⁶⁰, sugar alcohols⁶¹ and disaccharides⁵⁹. To continue with trisaccharides^{37,62,63} and saccharides of higher DP^{64,65} until N-glycans released from glycoproteins^{64,66} and glycosaminoglycans were investigated⁶⁷.

Reliable glycan analysis finds practical application in elucidation of complex samples and metabolomics. One example is disease diagnosis by sugar identification in biological matrix (urine, plasma, platelets and red blood cells)^{60,68} or food control by IM-MS analyses of honey³⁷. Finally, the valuable contribution of IM-MS to carbohydrate synthesis control and sequencing should be mentioned with one of the first instances utilised by Gabryelski and Froese (2003) with FAIMS to separate disaccharide isomers^{59,63,69}. The ions formed complexes with alkali metal ions (Li^+ , Li^+ , NH_4^+ , Na^+ , K^+ , Rb^+ , Cs^+) or anions (Cl^- , A^- , MCA^- , DCA^- , TCA^- , MBA^- , DBA^- , TBA^- , BCA^- , CDBA^- , BDCA^-) in positive or negative mode, respectively. The formation of adducts enabled better isomer separation since mobility differences of single ions are sometimes too small for effective separation^{70,71,72}.

By adduct formation the ions increase their size, which hence increase their mobility and differentiation. Furthermore, the oxophilicity of alkali metals affects folding of carbohydrates due to stereochemically dependent interactions^{73,74}. As follows, the observed trend was a direct, but not a monotonic correlation of mobility and complex ion radii^{37,59,73}.

In other studies, manifold more adducts were tested as for example the formation of dimers⁷⁵, Zn-ligands⁷⁶ or non-covalent peptide complexes⁷⁷.

Sometimes it appeared that one injected pure glycan gave more than one mobility peak. This strange fact may be reasoned by the ability of cations to coordinate at more than one position of the carbohydrate, leading to coexisting conformations.^{5,64,76} Furthermore, reducing sugars have the possibility to isomerise.

Monosaccharides equilibrate between the acyclic and cyclic form and can change between the α - and β -pyranose and α - and β -furanose forms^{64,70,74}.

This phenomenon complicates the characterization, especially in already complex mixtures of various saccharides. To reduce the ion mobility spectrum, a conversion of reducing sugars by disabling mutarotation is possible. For example, ammonium adducts just give one peak as well as purposeful reduction of oligosaccharides to alditols prevents interconversion^{37,62,64}.

The benefits of polarity are analyte dependent, for monosaccharides⁷⁸ as well as alditols^{62,64} good differentiation for sodium adducts in positive mode were achieved. On the opposite, negative mode was preferable for disaccharides, whereby the complexes formed in this mode were less stable than in positive polarity⁵⁹. Also for higher order oligosaccharides negative polarisation gave better outcomes and therefore, more anion complexes were requested such as $[M+I]^-$, $[M+Br]^-$ or $[M+NO]^-$ ^{75,78,74}.

In order to increase the ability to distinguish glycans, various parameters were investigated including polarity, adduct formation and derivatisation, as well as the variation of instrument settings. One possibility is the choice of drift gas since polarity and density of the gas have a great impact on the molecular interaction and mobility. For instance α - and β - methyl-mannopyranoside were not separated in nitrogen (N_2), but in carbon dioxide (CO_2) and a report by Pagel and Harvey observed larger CCS values for sodiated N-linked glycans in nitrogen than in helium (He)^{79,66}.

Over the time course, different IM instruments have been applied starting from the early home-build⁸⁰ to commercially available like FAIMS⁵⁹, DTIMS^{61,78,81}, TWIMS^{60,65,66,78,81} or finally TIMS^{37,67,82}, which just recently entered the market. Further technical enhancements were developed to increase the ability to resolve specified ions and raise carbohydrate isomer resolution. The Clemmner group elongated the drift tube until 3 m in DTIMS experiments, and further presented a cyclotron geometry drift tube equipped with four ion funnels^{83,84}. More recently a tailored serpentine ion pathway and a cyclic TWIMS allowing multipass separations were reported^{70,85}. Li et al. suggested tandem IMS by coupling DTIMS separator to a commercial TWIMS instrument with a TOF-MS analyser and differentiated raffinose and maltotriose or isomeric pentasaccharides successfully⁸⁶. Additionally, CID was implemented to support structure characterization of carbohydrates as some disaccharide isomers have the same mobility for the precursor ion, but show different mobility patterns for monosaccharide-glycolaldehyde product ions after dis-

sociation⁷⁴. Hereby the lability of the glycosidic bond is addressed, whereby linkage isomers can be distinguished by the bond strength as (1,2)- and (1,6)-linked disaccharides display the phenomenon of auto-dissociation^{73,74}. Further, the relation of product ions depends on anomer configuration of the initial ion⁷⁵.

Oligosaccharides or other glycans can be fragmented into smaller intact ions equal to the general saccharide building blocks⁶⁰. Thus, complex structures can be illuminated by comparing fragment mobilities to their counterpart standards⁶³.

To identify complex mixtures, no matter which IMS technique is used, a comprehensive mobility database will help enormously. This should include both polarities, various drift gas, adduct ions, chemical modifications and perhaps fragment data as well^{6,64}. To enable a universal IM-MS application across multiple samples, instruments and timeframes, the transformation of mobility values into CCS was proposed⁵². To date, a few groups presented CCS databases including glycans (Table 1).

Table 1: Available CCS databases of carbohydrates.

Research group	Website	Reference
Pacific Northwest National Laboratory	metabolomics.pnnl.gov & panomics.pnnl.gov/metabolites/	Zheng et al. (2017) ⁷⁸
Mc Lean Research Group	mcleanresearchgroup.shinyapps.io/CCS-Compendium/	Picache et al. (2019) ⁸⁷
Libin Xu Lab	ccsbase.net	Ross et al. (2020) ⁸⁸
Zhu Lab	allccs.zhulab.cn	Zhou et al. (2020) ⁸⁹

1.5. Aim of this Work

The aim of this study is the generation of an UHPLC-ion mobility-MS library, which further will be applied to the analysis of complex saccharide mixtures. Biological samples of phloem sap and aphid honeydew of plant fed and artificial fed aphids will be analysed, as outlined herein. At first, an instrument method for saccharide discrimination via timsTOF will be developed. Second, a library of mobilities and CCS values will be created by measuring 47 commercially available sugar standards of mono-, di- and oligosaccharides (DP 1-7) as well as sugar alcohols. This should contribute to the development of a comprehensive CCS database and will offer CCS data with regards to larger oligosaccharides and a multitude of disaccharide isomers, which are actually lacking in literature. Finally, the library will find application in the analysis of biological samples. Here, the observation of aphid honeydew is of

special interest, whereby the presence of many structural isomers in a biological glycan mixture is challenging. The utilisation of modern ion mobility techniques can offer new analytical dimensions to distinguish and identify sugar isomers. The first section will compare the sugar composition of maize plant sap and honeydew of aphids feeding on maize to elucidate aphid metabolism. The second section will gain deeper knowledge of sugar transformation in aphids and is led by the question: What impact does the sucrose levels in diet have on aphid honeydew composition? This question will be examined by feeding assays of the cabbage aphid *Brevicoryne brassicae* in an artificial diet setup.

2. Materials and Methods

2.1. Materials

2.1.1. Chemicals

All chemicals were commercially available and if not stated otherwise, were used without further purification. Water was obtained from purification system Millipore Milli-Q Synthesis A10 equipped with a 0.22 μm Millipak 40 filter (Millipore, Billerica, MA, USA). Milli-Q water was used to prepare standards, biological samples and for HPLC analyses. Acetonitrile (ACN) in HPLC LC-MS grade was obtained from VWR BDH chemicals (Darmstadt, Germany). ESI-L Low Concentration Tune Mix was purchased from Agilent Technologies (Santa Clara, CA, USA) and stored at 4 °C. Origin of sugar standards utilised in this study and ingredients of the artificial diet are listed in the appendix (Table II, Table III).

2.1.2. Preparation of Standards

For sugar standard preparation 2 μmol of each substance were weighed out in a 1.5 mL glass vial (Macherey-Nagel GmbH&Co.KG, Düren, Germany) with a high performance balance (Mettler Toledo XP26, Gießen, Germany) and dissolved in 1.0 mL milli-Q water to reach a stock concentration of 2.0 mM. The highly concentrated stock solutions were diluted with milli-Q water. Monosaccharides and polyols ($M \leq 182.17 \text{ g/mol}$) were diluted to a final concentration of 50 μM , all other sugar standards were diluted to 10 μM in glass vials, closed with caps and stored at -20 °C or placed directly into the autosampler. Before chemical analysis, they were thawed to room temperature, mixed thoroughly by vortex and placed in the autosampler cooled to 10 °C.

2.1.3. Aphid and Plant Species

The cabbage aphid *Brevicoryne brassicae* was reared on brussels sprout plants *Brassica oleraceae* var. *gemmifera*. The plants were grown in climate-controlled short-day environmental chambers at 14:10 h light:dark photoperiod, 60% relative humidity and 21 °C. The aphids were reared under conditions of 16:8 h light:dark photoperiod, 60% relative humidity and 23 °C. The aphids *B. brassicae* were generously provided by Dr. Rieta Gols (Wageningen University & Research, Wageningen, Netherlands).

The maize feeding aphids *Rhopalosiphum padi* and *Sitobion avenae* were reared on *Zea mays* plants of different ages (4 weeks - 4 months old). The seeds were obtained commercially (Badischer Gelber variety, Kiepenkerl, Germany) and grown under 16:8 h light:dark photoperiod and 21 °C. The aphids were obtained as a mix from Katz Biotech (Baruth, Germany).

2.1.4. Artificial Diet

In this study, the recipe was adapted from A₀ by Febvay et al.⁹⁰. All substances except sucrose were dissolved successively in milli-Q water following the exact order of the recipe (appendix Table IV). A magnetic stirrer was set up and each ingredient was fully dissolved, before the next one was added. Finally, the pH was adjusted to pH 7,5 with potassium hydroxide (KOH), divided into 50 mL aliquots and stored at -20 °C. Before use, the diet was thawed and sterilized by pushing through a syringe filter holder (0.20 µm, Sarstedt, Germany). As feeding stimulator 0.1% sinigrin (monohydrate, Rotichrom CHR, Karlsruhe, Germany) was added. The sucrose addition depended on the required sucrose level. The standard concentration is 20%, modified in this study to 5%, 10%, 40% and 60% sucrose, respectively.

2.1.5. Software

Table 2: Software

Name	Purpose
Analyst (Version 1.5.2)	View on Data
Analyst (Version 1.6.3)	Analysis of LC-MS/MS data
Bruker Compass HyStar (Version 5.1.8.1)	IM-MS Acquisition
Compass DataAnalysis (Version 5.3)	View on Data, EIC Extraction, Mobility determination
Compass QuantAnalysis (Version 5.3)	Quantification
Microsoft Excel for Mac (Version 16.49)	Data Processing
otofControl (Version 6.0)	MS-parameter, tuning
RStudio (Version 1.2.5042)	Calculations
ChemDraw Professional (17.1)	Drawing of chemical structures

2.2. Methods

For chemical analyses two different columns, positive and negative ESI mode and two MS-instruments were applied and listed in Table 3 for an overview.

First, the amine column apHeraNH₂ Polymer (150 × 4.6 mm, 5 μm particles, Supelco Analytical, Munich, Germany) equipped with an HILIC precolumn (Phenomenex, Aschaffenburg, Germany) was used. The covalent bonded polyamines provided a good separation of mono and oligosaccharides. As standard, the negative ionisation mode was used. For monosaccharide analyses the amine column with HILIC precolumn and an upstream HPLC In-line-filter AFO-8497 (0.5 μm, Phenomenex, Aschaffenburg, Germany) was connected to an Agilent Technologies 1260 Series HPLC (Agilent Technologies) coupled to an API5000 triple-quadrupole mass spectrometer (Applied Biosystems Sciex, Darmstadt, Germany). For di- and oligosaccharides a Thermo Scientific Dionex UHPLC* (Waltham, MA, USA) connected to a trapped ion mobility cell coupled to quadrupole, time-of-flight mass spectrometer (TIMS-qTOF-MS or device name timsTOF, Bruker Daltonics, Bremen, Germany) was used. There, the amine column with HILIC precolumn was utilised in negative electrospray mode for qualitative and quantitative analysis. Moreover, the compound identification was supported by runs in positive electrospray mode. Second, a porous graphitic carbon column (PGC, Hypercarb) (100 × 2.1 mm, 3 μm, ThermoFisher Scientific, Waltham, MA, USA) equipped with a C18 precolumn (Phenomenex, Aschaffenburg, Germany) was used to further confirm the sugar identification via timsTOF measurements in negative electrospray mode.

Table 3: Analytical methods.

Compound	Precolumn	Column	MS-Instrument	Electrospray ionisation mode	Type of Analysis
Monosacch.	filter+HILIC	NH ₂	API5000	negative	qual., quan.
Di- & Oligosacch.	HILIC	NH ₂	timsTOF	negative	qual., quant.
	HILIC	NH ₂	timsTOF	positive	qual.
	C18	PGC	timsTOF	negative	qual.

2.2.1. UHPLC Methods

The instrument was purged for 5 min at a flow rate of 1 mL/min before acquisition. Five microliters of authentic standard were injected into UHPLC, following

chromatographic gradients listed in Table 4.

First, the UHPLC was equipped with the amine column and the HILIC precolumn using the following parameters: Mobile phase consisting of water (solvent A) and acetonitrile (solvent B) at a flow rate of 1 mL/min (split 1:3 source:waste) at 20 °C. Second, the PGC column with C18 precolumn was used: Mobile phase consisting of water (solvent A) and acetonitrile (solvent B) at a flow rate of 0.25 mL/min at 12 °C.

Table 4: Chromatographic gradients.

apHeraNH2 Polymer column		Hypercarb PGC column	
time [min]	ACN [%]	time [min]	ACN [%]
0.00	80.00	0.00	0.00
0.50	80.00	2.00	0.00
13.00	55.00	20.00	25.00
14.00	80.00	22.00	0.00
18.00	80.00	30.00	0.00

2.2.2. Mass Spectrometry Analyses

Monosaccharides were detected using the API5000 in negative ionisation mode with a collision gas value set at 5, curtain gas pressure set at 20 psi and turbo spray gas 1 and 2 set at 50 psi and 60 psi, respectively. Ion spray voltage was set at -4500 V, and turbogas temperature at 600 °C with interface heater on. The instrument was operated in scheduled multiple reaction monitoring (MRM) with a detection window of 300 sec and target scan time of 0.4 sec. The MRM parameters are listed in appendix (Table V). Moreover, the declustering and entrance potential were set at -50 V and -9.5 V, respectively. The collision energy set at -10 V, the collision cell exit potential at 0.0 V.

Di- and oligosaccharides were detected using timsTOF with enabled TIMS to perform mobility measurements. The recorded mass range was from m/z 50-1500, the inverse reduced mobility ($1/K_0$) data were measured in survey mode in a range of 0.40 to 1.80 V·s·cm⁻² with a ramp time of 70.2 ms, spectra rate at 13.31 Hz, an accumulation time of 20 ms, duty cycle locked at 100% and the rolling average at 3x.

In both positive and negative ionisation mode the settings were as following: **Source:** The voltage of the end plate offset and capillary tip was set at 500 V and 4500 V,

respectively. The pressure of nebulizer was set at 1.8 bar, the dry gas flowed at a rate of 10.0 L/min and dry temperature set at 230 °C. **General Tune:** The transfer funnel 1 RF and 2 RF were set at 150 Vpp and 300 Vpp, respectively. The in source collision induced dissociation (isCID) energy was set at 0.0 eV, the multipole RF at 150 Vpp.

In negative mode, the deflection delta was set at -70.0 V, the quadrupole ion energy at 6.0 eV, the low mass at m/z 100, the collision energy at 10 eV, the collision RF at 400 Vpp, the transfer time at 50.5 μ s and the pre-pulse storage at 5.0 μ s. **Tims Tune:** Δ 1: 20.0 V, Δ 2: 120.0 V, Δ 3: -70 V, Δ 4: -60.0 V, Δ 5: 0.0 V, Δ 6: -100.0 V. Funnel 1RF 250 Vpp, Collision Cell In -300.0 V.

In positive mode, the deflection delta at 30.0 V, the quadrupole ion energy at 5.0 eV, the low mass at m/z 100, the collision energy at 15 eV, the collision RF at 400 Vpp, the transfer time at 50.0 μ s and the pre-pulse storage at 10.0 μ s. **Tims Tune:** Δ 1: -20.0 V, Δ 2: -120.0 V, Δ 3: 70 V, Δ 4: 100.0 V, Δ 5: 0.0 V, Δ 6: 100.0 V. Funnel 1RF 350 Vpp, Collision Cell In 300.0 V.

Nitrogen (nippon gases, Erfurt, Germany) was used as dry and IMS gas. Before entering the instrument, nitrogen was piped through an oxygen and moisture trap BIG SupelPURE HC (Supelco, Bellefonte, Pennsylvania, USA).

The timsTOF parameters are reported according the recommendations of Gabelica et al. for reporting IM-MS measurements⁵².

2.2.3. timsTOF Calibration

Ion mobility and m/z measurements were calibrated using Agilent ESI-L Low Concentration Tune Mix (Agilent Technologies, Santa Clara, CA, USA) under the same timsTOF instrument settings as for the measurements of samples. Before each set of analyses, the instrument was calibrated by injecting the calibration mix directly into ESI source. At first, m/z was calibrated, then the nitrogen flow adjusted and finally the mobility calibrated. Mobility and mass were calibrated by using at least three calibration points from the tune mix default values (negative mode: m/z 302, 602, 1034; positive mode: m/z 322, 622, 922). The nitrogen flow was regulated by turning the flow rate valve at the machine until the elution voltage -119 V for the EIM of m/z 602 was reached in negative mode or 132 V for m/z 622 in positive mode, respectively.

At the beginning of each run, the tune mix was injected for internal calibration through a 20 μ L loop. The loop was automated filled by a syringe (2.5 mL, Hamilton,

Langerwehe, Germany) during chromatographic run time of 18 min or 30 min with a flow rate of 1 $\mu\text{L}/\text{min}$ or 0.66 $\mu\text{L}/\text{min}$, respectively.

2.2.4. Mobility Data Processing and CCS Determination

For mobility determination the runs were processed with DataAnalysis Software. At first, the runs were automatically calibrated by the software to guarantee equality, calibration parameters are listed in appendix (Table VI, Table VII). Then, the chromatographic peaks were visually selected from their base peak chromatograms, the time at maximum peak intensity was taken as RT. The ion mobility was obtained from EIM. The EIM were generated for the expected m/z for following major ion species: In negative mode, $[\text{M}-\text{H}]^-$, $[\text{M}+\text{Cl}]^-$, $[\text{M}+\text{HCOO}]^-$ and $[2\text{M}-\text{H}]^-$. In positive mode, $[\text{M}+\text{H}]^+$, $[\text{M}+\text{Na}]^+$, $[\text{M}+\text{K}]^+$ and $[2\text{M}+\text{Na}]^+$. Next, the Mobilities were transferred to Microsoft Office Excel, where the averages, standard deviations, and relative standard deviations were calculated. Finally, mean mobilities were transformed into CCS data in Microsoft Office Excel applying the Mason-Schamp equation (chapter 1.3.2), with the used constants listed in appendix (Table VIII). DataAnalysis provides CCS calculation as well, but the equation and values were hidden. To enable transparency it was decided to do not take the software provided CCS calculation and instead do it in Microsoft Office Excel following Gabelica et al.⁵². The gained CCS values corresponded to the CCS output of DataAnalysis for all tested examples.

2.2.5. Quantitative Calibration and Analysis

For quantitative analysis, calibration curves were created for all available standards of identified sugars in honeydew (appendix Figure VI). For the unknown compounds representative standards were chosen according their polymerization grade. Dilution series of glucose, fructose, mannitol, sucrose, trehalose, gentiobiose, melezitose, kestose, nystose, raffinose, panose and the maltooligosaccharides maltose, maltotriose, maltotetraose, maltopentaose, maltohexaose and maltoheptaose were prepared the following:

High concentrated stock solutions ($V = 0.6$ to 1 mL) of 10 mM were prepared in milli-Q water. The dilution series was done in triplicates (A, B, C) in glass vials. The stock solution was diluted to 1000 μM , 500 μM , 200 μM (all $V = 1$ mL) and 100 μM ($V = 4$ mL). The replicate B 100 μM solution was further diluted to 50 μM , 20 μM , 10 μM , 5 μM (all $V = 1$ mL) and 1 μM ($V = 4$ mL). At last, the replicate B 1 μM was

diluted to obtain concentrations of 0.5 μM , 0.2 μM , 0.05 μM , 0.02 μM and finally 0.01 μM (all $V = 1 \text{ mL}$).

The expected concentrations for glucose and fructose in biological samples were higher than for other saccharides. Moreover, the detection limit of timsTOF was less sensitive for small molecules. Due to the fact that the calibration curve should have sufficient data points, the dilution series was adapted. Stocks (2 mL) of 10 mM were diluted to 1500 μM , 1200 μM , 1000 μM , 800 μM , 500 μM , 300 μM , 200 μM and 100 μM . The B replicate of 100 μM was further diluted to 80 μM , 50 μM , 20 μM , 10 μM , 5 μM and 1 μM being the detection limit.

The dilution series were measured from lowest to highest concentration utilising the standard UHPLC-IM-MS method (chapter 2.2.2). The data were processed with Compass QuantAnalysis Software provided by Bruker. The extracted ion chromatograms (EIC) for $[\text{M-H}]^-$ were generated and integrated with the algorithm version 3.0. The sensitivity was set at 100, absolute area and intensity threshold were set at 5 and 1, respectively with minimum peak valley set at 10. To identify compounds based on their mobility the EIM $[\text{M-H}]^-$ was integrated, too.

For quantitative analyses of the plant sap and honeydew samples, the runs were processed the same way. The intensities of runs were different, therefore peak areas were normalized by dividing by the sum of the peak areas of all compounds of this run. To transform the peak areas into concentrations a custom R script was used. There, the calibration curve was fitted with base functions $\text{sqrt}(x)$ and $\text{log}(x+1)$. Then, the inverse of the fitted function was locally approximated and given as an output (appendix A.2.2).

2.3. Preparation of Biological Samples

2.3.1. Phloem Sap

To study the impact of darkness on the plant metabolism, the phloem sap was collected from plants grown continuously under standard conditions and plants being in the dark for 48 h before collection. The phloem sap of maize plants was obtained by Dr. Torsten Knauer in October 2019 by stylectomy⁹¹. This method allows the collection of pure phloem sap by radio frequency microcautery. Fixed maize leaves were infested with 100 adult apterous aphids (*S. avenaie*), which inserted their stylets into the leaves for ingestion. After 24 h of feeding, the stylets were cut with a microcautery device. In this vein, a straight access to the sieve tubes was provided.

Finally, the exuding phloem sap was collected and transferred into PCR tube with a micro capillary after 24 h. The samples were stored at -20°C . By this method, 10 nL of plant sap were gained, which were thawed and diluted with 50 μL water (1:5000) for chemical analysis.

2.3.2. Honeydew

Maize feeder:

Honeydew from the maize plant reared aphids *R. padi* and *S. avenae* was collected by Bettina Raguschke and Dr. Daniel Giddings Vassão in the summer of 2019. For collection, the visible deposits of honeydew present in the cages where the aphids were grown were wiped with a water-wetted cotton into a Falcon tube (50 mL). Then, the solution was filtered, frozen, freeze dried and stored at -20°C . The collected honeydew was pulverized and stock solutions prepared by dissolving 30-60 mg dried honeydew into 300-600 μL water (1:10) in five replicates. For chemical analysis, the 10 μL of stock solutions were diluted with 990 μL water (final degree of dilution 1:1000).

Cabbage feeder:

For cabbage aphids an artificial bioassay was set up, developed for aphid feeding studies by Dr. Grit Kunert and Daniel Veit. The artificial diet was provided to the aphids *B. brassicae* through a parafilm membrane. The equipment was sterilized before use and setup as followed: Three plates with nine hollows each were covered with stretched parafilm. In each hollow a drop of 120 μL diet (20% sucrose, 0.13% sinigrin) was placed and fixed by a second layer of parafilm. The projecting flaps were pulled down and tighten on the reverse side of the plates. Then, twenty apterous adult cabbage aphids were placed in each hollow and covered with a magnetic attached cage lid (inner $\text{Ø} = 1.8\text{ cm}$) (Figure 6).

The artificial setup was kept under same climate chamber conditions as the plants (16 h light, 8 h dark, 60% humidity, 23°C). Then, the adult aphids were giving nymphs, which - accustomed to the artificial setup - may had a better survival rate than plant reared aphids⁴¹. After 48 h, the adults were removed and the 1-2 day old nymphs were left in the cage. After two more days, the nymphs were transferred by lifting them carefully with a brush to a fresh setup equipped with 150 μL diet (20% sucrose, 0.1% sinigrin). Before getting distributed to diets with different sucrose levels, they grew three more days on normal artificial diet. Five replicates per

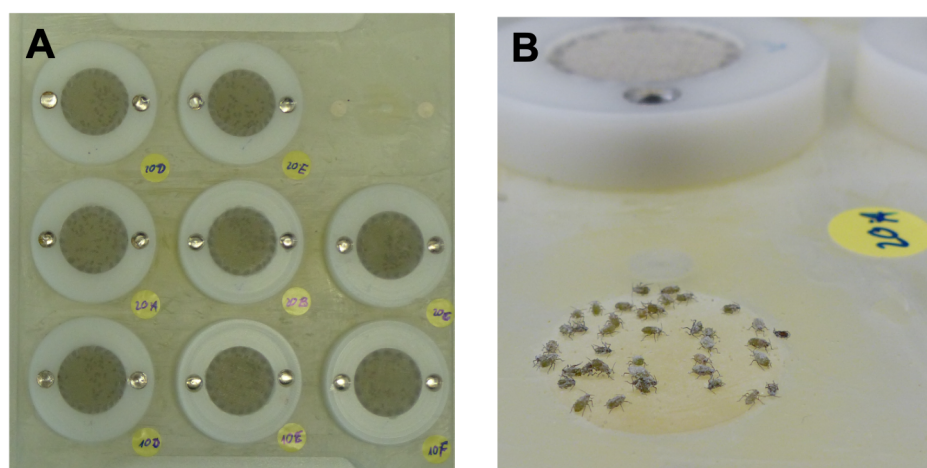


Figure 6: Setup of the feeding assay. Each plate has nine cages covered with mesh lids (A), *Brevicoryne brassicae* feeds on artificial diet provided through a parafilm membrane (B).

sucrose level were performed. Therefore, the 6-7 day old nymphs of all 27 cages were divided into 25 roughly same sized colonies. The colonies were placed on fresh setups supplying diets with 5%, 10%, 20%, 40% or 60% sucrose, respectively and 0.1% sinigrin. The cages were turned, so the aphids fed in an upside-down position and honeydew was allowed to fall into the cage lid. The next day, the cages were turned upside-up again and the winged aphids were removed. At day ten, the cages were cleaned and remaining aphids counted. Dead and winged aphids as well as deposits were removed and the cage lids replaced. After two days feeding on different sucrose levels, the honeydew was collected. The aphids were counted and removed carefully. Then, the outer parafilm membrane and cage lids were washed three times with 200 μ L milli-Q water at room temperature. The wash solutions were united in one pre-weighed Eppendorf tube each. The honeydew solutions were frozen with liquid nitrogen and freeze dried in an Alpha Christ LPH4 1-4 LDplus (Osterode am Harz, Germany) at 0.22 bar for 48 h. The tubes with dry honeydew were weighed and stored at -20°C prior to chemical analysis. For UHPLC-IM-MS measurements, 1 mg dried honeydew was resolved into 100 μ L mili-Q water (dilution 1:100) and transferred into 0.3 mL plastic vials (Macherey-Nagel GmbH&Co.KG, Düren, Germany).

3. Results

3.1. Method Development

For chromatographic analyses of saccharides, pre-established UHPLC methods for sugar separation were taken. Additives in the mobile phases were omitted and neutral chromatographic conditions chosen. This avoided changes in mobile phases performing measurements in negative and positive ionisation mode and thus, the RT in both modes were comparable.

To create an ion mobility library for saccharides, an IM-MS method was developed for timsTOF instrument based on software provided default settings for direct infusion of small molecules in negative ionisation. Aqueous solutions of glucose and sucrose were injected directly into the instrument and achieved sufficient peak intensities for sugar concentrations of 50 μM for glucose and 10 μM for sucrose.

TIMS was enabled, whereby the instrument offers three different resolution modes for mobility: survey, detect and ultra mode. To create one comprehensive method for all tested sugar standards and their adducts, the demanded mobility range was 0.5 - 1.5 $\text{V}\cdot\text{s}\cdot\text{cm}^{-2}$. This was only covered by the survey mode providing a mobility range of 0.4 - 1.8 $\text{V}\cdot\text{s}\cdot\text{cm}^{-2}$, a mass range of 50 - 1500 g/mol and a ramp time of 70.5 s. Ramp time is the time in which the specified mobility range is scanned, and was set automatically based on mobilities $1/K_{0,start}$ and $1/K_{0,end}$. The accumulation time of ions in the storage cell before entering the TIMS cell for mobility separation was the same as the ramp time to achieve a duty cycle of 100%. It should be considered that too long of an accumulation time results in overloading which could lead to peak broadening. The method was optimised for di- and oligosaccharide analyses by changing the instrument settings systematically. Values giving best peak intensities were taken. The method refrained from fragmentation, as the full scan mode uses a low collision energy, no isCID and no isolation in quadrupole.

The limit of detection for each analyte were not determined in this study. For calibration purposes, standard concentrations in the ranges of 0.01 - 1000 μM for di- and oligosaccharides or 1-1500 μM for monosaccharides, respectively were recorded and ion chromatograms extracted. From them, an estimated detection limit was derived as follows, for monosaccharides in general below 1 μM and for di- and oligosaccharides in general below 0.01 μM . The standards mannitol, gentiobiose, raffinose and kestose were detected at 0.02 μM and trehalulose at 0.5 μM onwards. Monomer peaks of 50 μM monosaccharides solutions were small or not detected and therefore the

mobility recording unreliable. Previously, good results for monosaccharide analysis were achieved using API5000 triple-quadrupole MS. For this reason, the dominant monosaccharides fructose and glucose were quantified there without recording the ion mobility, whereby the EIC gave a peak area 400 times higher than the timsTOF recordings.

3.2. Generation of CCS Library

Chromatography using an amine-functionalized HILIC stationary phase allowed a rough separation of all 47 tested sugar standards (12 mono-, 17 di-, 7 tri-, 3 tetra-, 1 penta-, 1 hexa-, 1 heptasaccharides, 5 sugar alcohols) (appendix A.1). The RT is dependent on the interaction of the analyte with the stationary phase. Regarding the molecule mass, smaller saccharide molecules generally elute earlier, while larger molecules have longer RT due to more hydroxyl groups involved in hydrophilic interactions. An overlay of chromatograms of all sugar standards shows clusters in dependence on their DP (Figure 7). Monosaccharides (m/z 150.13-182.17) eluted in a time range from 1.23 to 6.78 min and disaccharides (m/z 326.30-342.30) from 7.82 to 10.34 min, followed by trisaccharides (m/z 504.44) detected in a window from 9.65 to 11.05 min and tetrasaccharides (m/z 666.58) from 10.88 to 11.89 min. Hereinafter eluted maltopentaose at 13.07 min, maltohexaose at 13.96 min and maltoheptaose at 14.00-14.40 min (Table 5).

With simple chromatography the sugar class was estimated, whereby sugar alcohols conducted different than aldoses and ketoses. The disaccharide alcohol galactinol (RT = 10.34 min) eluted in the time window of trisaccharides (Table 5). Further, overlapping areas made a classification difficult. For example, the trisaccharide isomaltotriose (RT = 11.05 min) retained longer than the tetrasaccharide nystose (RT = 10.88 min) (Table IX).

To gain a next level of chemical analysis, UHPLC was coupled to MS. The second dimension of mass determination was added to the RT. This guaranteed the correct sugar classification despite overlapping elution areas, but did not help to identify the compounds specifically.

The disaccharide isomers trehalose, also named α, α -trehalose, α, β -trehalose, maltose, cellobiose and lactose have all the same mass and just differ in their composition, connection or configuration (Figure 8). Consequently, MS alone did not help to distinguish among them. Moreover, they were not chromatographically separable with the amine column (Figure 9 A), and thus a further analytical dimension was de-

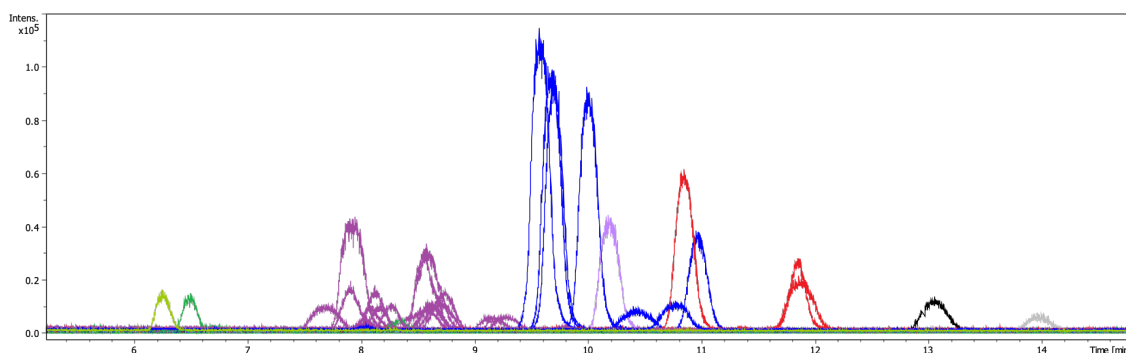


Figure 7: Overlaid chromatograms of sugar standards. Single sugar standards were separated via amine column: 12 mono- (green), 17 di- (violet), 7 tri- (blue), 3 tetra- (red), 1 penta-(black), 1 hexa- (grey), 1 heptasaccharides (not visible), 5 sugar alcohols (light green/violet). All chromatograms were overlaid forming clusters according to their degree of polymerisation. Overlapping peaks disabled a reliable separation of sugars by applying only UHPLC.

Table 5: Retention time ranges of saccharide classes.

Sugar class	Retention time [min]
Monosaccharides & -sugaralcohols	1.23 – 6.78
Disaccharides	7.82 – 9.37
Galactinol	10.34
Trisaccharides	9.65 – 11.05
Tetrasaccharides	10.88 – 11.89
Pentasaccharide	13.07
Hexasaccharide	13.96
Heptasaccharide	14.00 - 14.40

manded. Here, ion mobility offers the possibility to discriminate isobaric compounds with identical retention times with regards to structural variation of the molecules three dimensional size. The resulting mobilograms allowed separate detection of the isomers (Figure 9 F, K), whereby the deprotonated monomers in the second column (Figure 9 F-J) divided less than the deprotonated dimers shown in third column (Figure 9 K-O). Outstandingly, ion mobility allowed even baseline separation for the anomers trehalose/ α , β -trehalose and maltose/cellobiose (Figure 9 L, M), which were impossible to discriminate through the amine column (Figure 9 B,C).

Unfortunately, IM did not provide separation of all tested isomers. In contrast to the mentioned anomers, the compositional isomers cellobiose/lactose (Figure 9 D, I,

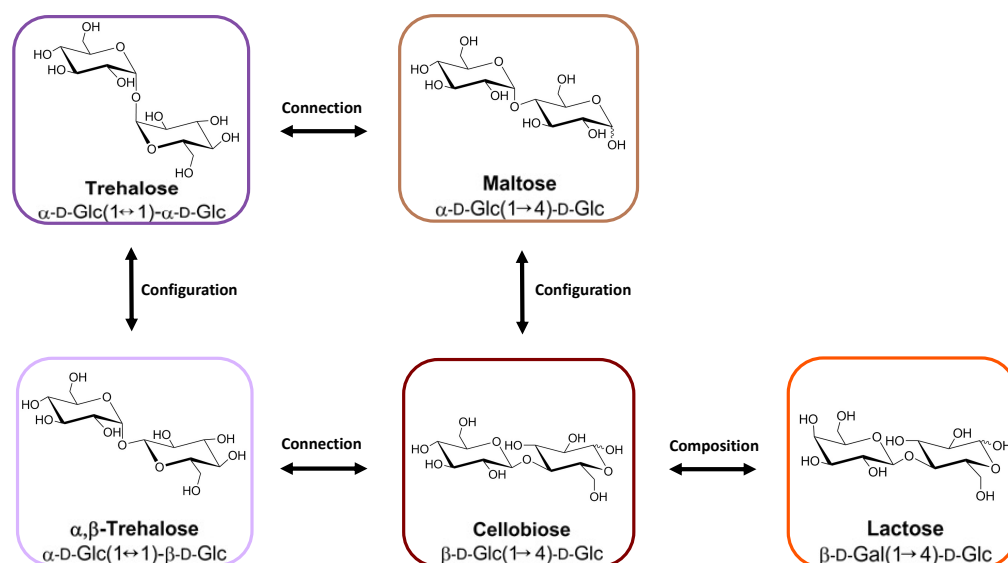


Figure 8: Disaccharide isomers. The disaccharides trehalose (violet), α , β -trehalose (light violet), maltose (brown), cellobiose (dark brown) and lactose (orange) differ in their composition, configuration or connection, respectively.

N) were neither differentiated by the amine column nor by their ion mobilities. To provide an additional discrimination method, a second chromatographic procedure was complemented using a PGC column. The stereo-selective surface consists of porous graphite and provides distinction of polar and closely related structures⁹². In contrast to the amine column (Figure 10 A-C), the isomers cellobiose/lactose (Figure 10 D) and kestose/erlose (Figure 10 F) gained baseline separation. Maltose and lactose still overlapped (Figure 10 B, E), but in turn, were able to distinguish by their mobility (Figure 9 O).

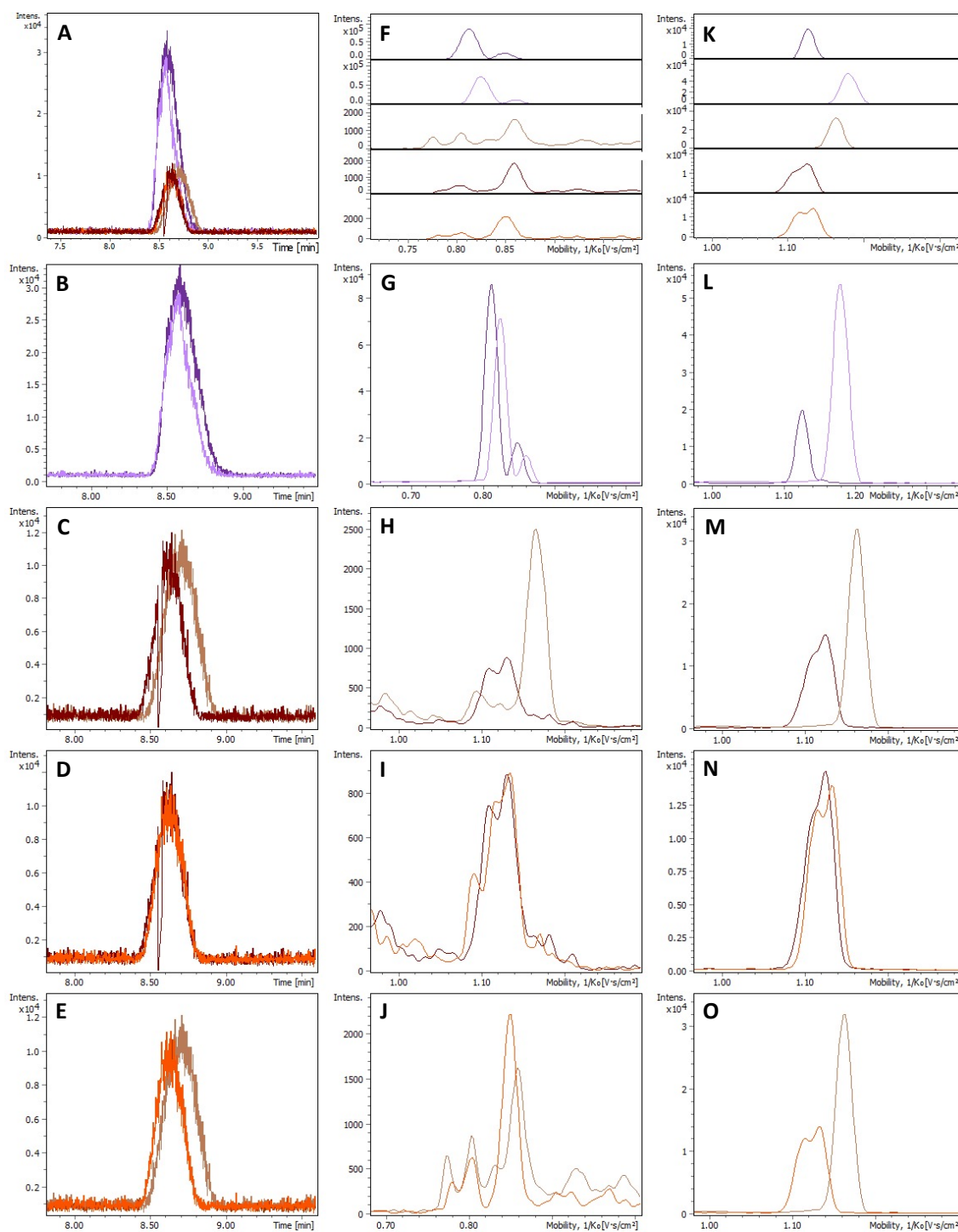


Figure 9: Chromatograms and mobilograms of selected isobaric disaccharides. Overlaid chromatograms of trehalose (violet), α,β -trehalose (light violet), maltose (brown), cellobiose (dark brown) and lactose (orange) are shown (A-E). Enhanced discrimination was gained by extraction of ion mobilograms of $[M-H]^-$ (F-J) and $[2M-H]^-$ (K-O).

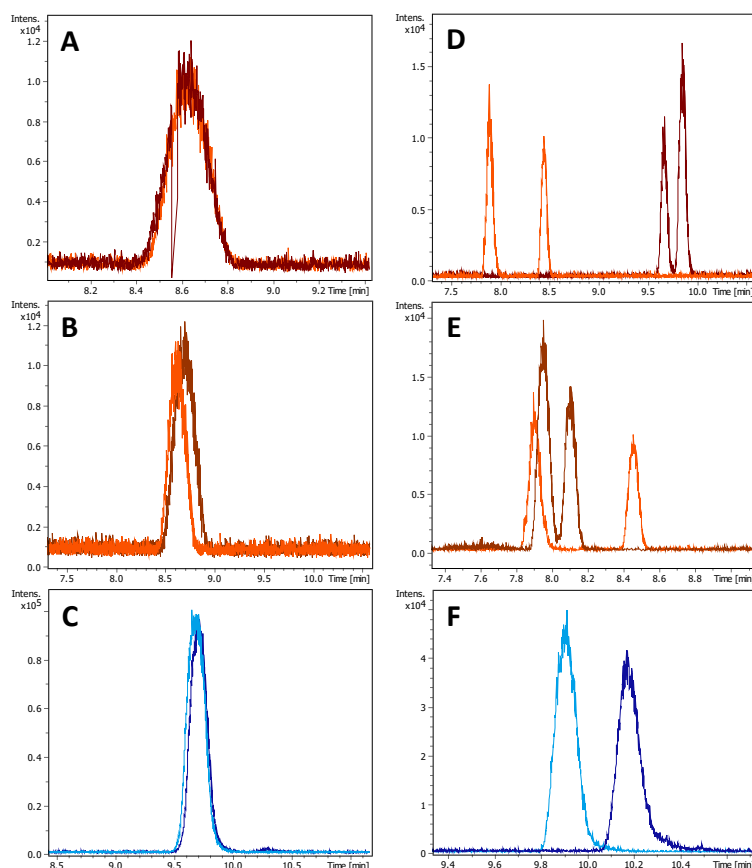


Figure 10: Chromatographic separation via two different columns. The isomers cellobiose (dark brown)/lactose (orange), maltose (brown)/lactose (orange) and erlose (blue)/kestose (light blue) show different separation behaviours in amine (A-C) and graphite column (D-F).

Figure 9 shows that IMS can be a possibility to separate isomers through mobility differences of the ion species $[M-H]^-$ (Figure 9 F), but in case of disaccharides, 11 of 16 tested disaccharide standards shared the mobility $1/K_0 = 0.805 \pm 0.002 \text{ V}\cdot\text{s}\cdot\text{cm}^{-2}$ for their deprotonated monomers (Table IX, Figure 11 A). As a potential solution to this problem, further ion species such as chloride and formate adducts $[M+Cl]^-$, $[M+HCOO]^-$ were included into the mobility library. In contrast to $[M-H]^-$ ions of multiple disaccharides (Figure 11 A), the mobilities of $[M+Cl]^-$ (B) distributed more and the $[2M-H]^-$ (C) the most. Besides negative ionisation mode, various ion mobilities were also recorded in positive mode in order to further add diagnostic signals for saccharides. The sodium adducts $[M+Na]^+$ and $[2M+Na]^+$ as well as the potassium adduct $[M+K]^+$ were considered and supported the compound identification providing additional indicators.

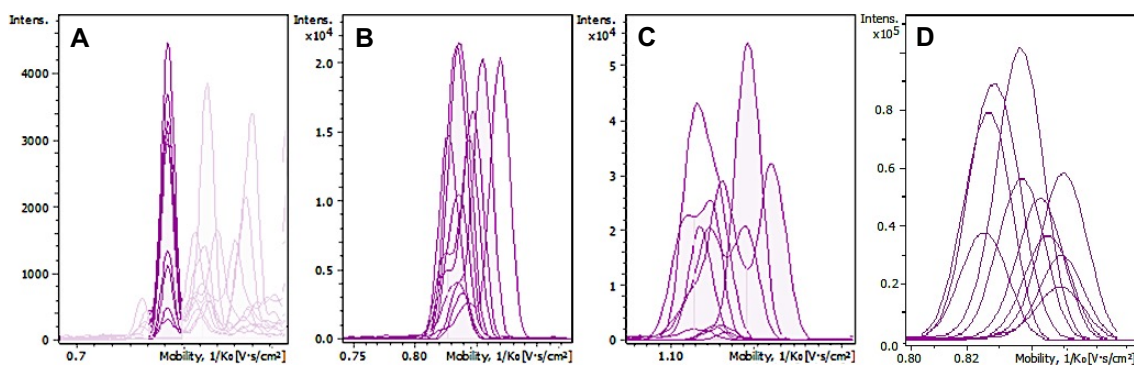


Figure 11: Disaccharide discrimination via ion mobility. 11 of 16 tested disaccharides had a mobility of $1/K_0=0.805\pm 0.002$ V·s·cm⁻² for their deprotonated monomer [M-H]⁻ (A), better separation was achieved for [M+Cl]⁻ (B), [2M-H]⁻ (C) or even [M+Na]⁺ (D).

To conclude, there was not one universal analytical parameter providing a discrimination of all 47 sugar standards. In order to provide a comprehensive library for a potential user, the mobility and CCS library presented here consists of the compound name, molecular weight, RT for amine and PGC column and mobilities for up to six different ion species plus/minus standard deviation of three technical replicates (appendix Table IX). For universal application and inter-laboratory comparison, the mobilities were transferred into CCS values using the Mason-Schamp equation.

3.3. CCS Patterns

Generally, the mobility depends on the molecular size of the ion in question. Higher molecule or ion sizes, respectively mean larger cross-sectional areas and thus higher CCS values. Larger structures experience a stronger push through the gas flow in the mobility cell, which in turn means that their mobility decreases. The mobilograms displayed within this work show the inverse reduced mobility $1/K_0$ on the horizontal axis versus the intensity on the vertical axis. Following this rationale, mobility peaks of larger ions with smaller mobility are shifted to the right (Figure 12).

In Figure 13, the mobilities of all tested sugar standards were plotted with respect to their mass. It is quite plain to see that the inverse reduced mobility of deprotonated single charged sugar monomers rises proportionally with the molecular weight.

The question arises however, if further molecule characterisation is possible through IMS, or can CCS and mobility patterns help with structural elucidation? As a preface, the IM-MS method employed in this study mainly focused on di- and oligosaccharides, as mobilities for monosaccharides were difficult to determine and

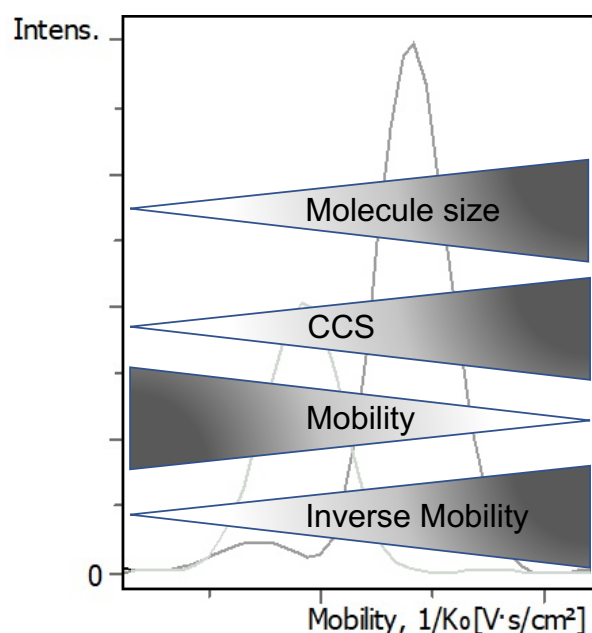


Figure 12: Schematic ion mobilogram. The mobilogram displays the inverse of reduced mobility $1/K_0$ on the horizontal axis. Rightwards, the size of the molecule and the collision cross section (CCS) increase with higher inverse mobility values whereby the ion mobility decreases.

not achieved for all tested monosaccharides. However, influences caused by saccharide composition, configuration or connection were indeed observed comparing mobility values of respective $[M+Cl]^-$ complexes.

At first, mobility can give information about the saccharide composition, for example whether a saccharide is constituted of a fructose or a glucose moiety. Regarding the building blocks of disaccharides, pairs of the composition fructose-glucose/glucose-glucose (fru-glc/glc-glc) were compared (Figure 14). The created database provided the pairs trehalulose/trehalose (Figure 14 A), turanose/nigerose (Figure 14 B), maltulose/maltose (Figure 14 C) and isomaltulose/isomaltose (Figure 14 D). In all considered cases, the disaccharides containing a fructose (light violet) rather than a glucose (violet) building block had higher mobilities, means smaller inverse mobilities (Figure 14, Table IX). Moreover, the trisaccharides maltotriose/erlose (Figure 14 E) confirmed this trend with the fructose containing erlose (light blue) having a lower inverse mobility than maltotriose (blue) consisting of three glucose building blocks.

On the other side, a differentiation between galactose and glucose moiety was not possible. Comparing the pairs lactose/cellobiose (Figure 14 F), lactose/maltose

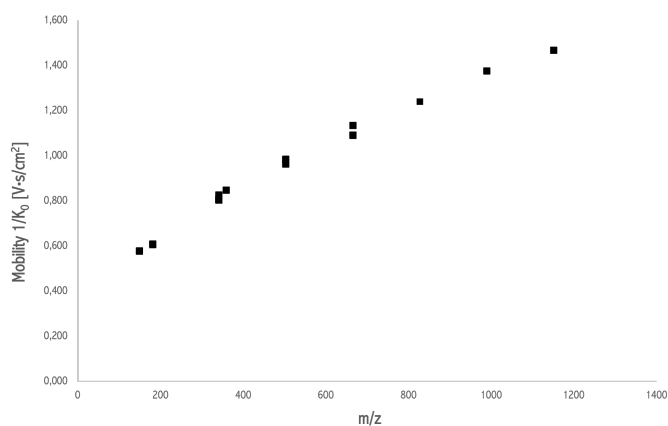


Figure 13: Plot of mobility as a function of m/z . Mobilities of single charged, deprotonated monomers in negative mode of sugar standards were recorded using timsTOF.

(Figure 14 G) and melibiose/isomaltose (Figure 14 H), the galactose containing lactose (orange) was more compact and mobile than cellobiose or maltose (brown), respectively. In contrast, melibiose had a smaller mobility and the peak was shifted more to the right than the glucose-compositional isomer isomaltose.

A final point, regarding the constitution, is that no trend was observed in dependence of reducing and non-reducing properties of the sugar.

Second, it might be obvious that the configuration influences the molecule structure and thus the mobility. However, comparing the anomers maltose/cellobiose, the trend in mobility was not so clear. In dependence on the ion species, the mobilities were almost the same for the deprotonated monomers and chloride adducts (Figure 15 A), but the deprotonated dimer of β -linked cellobiose had a higher mobility, than the α -configured maltose (appendix Table IX). For the pairs trehalose/ α, β -trehalose (Figure 15 B) and isomaltose/gentiobiose (Figure 15 C) the α -anomer had a higher mobility and was the more compact configuration.

A third structural property besides constitution and configuration is the connectivity of saccharide building blocks. The regioisomers trehalose/maltose (Figure 15 D), trehalulose/maltulose (Figure 15 E) and α, β -trehalose/cellobiose (Figure 15 F) were (1,1)- or (1,4)-linked, respectively, where the first two pairs showed lower mobilities if the building blocks were (1,1)-linked. However, the mobility relations of the last mentioned isomers were ambiguous and thus the trend adduct dependent. Moreover, isomers either (1,6)- or (1,4)-linked were compared represented by the pairs maltulose/isomaltulose (Figure 15 G) and maltose/isomaltose (Figure 15 H).

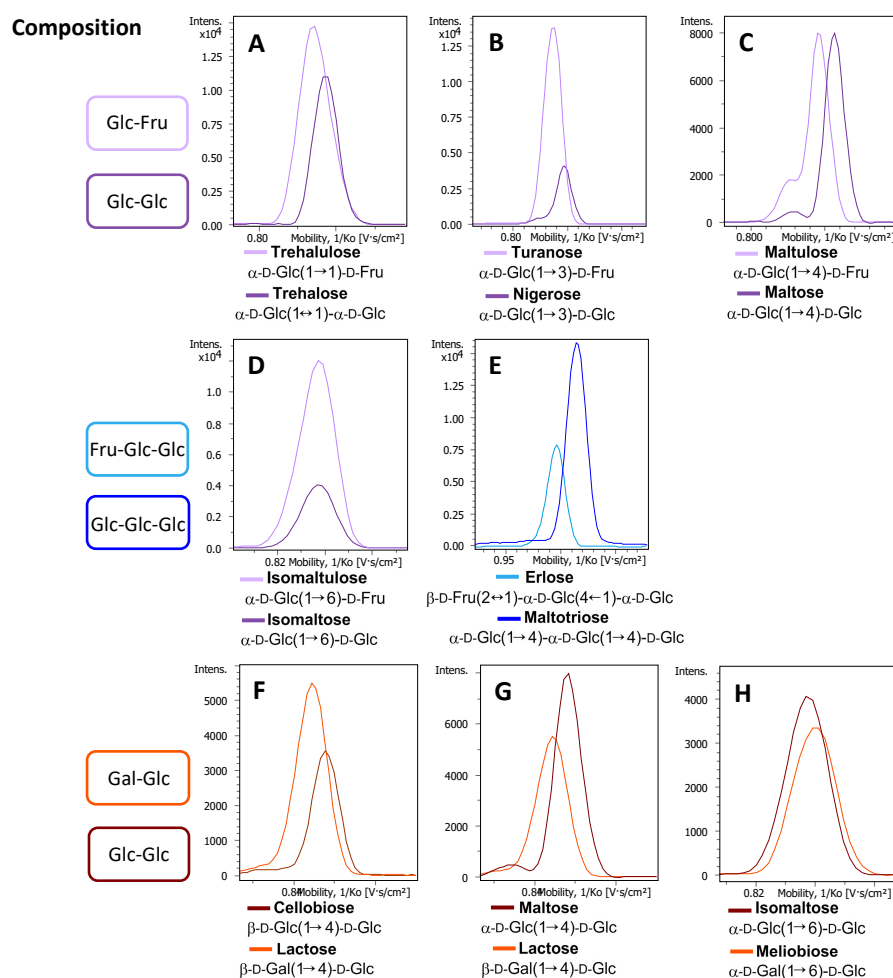


Figure 14: Mobility in dependence on composition. Overlaid mobilityograms of $[M+Cl]^-$ adducts allowed the discrimination of fructose than glucose containing disaccharides (A-C) and trisaccharides (D,E), but not galactose than glucose (F-H).

It was clear assigned that the (1,6)-linkage resulted in more compact structures than the (1,4)-bonded having lower inverse mobilities.

Besides comparison of (1,4)- and (1,1)- or (1,6)-linked isomers also the regioisomers with the structure $glc(1,x)-fru$ (trehalulose $x=1$, sucrose $x=2$, turanose $x=3$, maltulose $x=4$, leucrose $x=5$, isomaltulose $x=6$) were examined. The mobility pattern was adduct dependent. For the monomer ions, the mobility did not differ much (Figure 11 A). For the dimer and sodium adduct, the inverse mobility had the orders $[2M-H]^-$: $x=2, 3, 6, 1, 4, 5$ and $[M+Na]^+$: $x=5, 2, 3, 6, 1, 4$. The regioisomers with the structure $glc(1,x)-glc$ (trehalose $x=1$, nigerose $x=3$, maltose $x=4$, isomaltose $x=6$) had the pattern $[2M-H]^-$: $x=1, 6, 3, 4$ and $[M+Na]^+$: $x=1, 3, 6, 4$

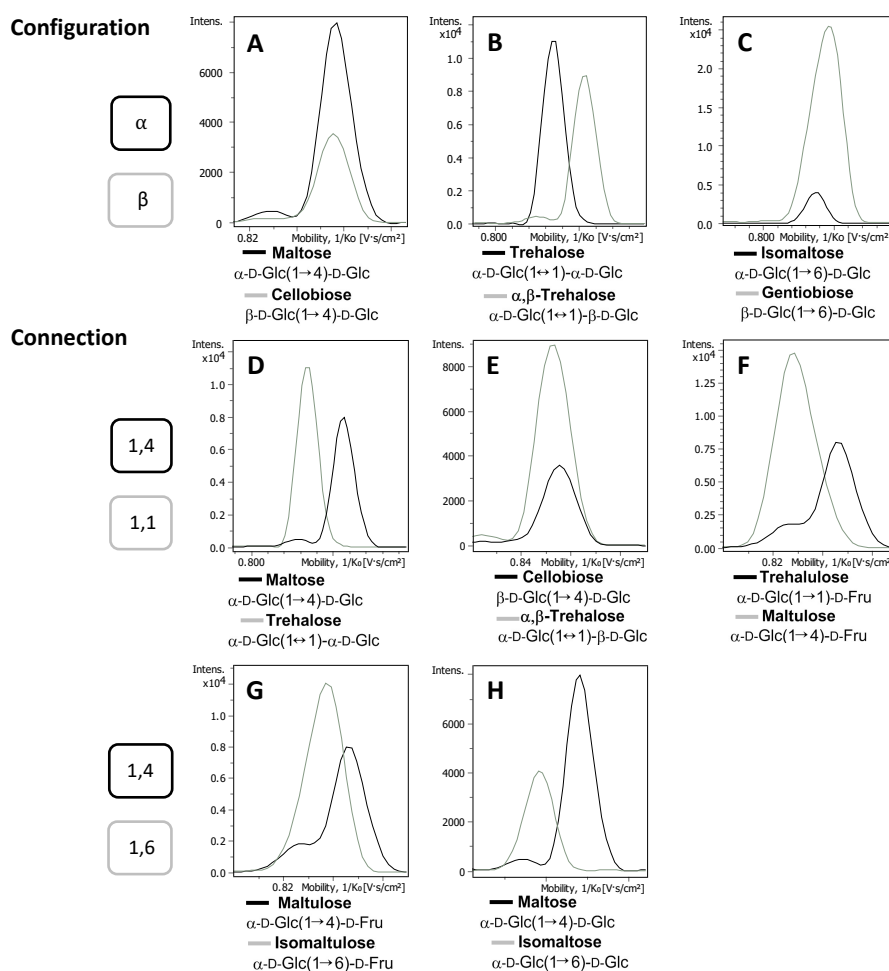


Figure 15: Mobility in dependence on linkage. Overlaid mobilograms of $[M+Cl]^-$ complexes allowed the discrimination of some anomers (B). Regioisomers differed in their mobilities, (1,4)-linked saccharides gave larger inverse mobilities than (1,1)- or (1,6)-linked, respectively.

or regarding the second mobility peak $[M+Na]^{+}$: $x = 3, 1, 6, 4$. Concluding, (1,1)- and (1,3)-linked building blocks resulted in more compact disaccharides than their (1,4)-bonded regioisomers. Moreover, the adduct influenced the mobility, pointing out that leucrose containing a (1,5)-glycosidic bond had the largest mobility of all compared regioisomers as deprotonated dimer, but the lowest as sodium complex. In negative mode the mobility of adduct followed the trend $[M-H]^- < [M+Cl]^- < [M+HCOO]^- < [2M-H]^-$, in contrast, complexes in positive mode did not show a consistent behaviour.

3.4. Application of CCS Library to Natural Samples

To further demonstrate the utility and application of our CCS library, UHPLC-IM-MS was applied for the analysis of sugars in selected biological samples. Phloem sap of *Z. mays* plants and aphid honeydew produced by *Z. mays*-fed *R. padi* and *S. avenae* aphids, as well as by artificial diet-fed *B. brassicae* aphids, were analysed with the presented methods. The treatments were performed in biological replicates ($n = 5-6$), the measurements in technical replicates ($n = 3$). The median of relative standard error within the artificial feeding experiment was 6.7%. For quantification, the peak areas were converted into absolute sugar concentrations in μM based on calibration curves. The median of relative standard error of peak areas based on timsTOF data was 8.9%. For better comparison between samples, relative compound concentrations were represented as percent, with the total of all quantified sugars in one sample was assumed to be 100%.

3.4.1. Maize Phloem Sap and Honeydew

Phloem sap of maize was obtained through stylectomy and analysed with UHPLC-IM-MS. In almost all samples sucrose was found as sole sugar independent of light cycle (Figure 16 A). Just one sample of maize plant grown under standard conditions contained additionally trehalose, while one sample kept dark for 48 h also contained trehalose, kestose and one unidentified tri- and one tetrasaccharide (Figure 16 B, appendix Table XI).

In contrast to the almost uniform and sucrose-dominated sugar composition of phloem sap, the mixed honeydews of maize feeding aphids *R. padi* and *S. avenae* contained various sugars. Applying the amine column for separation, 22 different compounds were detected from which 12 sugars were identified (Table XV). Monosaccharides made up the greatest portion of identified sugars with fructose (28%), glucose (10%) and mannitol (5%) (Figure 16 C). A lower proportion had disaccharides with sucrose (4%), trehalose (1%) and maltose (>1%) being identified and further erlose (3%), melezitose (1%) and unidentified trisaccharide (>1%) were found. Moreover, unspecified oligosaccharides remained with tetra- (19%), penta- (9%), hexa- (1%) and heptasaccharides (20%). Furthermore, mobility values suggested that maltulose, raffinose, stachyose and the malto-oligosaccharides were present in aphids honeydew as well (appendix Table XV).

Aphids as phloem-feeding insects mainly hydrolyse and incorporate sucrose through their diet and excrete honeydew consisting of a blend of multiple saccharides. It

can be derived that aphids or endosymbiotic bacteria have the enzymatic capacity to transform sucrose into various saccharides. On the one hand, sucrose was cleaved into its constituents fructose and glucose. On the other hand, further monosaccharide building blocks were added to sucrose. An addition of glucose via (1,3)-linkage resulted in melezitose, fructose in (1,4)-linkage resulted in erlose. A galactose linked in (1,6)-position to sucrose led to raffinose with a second galactose unit to stachyose. Moreover, glucose and fructose were isomerised and reconnected by a (1,4)-linkage resulting in maltulose, whereby reassembling glucose units in the same manner formed maltose and in repetitive chain malto-oligosaccharides.

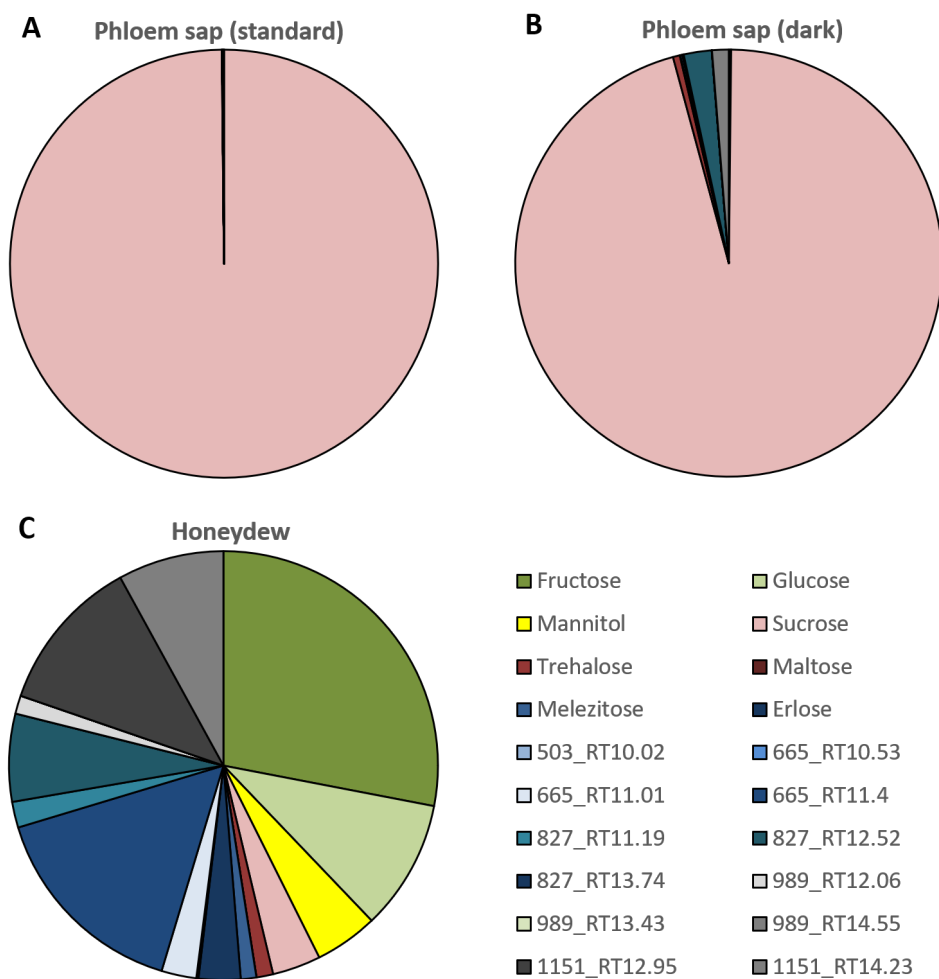


Figure 16: Sugar composition of maize phloem sap and aphid honeydew. The pie charts show relative saccharide proportions in phloem sap of *Zea mays* grown under standard conditions (A) and kept dark for 48 h prior to collection (B), as well as honeydew composition of maize fed aphids *Rhopalosiphum padi* and *Sitobion avenae* (C).

3.4.2. Sucrose Feeding Experiment

Once more, the created saccharide library was applied to identify insect saccharides in aphid honeydew. With this experiment the impact of dietary sucrose levels on aphid honeydew composition was investigated, having this goal, *B. brassicae* was fed with artificial diet where the sucrose concentrations were adjusted to 5%, 10%, 20%, 40% or 60%, respectively.

Runs with the amine column showed 40 peaks of which 15 could be assigned applying the created mobility library of sugar standards, whereby the PGC column showed

34 peaks of which 8 sugars were identified (Figure 17, appendix Table XVII).

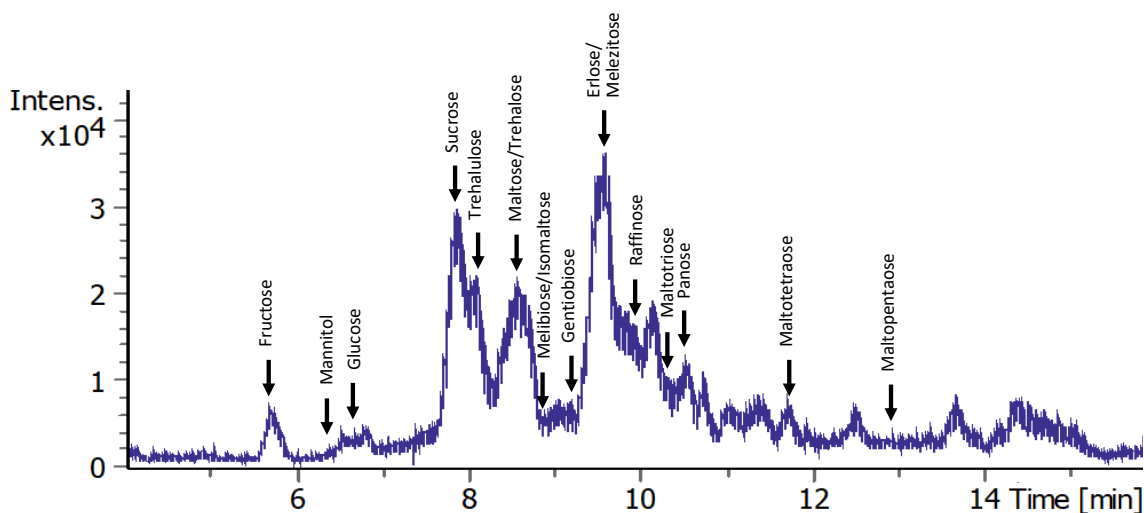


Figure 17: Chromatographic separation of aphid honeydew. The chromatographic amine column was utilised to separate honeydew of *Brevicoryne brassicae* fed on 40% sucrose level, the dried honeydew was diluted 1:100. The peaks were assigned with aid of saccharide standards by comparing retention times and ion mobility values.

Qualitatively, the honeydew was composed of the monosaccharides fructose, mannitol and glucose. As disaccharides sucrose, trehalose, trehalulose, maltose and gentiobiose were found whereby melibiose as well as isomaltose were identified with some level of ambiguity, since the two recorded mobility values were in accordance with both compounds. The assigned trisaccharides were melezitose, erlose, raffinose, maltotriose and panose. Furthermore, representative larger order saccharides maltotetraose and -pentaose were present as well. Saccharides of higher polymerisation grade were not included in the method and thus not detected. The graphite column runs provided even further support for the assignment of sucrose, trehalose, maltose, gentiobiose, melezitose, erlose and raffinose.

The compounds were roughly identified regarding the RT, with more accurate confirmation based upon comparison of mobilities. Here, EIM of the ion species $[M-H]^-$, $[M+Cl]^-$, $[M+HCOO]^-$, $[2M-H]^-$, $[M+Na]^+$, $[M+K]^+$ and $[2M+Na]^+$ were considered if detectable. The assignment of three monosaccharide peaks eluting in advance of fructose was not possible, however their detection is noted. The vast amount of included disaccharide standards permitted the identification of all but two disaccharide peaks (Figure 17). Five of eight detected trisaccharides were identified. The

largest void in the created library were saccharides of higher polymerization grade, mainly due their availability as standards. Only one tetra- and one pentasaccharide could be named. Moreover, the detection of hexasaccharides and larger molecules was constrained by the method and ability to separate these large sugar polymers on an HPLC system alone.

One of the largest advantages of applying ion mobility for the analysis of complex mixtures is the ability to identify overlapping saccharides in HPLC separation. For example, the separation of honeydew by the amine column displayed one peak at 8.57 min (Figure 18 A). In a further step, ion mobilograms were extracted showing a second peak (Figure 18 B). This indicated the presence of one compound in different structural constitutions or elution of more than one compound with same RT. Considering the mobilities of all ion species, the regioisomers maltose and trehalose were identified by comparison to their pure standards.

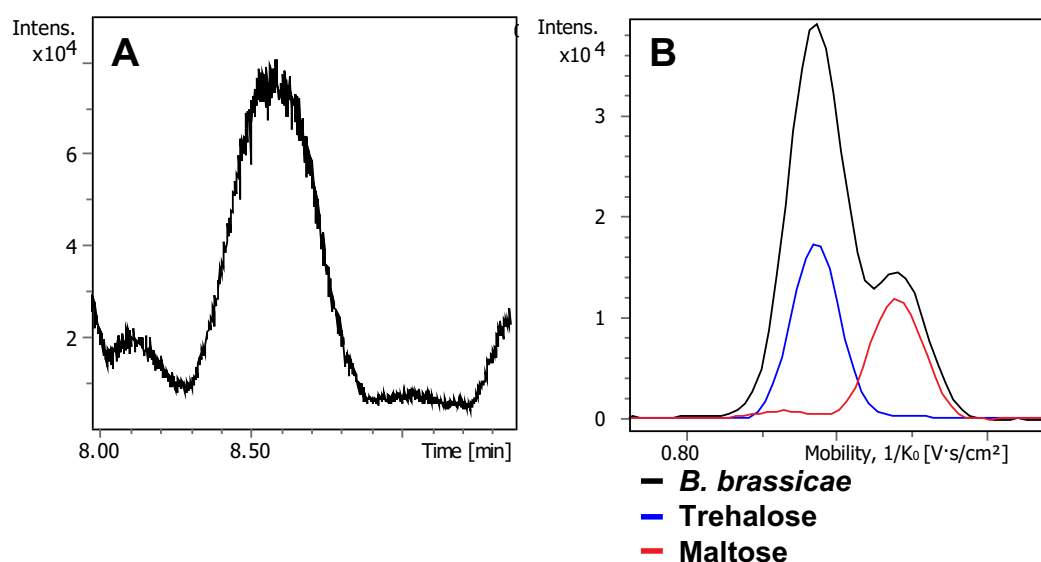


Figure 18: Extracted ion mobility aids in compound identification.

The chromatogram of *Brevicoryne brassicae* showed a single peak at 8.57 min (A). The extraction of the ion mobilogram (m/z 377.085) showed indeed overlapping compound peaks (black), which were assigned to trehalose (blue) and maltose (red) through comparisons with saccharides standards (B).

In general, the sugar profile of honeydew was not qualitatively changed after feeding on different sucrose levels with only a few exceptions observed. One monosaccharide peak at 3.39 min was present at 5% and 10% sucrose, but not at higher levels. In contrast, three unidentified oligosaccharides only appeared at 40% and 60% sucrose

(RT 10.14 min (NH₂), 12.24 min (NH₂), 13.48 min (PGC)) (data not shown).

To sum up the qualitative analysis, the created library was successfully applied to honeydew samples of *B. brassicae*.

The next section deals with the aphid survival rate and quantitative honeydew composition. The aphids in each treatment were counted at the beginning and end of the experiment, and from that, the survival rates ($n^{\circ}_{end}/n^{\circ}_{start}$) were calculated (Table 6). Aphids feeding on diet with 10% sucrose survived the best whereby 60% was the worst. In addition to this level of fitness, the amount of collected honeydew per average aphid number was determined for each treatment, where it was observed that the honeydew production raised with increasing dietary sucrose level.

Table 6: Fitness of *Brevicoryne brassicae*.

Sucrose level	Survival rate	dry weight of honeydew [mg/aphid]
5%	69.4%	0.05
10%	79.1%	0.05
20%	58.3%	0.09
40%	73.0%	0.12
60%	55.6%	0.17

In general, monosaccharides constantly had the greatest proportion in honeydew, followed by disaccharides. From this point, however, the composition diverged as oligosaccharides ranked according to their chain length, with decreasing polymerization grade the observed proportion in the honeydew also decreased ($7 > 6 > 5 > 4 = 3$) (Figure 19).

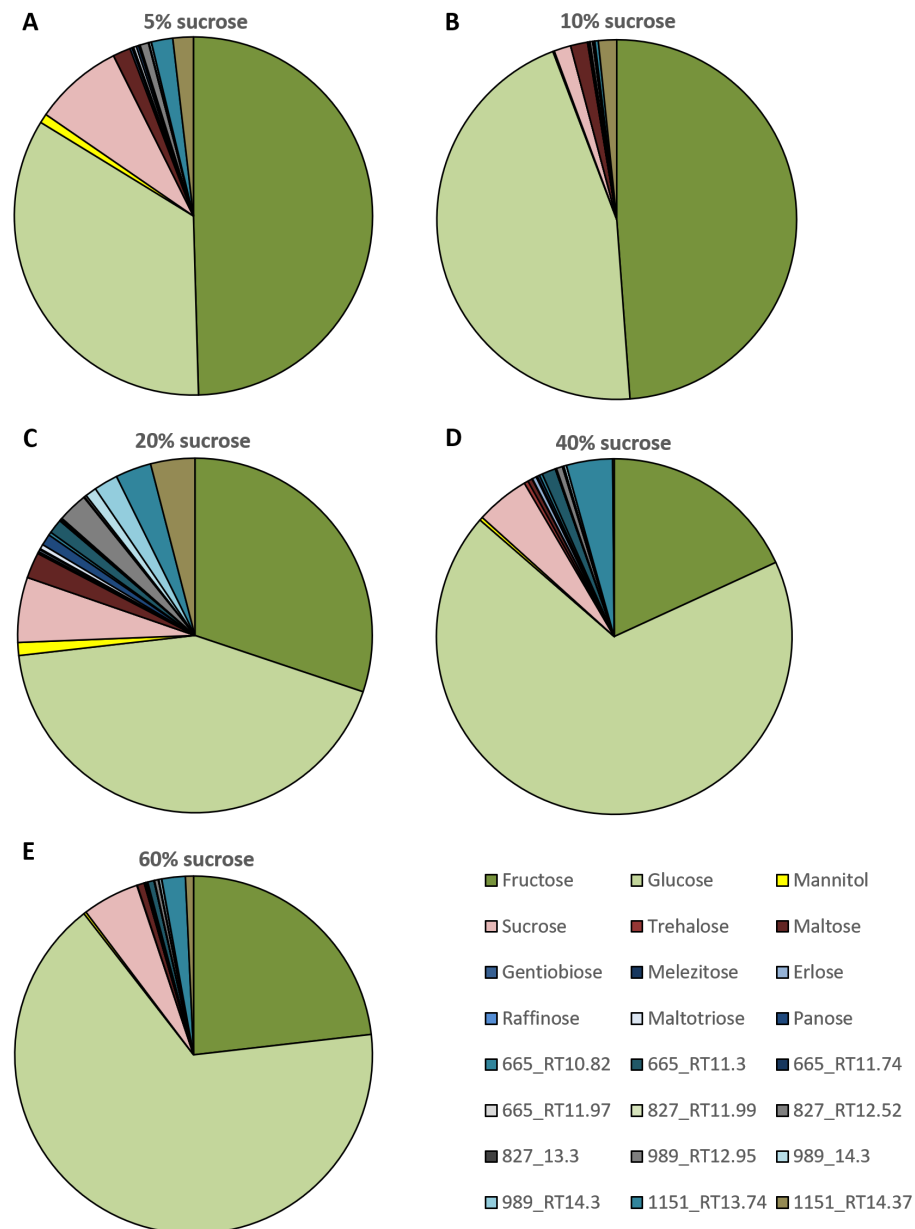


Figure 19: Sugar composition honeydew of *Brevicoryne brassicae*. Pie charts show the honeydew composition after the artificial feeding experiment. The aphids were supplied with diet containing following sucrose levels: 5% (A), 10% (B), 20% (C), 40% (D) and 60% (E).

Comparing the honeydew composition quantitatively, changes related to dietary sucrose level were observed. Regarding monosaccharides, the highest proportion was reached at 10% sucrose level amounting 94% of the total honeydew sugar, whereby all other saccharides had their lowest concentration at this sucrose level. In this treatment the relation of fructose and glucose was balanced. At 5% the honeydew

composed of more fructose than glucose (Figure 20). At high sucrose levels, this relation changed accompanied by a 3.8-fold glucose concentration increase. Fructose was high at low sucrose level and decreased with raising dietary sucrose, with glucose levels behaving contrarily. Besides fructose, also disaccharides had their maximum at sucrose level of 5% amounting to 9.8% of the total honeydew. Sucrose was the most dominant disaccharide in honeydew, whereby the proportion in tendency decreased with increasing sucrose level with a minimum at 10% dietary sucrose. The most oligosaccharides were produced at 20% dietary sucrose level amounting 17.2% of the total sugar blend. Identified oligosaccharides were panose (1.0%), maltotriose (0.4%), erlose (0.2%), melezitose (0.1%) and raffinose (0.1%). From this derived, the oligosaccharide building blocks were first of all glucose, then fructose and rarest galactose units (47:6:1).

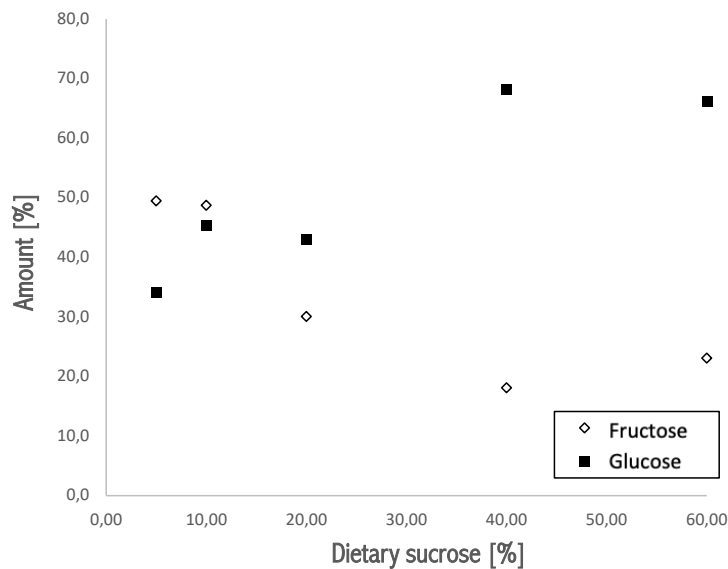


Figure 20: Fructose and glucose level in honeydew. Concentration of dominating monosaccharides fructose and glucose in dependence on dietary sucrose levels in honeydew of *Brevicoryne brassicae*.

4. Discussion

In this study, an ion mobility library for saccharides of different compositions and oligomerisation degrees was generated. Its application, firstly, gave further insights into aphid saccharide metabolism and, secondly, demonstrated the advantages of an ion mobility separation for saccharide analysis. The first time reported, phloem sap as well as honeydew of plant and artificial fed aphids were analysed by UHPLC-IM-MS which will be discussed, in turn, under revision of the literature. Additionally, the method as well as observed relations of ion mobility and molecular structure will be examined and finalised with suggested improvements and applications to the aforementioned method.

4.1. Saccharide Identification in Plant and Insect Samples

In the first experiment, the generated ion mobility library was applied and allowed the identification of up to three sugars in maize phloem sap and of 12 sugars in honeydew of maize-feeding aphids. The phloem sap was obtained through stylectomy providing low sample volume of only nL. The low quantity complicated the analyses and required a high dilution, which had a negative impact on compound detection as far as some compound concentrations remained below detection limit. On the other hand, stylectomy is to date one of the best methods to achieve pure phloem sap in which sample contaminations are avoided, and a real picture of phloem sap composition is obtained. In *Z. mays* (Poaceae) sucrose was, besides traces of trehalose, the sole sugar in maize phloem when grown under standard conditions. Many more plant families have been reported to compose of sucrose as the only detected sugar in phloem sap (e.g. Fabacea). According to Ziegler 1975, these plants belong to the first main type of sugar composition in the sieve-tube sap in which sucrose is predominant besides low concentrations of sugars of raffinose type¹⁰. Even though trehalose has another structure than raffinose, it is a non-reducing sugar and therefore a probable transport sugar in plants.

A secondary treatment kept plants in dark for 48 h before phloem sap collection. In these samples again sucrose was dominant, but additionally kestose and trehalose were observed. Under certain conditions, as darkness or low carbon dioxide concentration, photosynthesis is inhibited. In these cases, nutrients and sucrose are provided by accessing specific pools for translocation⁹³. The change of supply may lead to varied phloem sap compositions at different growing conditions, as was ob-

served here. However, the uptake of nutrients by aphids depends on the feeding plant, whether the xylem is broached and other factors such as light or water supply¹⁰.

Comparing phloem sap and aphid honeydew - the in- and output of aphids - it can be concluded that aphids or their associated bacteria transform the ingested sucrose to a blend of mono-, di- and oligosaccharides.

Since plant raised aphids are subjected to dietary changes, an artificial set-up with chemically defined diets provided further insights into aphid metabolism. Here, *B. brassicae* was fed with different sucrose levels. UHPLC-IM-MS analyses of honeydew achieved an identification of 15 sugars. The honeydew produced by *R. padi*, *S. avenae* (both plant fed) and *B. brassicae* (artificial diet fed) showed similar sugar profiles. In all aphid honeydew samples were 12 common compounds (fructose, glucose, mannitol, sucrose, trehalose, maltose, melezitose, maltotriose, erlose, raffinose, stachyose, maltotetraose). The maize aphids excreted further maltulose and maltohexaose whereby in the honeydew of cabbage aphid gentiobiose, melibiose, trehalulose and panose were detected.

Many previous studies investigated honeydew composition for various different aphid species, however, these results are not transferable to *R. padi*, *S. avenae* and *B. brassicae* since honeydew production varies between species, with many unusual species-specific sugars having been characterized in honeydews from different species^{21,39,43,94}. Some other sugars were just reported punctually as trehalulose and bemisiose being found predominantly in whitefly honeydew^{22,25}. In scale insects *Stigmacoccus* stigmatriose, - tetraose and - pentaose were uniquely reported⁹⁵. These oligosaccharides are composed of subsequent glucose unit(s) linked in (1,4)-position to the glucose of sucrose. Because standards of unusual saccharides are not commercially available, they have not been included into the ion mobility library reported here.

Nevertheless, in general a great intersection of honeydew compounds stated here and in literature exists, with frequently reported saccharides being fructose, glucose, sucrose, maltose, melezitose, raffinose^{13,21,27,94} and further erlose^{31,43,96} and stachyose^{19,30}.

It has been suggested to divide honeydew into erlose and melezitose type³⁴, but this is rebutted by the herein reported detection of both trisaccharides in honeydew using our analytical methods. Despite simultaneous elution from the amine column, great benefit was gained by the additional separation through the graphite column and the proofed identification based on mobility values.

Regarding the methods, Fischer and Shingleton (2001) applied HPLC coupled to an electrochemical detector (EIC) and identified a broader spectrum of monosaccharides including arabinose, xylose and rhamnose³⁰. This method did not cover sugar alcohols or many oligosaccharides. Complementarily, Neerbos et al. used the same analytical instrumentation to identify sorbitol and mannitol in addition to mono and disaccharides⁹⁴. An HILIC-MS method was recently developed for fast analysis with a 7 min chromatographic run time, but just covered three mono and four disaccharides²⁷. A broader analytical spectrum of 17 sugars has been provided by Shaaban et al. using an HPLC with anion exchange column and pulse amperometric detection. Honeydew of *Physokermes* and *Cinara* aphids were analysed and a total of eight sugars identified. Unfortunately, 1-kestose could not be detected reliably with this method, since it overlapped with nigerose and stachyose⁴³.

Just recently, another ion mobility method for saccharide analyses was published by Przybylski and Bonnet (2021) using ESI-TIMS in positive mode³⁷. They created a library of 13 isomeric trisaccharides to support quality control of honey. Comparing with the here presented methods, at least 12 sugars were identified in honeydew samples and a differentiation and identification of the aforementioned saccharides was possible using IM-MS.

To conclude, the generated ion mobility library with three analytical dimensions and multiple recorded ion species in positive and negative ionisation mode provided a profound sugar identification in biological samples. Its application of the generated ion mobility library allowed higher dimensional analysis of sugars than traditional methods. Nevertheless, many honeydew sugars remain unknown and require the inclusion of further oligosaccharide standards or improved structure elucidation.

4.1.1. Influence of Dietary Sucrose Content

At this point it will be refrained from further comparisons of divergent methods and aphid species. Following, the artificial feeding experiment will be discussed in which the sucrose concentration in diet was manipulated. First of all, the survival rate of artificial diet-fed aphids was dependent on sucrose levels in the diet. The aphid *B. brassicae* showed the highest survival rate on 10% sucrose followed by 40% and performing worst at 60% being consistent with literature reports that certain sucrose levels have a negative impact on the aphid's fitness^{19,97}. In one study, highest survivorship was reported for 1.0 M (34.2%) sucrose and lowest for 1.5 M (52.3%), which was the highest concentration tested in the referring study¹⁹. Developers

of artificial diet recommended a sucrose concentration of 20-35% for optimal sugar supply^{90,98}. Consistent to our finding is the negative influence of high sucrose levels on aphid performance, although the best sucrose level was not identical. Besides manipulation of the diet, the survival rate in this study may be influenced by the fact that cages were turned up-side down after aphid transfer. This could have made it difficult for the aphids to find the diet and could be solved by establishment of a settling period of about one day before turning the cages. Generally, *B. brassicae* are generalist feeding aphids feeding on various plants of the cabbage family indicating a higher tolerance towards phloem sap compositions⁹⁹.

As second result, we observed that the amounts of excreted honeydew were dependent on dietary sucrose levels. The determination that a higher dietary sucrose level led to enhanced honeydew excretion is consistent with other reports^{32,100}. This supports the assumption that honeydew at least in part represents voided nutrients which may not be needed for aphid nutrition and function.

Moreover, the honeydew composition was changed with dietary sucrose level. The data showed steady monosaccharide concentration in honeydew displayed a maximum at 10% and minimum at 20% sucrose concentrations. Conversely, all other saccharides showed a minimum at 10%. Moreover, disaccharides in honeydew generally decreased with increasing dietary sucrose, whereby oligosaccharide values fluctuated and raised to an extreme maximum at 20%.

The literature reported that aphids feeding on a diet with low sucrose concentration produce honeydew rich in monosaccharides and sucrose, whereby a high concentrated diet leads to predominant oligosaccharide production^{13,15,17,19,32,39}. To remember, the formation of higher saccharides is attributed to osmoregulatory effects, where reducing the molarity avoids water loss from insect's body fluid to the gut resulting that the honeydew voided from the insect is isoosmotic with its haemolymph^{13,14,17}.

In accordance is the honeydew composition achieved at 5% sucrose level, where the honeydew of *B. brassicae* consisted of mainly monosaccharides and the sucrose proportion in honeydew reaches maximal values. In conflict with literature are saccharide proportions at higher dietary sucrose. In this experiment, the oligosaccharide level remained continuously low in comparison to monosaccharides. The high proportion of monosaccharides at high sucrose levels could be attributed to the need of reducing the viscosity of the diet to achieve sufficient ingestion rates¹¹. However, the decrease of detected oligosaccharides at sucrose levels higher than 20% could be

due the presence of even higher oligosaccharides ($DP \geq 8$), which may be expected to form at very high osmotic pressure, were not detected by the limited mass range of our method. Furthermore, it might also be stated that different quantification methods were used in this study for monosaccharide analyses than for di- and oligosaccharides. In principle, the absolute concentrations in samples were observed by comparisons with calibration curves. Therefore, the quantitative values should be comparable independent of the method. But, as discussed later, the quantification with tims-TOF did not achieve satisfactory results regarding reliability. The median of standard error was 8.9% that means the recorded concentrations could vary by an order of magnitude.

Focusing on the formation of honeydew components it can be presumed that detected saccharides, besides sucrose, originate from metabolism by aphids and are neither present in the ingested diet nor produced by associates. The first statement is supported by the chemically defined preparation of diet including sucrose as sole sugar, while the second statement is founded by the observation that antibiotic-treated and untreated aphids by Wilkinson et al. showed no major differences in the saccharides detected in the honeydew¹⁵.

4.1.2. Sucrose Modifications

The cleavage of sucrose into its constituents led to high fructose and glucose concentrations in aphid excreta. With raising dietary sucrose, the values showed reduced fructose occurrence coupled to simultaneous increase of glucose proportion from 34.2% to 68.2% in terms of molar concentration of the total sugar content in honeydew. An earlier analysis of *B. brevicoryne* states the finding of much glucose and some fructose in honeydew samples¹⁰¹. Occurrence of glucose in the same scale was reported for *B. tabaci*, where this monosaccharide represented up to 60% of the honeydew sugars¹⁰². Otherwise, for different aphid species it was reported that fructose is typically more abundant than glucose^{13,19,43}.

The current literature describes an enzyme with both α -glucosidase (sucrase) as well as transglucosidase activity as responsible for some of the transformations among different saccharides^{14,16}. Its first name reflects cleavage of sucrose to fructose and glucose, whereby the second is due to its involvement in the formation of oligosaccharides in the presence of an excess of the substrate sucrose¹⁶. Ashford et al. investigated the metabolism of sucrose by aphid gut homogenates of *A. pisum* in which they characterized the enzymatic activities fitting to a substrate inhibition model¹³.

The observed inhibition of glucose production at high sucrose levels might be due to a single enzyme mediating both sucrose hydrolysis and glucose-based oligosaccharide synthesis¹³. The decreasing glucose production and simultaneous fructose increase reported in Ashford et al. are contrary to our values, but as they observed extracted guts, the entire metabolism and assimilation of living aphids were neglected, in particular, the absorption of fructose, which is utilised preferentially over glucose as the primary metabolite in respiration¹³. The relation of respiration and diet is difficult to predict and while feeding through artificial membrane is presumed to be more stressful than feeding on plants, no relations were observed between respiration rate and dietary sucrose level in previous reports^{41,39}.

The formation of oligosaccharides has been reported to increase at a certain sucrose level where observations of *A. pisum* defined 0.5 M (17.1%) or rather 15% as lowest sucrose concentration for oligosaccharide synthesis, which is remarkably similar to the here observed sharp increase of oligosaccharide proportion at 20% fed sucrose^{15,17}.

The broad blend of oligosaccharides detected in honeydew samples indicated diverse enzymatic activities for the modification of sucrose. Many identified trisaccharides were synthesised from fructose, glucose or galactose moieties linked to sucrose by introduction of (1,3)- (melezitose), (1,4)- (erlose) as well as (1,6)-glycosidic linkages (raffinose). Moreover, the monosaccharides were reconnected by α -(1,4)-linkages to maltose-oligosaccharides or maltulose. In the trisaccharide panose, glucose units were bonded through a (1,4)- and further a (1,6)-linkage. Also, the rather uncommon α -(1,1)- or β -(1,6)-linkages were detected in products such as trehalulose or gentiobiose, respectively. It should be said that this composition was stated for only the identified compounds where sugar standards have been available. However, the variety of sugar addition may be even greater. Along this line of thought, the analyses of honeydew showed several additional unidentified saccharide peaks, which in a few cases only appeared at high dietary sucrose concentrations. Perhaps the higher concentrations of sucrose may allow the catalysis of rather minute reactions by sheer availability of acceptor molecules for transglucosidation.

Ashford et al. considered that all oligosaccharides consist of only glucose¹³. Here we were able to show that *B. brassicae* as well as *R. padi* and *S. avenae* produced oligosaccharides by glucose as well as galactose transfer such as melezitose, erlose and stachyose, respectively. Nevertheless, glucose units dominate the oligosaccharides in form of panose or malto-saccharides. Moreover, the modification of sucrose is com-

mon for phloem feeders in general, whereby the honeydew profiles differ, such as the trehalulose rich honeydew excreted by whiteflies^{22,23,103,104,105,106}. The disaccharide modification in inter alia *B. argentifolii* from (2,1)-linked sucrose to (1,1)-linked trehalulose at high dietary sucrose levels may be favourable due to the fact that the resulting isomer is less or non-hydrolysable to numerous glycosidases¹⁰⁴. Further, whiteflies and aphids differ in their polyol synthesis, where sorbitol has been reported to be present in whiteflies while this study detected mannitol in aphid honeydew in accordance with previous reports^{94,107}. The polyol synthesis uses fructose as substrate and is stimulated by elevated temperatures¹⁰⁷. In 2003, compositions of different hemipteran were compared, in which only a few saccharides were reported for *B. brassicae*¹⁰³, while in this study a plethora of saccharides were identified. This huge difference in compound detection is attributed to different analytical methods being the key for elucidation of biological mixtures. So far, few reports appear to have been published based on modern analytical techniques²⁷.

4.2. Mobility and CCS Library

Here, the state-to-the-art technique UHPLC-IM-MS was used to create an ion mobility library of 47 saccharide standards with 250 mobility or rather CCS values. The utility was demonstrated, as already discussed, by application on biological samples and allowed the satisfying identification of insect saccharides.

The first analytical dimension was gained through chromatographic RT, which changed during the timespan of analytical performance. The shift was greater in the amine than graphite column, which could be related to more frequent application, and is expected for the operation of most amine columns. After months of continuous analysis, the standards eluted around 0.15 min earlier from the amine column than initially recorded, requiring repeated injection of selected standards during new batches of analyses. However, the chromatographic separation allowed a good discrimination between many of the compounds being analysed. Previous reports applied HPLC methods with effective resolutions, but also less compounds were considered^{27,30}.

For peak assignment, primarily the amine column was used, with secondary support from PGC data. The reasons were first, the amine column was more well-established in saccharide analysis and second, the graphite column often resulted in double peaks for many compounds, especially reducing sugars. Reducing structures are known to switch between conformations in hour timescales, resulting in mixtures that could

be separated by this method and complicated the peak assignment. Furthermore, the automated quantAnalyses software did not consider two peaks simultaneously for peak area calculation which was the reason to do not include PGC runs into the quantitative analyses.

The second analytical dimension was provided by high resolution MS, which gave reliable accurate masses based on a calibration segment before each run. As outlined above, however, the large number of isobars required a third dimension of separation.

The ion mobility was calibrated internally as well and the values were constant over the last year and therefore, the inclusion of mobility data into saccharide analyses allowed a differentiated and reliable compound identification method. Moreover, the calculation of inter-instrumental CCS values raises the worth of the library generated herein for application in other laboratory settings. Unfortunately, for monosaccharide standards only insufficient peak intensities and thus estimated mobilities were achieved. In many cases, recorded inverse mobilities of monosaccharides were higher than for disaccharides. This could be explained by the fact that monomer peaks were dominated by larger ion species. Consequently, monosaccharides are excluded from further considerations, but are nevertheless presented in the ion mobility library for the sake of completeness.

The mobilities were measured in technical replicates of three with an average standard deviation for all standards ($M \geq 326.30$ g/mol) of $0.001 \text{ V}\cdot\text{s}\cdot\text{cm}^{-2}$ and maximal deviation of $0.007 \text{ V}\cdot\text{s}\cdot\text{cm}^{-2}$ (maltoheptaose). In general, the major ion species observed were $[\text{M}-\text{H}]^-$, $[\text{M}+\text{Cl}]^-$, $[\text{M}+\text{HCOO}]^-$ and $[\text{2M}-\text{H}]^-$ in negative as well as $[\text{M}+\text{Na}]^+$ and $[\text{M}+\text{K}]^+$ in positive mode.

The positive mode was only recorded with the amine column, but theoretically and experimentally mobility values for a given compound are independent of the chromatographic method. The deviation of mobility values between both columns were maximal $0.005 \text{ V}\cdot\text{s}\cdot\text{cm}^{-2}$. Deprotonated monomers were initially the preferred diagnostic ions on account of the fact that mobilities of these basic ions are immediately related to the molecules respective structures. However, often the peak intensity was too low and thus the mobility peaks broad, vague and MS were dominated by formate or other ion clusters. Consistent with this is the fact that monomers of larger molecules ionized better and thus gave better mobility peaks. In contrast, chloride adducts were consistently formed for smaller saccharides ($DP \leq 3$), but not for larger chains. Interestingly, the formation of formate adducts was dependent on the chromatographic method and more abundant in graphite column runs although

the mobile phases were identical. Universally, the deprotonated dimer was the most reliable ion species for diagnosis of all saccharides ($M \leq 666.58$ g/mol), with the exclusion of larger molecules being attributed to the preferred mass detection range of this method. It was expected and also observed that high compound concentrations supported the formation of dimers (Figure 21).

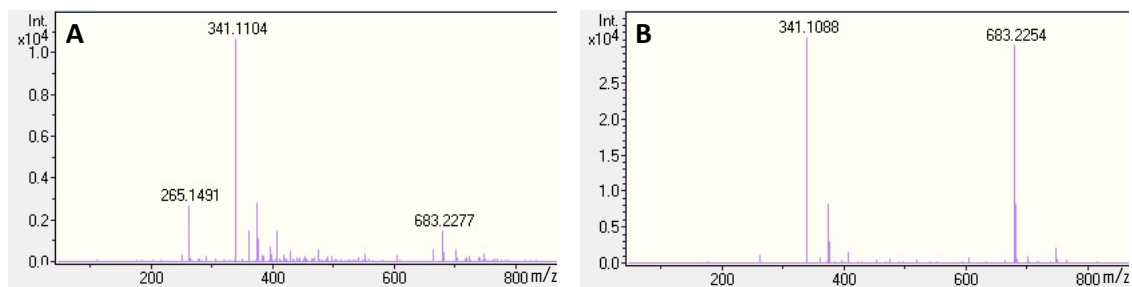


Figure 21: High concentrations promoted dimer formation. Mass spectra of sucrose were dominated by $[M-H]^-$ peaks at low concentrations $1 \mu\text{M}$ (A). An increasing concentration of $100 \mu\text{M}$ promoted the formation of $[2M-H]^-$ (B).

The isomer separation was dependent on ionisation mode and ion species, with a discrimination being possible at an estimated mobility difference of $\Delta 1/K_0 \geq 0.03 \text{ V} \cdot \text{s} \cdot \text{cm}^{-2}$. Mobilities of $[M-H]^-$ and $[M+Cl]^-$ were quite similar for many disaccharides, but differed sufficient for oligosaccharides. Adducts such as $[2M-H]^-$, $[M+Na]^+$ and $[M+K]^+$ were utilised in the discrimination of disaccharides, as these gained better separation. It can also be stated that isomers as well as complexes of isomers were easier to resolve as they increased in size^{70,71,72}.

For the representative ion species $[M-H]^-$ for all saccharide standards recorded here, a linear trend of mobility and m/z was observed. In general, the mobilities were proportional to their molecule weight and the array of mobilities of anion adducts was also stable. Furthermore, for other metabolites this behaviour is well established and can help to classify compounds^{55,71,72}. In contrast, mobilities of alkali metal adducts did not necessarily correlate to the metal ion radii and showed anomalous behavior^{73,108}.

Previous reports tested the formation of diverse complexes and stated that the influence on ion mobility is compound dependent and cannot always be easily generalised. The characteristic change of conformation is related to physiochemical properties and could aid in structure elucidation^{72,108,109}. Moreover, the choice of complex ions could support isomer discrimination and promote reliability through structure stabilisation⁷³. Here, ion mobility of sodium and potassium adducts provided valuable

support in sugar identification. For example, turanose and leucrose were impossible to separate in negative, but resolved in positive ionisation. Often, alkali metal adducts showed more than one mobility peak, which arose from the formation of different spatial structures. In these cases, the charge carrier most likely adhered to multiple positions^{79,110}. The preferred coordination corresponds to low-energy structures and could be determined by molecular dynamics calculations⁸¹.

The high reproducibility of the reported data illustrates the precision of ion mobility values and high level of importance for chemical analysis. The measurements in both ionisation modes is a strong backbone for the ion mobility library. An enhanced glycan separation via UHPLC-IM-MS was realized by exploration and inclusion of the most promising ion complexes, with improvements found by the promotion of an optimal adduct formation. This could be achieved through additives in the mobile phase as alkali metal chlorides or formic acid.

4.2.1. CCS Pattern

To elucidate saccharide structures, ion mobility values can give valuable information. In this study, fructose-containing compounds were always the most compact within the sets of isobaric compounds tested being related to smaller structures of pyranosyl furanoses than pyranosyl pyranoses¹⁰⁸. Contrarily, galactose and glucose could not be separated, which may be related to the minimal structural difference of only one hydroxyl group differing in orientation⁶³.

In most cases α -disaccharides were more compact, which is also described for α -trisaccharides⁶³. An exception to this pattern is the pair cellobiose/maltose, where the trend was observed to be adduct dependent with tendency for β -anomers being more compact. Interestingly, similar observation was previously reported for cellopentaose/maltopentaose⁷¹.

In contrast, the mobility pattern for regioisomers was more consistent within the literature and our results. This study states a lower mobility for (1,4)-linked than for (1,1)-, (1,3)- or (1,6)-linked isomers, respectively, the issue that (1,3)- are more compact than (1,4)-linked has been confirmed by multiple previous reports^{63,73,71}.

4.2.2. Comparison of CCS Values with Published Data

The inverse reduced mobilities were converted into CCS values to give parameters independent of the instrument and laboratory properties. The CCS values recorded here were compared to previously published libraries. The entries of $[M-H]^-$ and

$[M+Na]^+$ matching 19 common saccharides (37 entries) with the Pacific Northwest National Laboratory (PNNL, <https://panomics.pnnl.gov/metabolites/>) had a relative deviation of 2.7%, whereas the database of the McLean Research Group (<https://mcleanresearchgroup.shinyapps.io/CCS-Compendium/>) had 17 compounds (33 entries) matching $[M-H]^-$, $[M+Na]^+$ or $[M+K]^+$ with a relative deviation of 1.2%. Furthermore, sodium and potassium complexes of seven trisaccharides were compared with Przybylski et al. and achieved a relative deviation of 1.7% (appendix Table X)³⁷. An overarching comparison with the current literature is not easy, since various groups used different chemical modification, adducts and instruments⁶. To prevent this in future, recommendations for IM-MS data were published which were followed in this thesis⁵². Besides consensus reports, an agreement on mobility calibration is required as different values for the tuning mix exist in literature¹¹¹.

The CCS library presented here covers a wide spectrum of disaccharides, also including a few trisaccharides and choice of larger saccharides. The developed UHPLC-IM-MS method contributes enormously to the separation and identification of disaccharide standards. The potential for oligosaccharides has not been exhausted by the contents of this thesis and thus can be expanded considerably. Desirable would be the inclusion of unusual compounds already reported in honeydew as bemisiose, isobemisiose, stigmatriose, -tetraose or -pentaose as well as other potential plant and insect oligosaccharides^{25,95,105}. Aspiring to include profound monosaccharide mobilities into the library, as it was reported by Paglia et al. would also be a noteworthy contribution⁶⁰. For monosaccharide measurements the API5000 was used because it provided sufficient peak intensities. Since a linear ion trap can store more ions than the quadrupole, coupling an ion mobility cell to this instrument could provide an optimal interface. But further optimisation of the timsTOF method would be promising as well⁶⁴. An UHPLC-IM-MS method detecting monosaccharides would support the detection, identification and quantification in our biological samples into a cohesive and all encompassing routine. Furthermore, the method could become expanded to an IM-MS/MS method, where fragmentation takes place. In this case an ion mobility library for monosaccharides would help to assign fragments and thus supports the elucidation of complex structures. Hofmann et al. fragmented higher oligosaccharides and observed identical CCS values for trisaccharide fragments as for their intact counterpart⁶³.

4.3. Quantification Method

In contrast to the stable and reliable sugar identification through IM-MS, the quantification using the timsTOF utilised here exhibited high technical deviation of 8.9% (median of relative standard errors). To quantify the sucrose concentration in honeydew, the peak areas of the EIC of the deprotonated monomer were taken. Even in three samples measured directly in row, the peak area varied about a 6-fold (Figure 22 A-C). In case the compounds were overlapping in the chromatogram, the EIM was taken for compound quantification. But also the EIM varied in their peak areas and corresponding mass spectra (Figure 22 D-E).

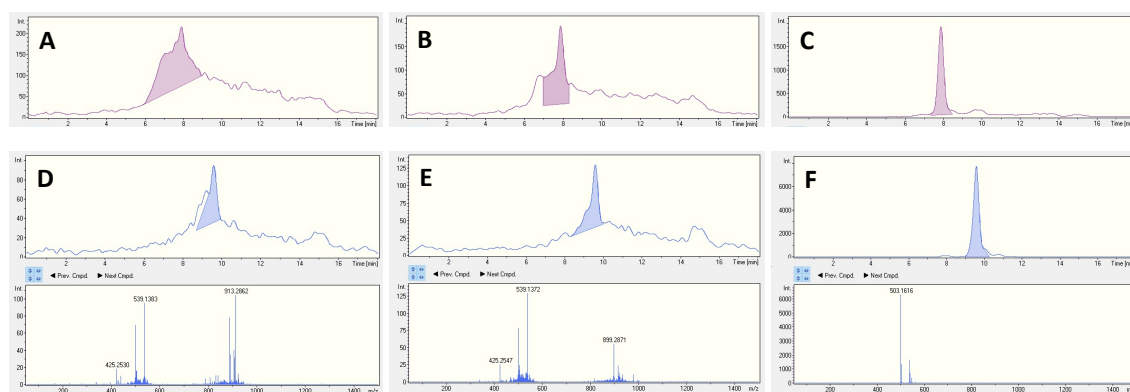


Figure 22: Deviating peak areas. Sucrose was measured in three technical replicates directly in a row (A-C), the ionisation of a unknown trisaccharide varied within the technical replicates (D-E).

To guarantee stable conditions, best efforts were made to eliminate contaminations running several blanks before each set. Nevertheless, one reason could be different grades of ionisation due to various ionisation efficiencies and the residual presence of complexing ions³⁷. In general, the mass spectra showed deprotonated molecules as well as a mixture of multiple ion adducts. It was assumed that the ion spectra are stable and compound characteristic. Concentration dependent shifts would have been hidden by the calibration curves, but running calibration curves of pure standards neglected the influence of other compounds in the complex biological matrix. To realise a complete compound quantification, all ion species need to be captured. However, here the question arises, how the various ion species should be rated and calibrated? Mobile phase additives could offer a solution by the promotion of the constant formation of a few peaks and thus simplify the analysis overall¹⁰⁹. Hofmann et al. reported a linear correlation of the IM-MS intensity for a broad range of concentrations⁶³. Contrary to this was the observation in this study, where the

calibration curves were not linear in the range of concentrations examined, and have been better described by a combination of root and logarithm functions. Therefore, the transformation of peak area to concentration was complicated and required a custom R script. A quantitative calibration through the calibration segment was discussed, but rejected. The volume of tune mix could not have been directly controlled since it was injected through a sample loop and further, split before entering the MS in case of the amine column method. Additionally, the observed quantitative variations could be caused by the technical issue that inconsistent injection volumes are drawn up from plastic vials at low sample volumes. Samples of maize honeydew were stored in glass vials, whereby the *B. brassicae* honeydew samples were stored in plastic vials and showed a 10-fold higher technical standard error (median SE = 13.2) than maize honeydew (median SE = 1.3).

4.4. Further Improvements and Application

Until now, several improvements were proposed. First, chemical additives in the mobile phase should be tested to stabilize the adduct formation and promote a more reliable basis for compound quantification. Besides this, the discrimination of close isomers could be enhanced by establishing a method in ultra mode for ion mobility scanning. Until now the lower-resolution survey mode was utilised in order to cover the whole mobility range. In contrast, the ultra mode provides a higher resolution in a much narrower mobility range. In literature, other approaches are taken, as coupling IM with infrared (IR) as combinations of IM/IR-MS/MS⁴⁴. Here, we successfully tested the utility of the generated ion mobility library on phloem sap and aphid honeydew samples. This work represents an important step for further sugar analyses and could help to elucidate the enzymatic sugar transformations in aphids due to physiological or ecological functions. Furthermore, the UHPLC-IM-MS method was applied on extracts of barley plants being infected with barley yellow dwarf virus. In young plants, the trisaccharide kestose has been identified, whereby it has not been detected in older plants (manuscript in preparation). The introduction already presented various application areas of this advanced saccharide analysis as medical diagnostic, where the support of adenocarcinoma screening by identification of lewis glyco-epitopes was reported⁶⁸. Moreover, the method is a promising tool in food quality control and prevention of adulteration as the origin of honey can be determined by the possibility to differentiate floral and extrafloral nectar as well as synthetic honey^{34,37}. Furthermore, the method may be beneficial in car-

bohydrate synthesis control, since TWIM-MS was already applied on disaccharides and glycopeptides synthesis⁶⁹. Finally a comprehensive library including multiple analytical dimensions will aid in the elucidation of insect and plant metabolomics⁵⁵.

5. Conclusion and Outlook

This work presents an ion mobility and collision cross section (CCS) library focused on plant and insect saccharides including 47 saccharide standards of 12 monosaccharides, 5 sugar alcohols, 17 disaccharides and 13 saccharides of higher polymerisation grade (DP 3-7). The three-dimensional data collection offers 250 ion mobility values in addition to retention times and mass-to-charge ratios. Mobility values were transformed into CCS values to, furthermore, allow the comparison across laboratories and instrumental settings. The CCS values reported here are in accordance with previous published data.

For data generation, UHPLC-IM-MS methods were developed and are reported herein. Two different chromatography columns were coupled to trapped ion mobility mass spectrometry (timsTOF, Bruker) operated in both the positive and negative ionisation modes.

Furthermore, isomers differing in composition, configuration or connectivity were compared and relations of ion mobility and molecular structure were discovered, possibly guiding future structural elucidation efforts. Additionally, this ion mobility library is expected to improve sugar identification in biological samples of plants and insects. These expectations were fulfilled by the successful identification of saccharides in phloem sap and aphid honeydew samples.

This study reports the detection of mainly sucrose in phloem sap of *Zea mays* plants and identification of a blend of 12 saccharides in honeydew of *Z. mays*-fed aphids *Rhopalosiphum padi* and *Sitobion avenae*. In an artificial set-up, 15 sugars in the honeydew of *Brevicoryne brassicae* were identified and the influence of dietary sucrose on the saccharide profile of excreted honeydew was investigated. A highly sugary diet lowered the proportion of fructose and raised the glucose level while the level of oligosaccharides was the highest at 20% dietary sucrose. Many trisaccharides were direct derivatives of sucrose extended by glucose or galactose addition in (1,3)-, (1,4)- or (1,6)-position. Furthermore, isomerised disaccharides in a (1,1)-, (1,4)- or (1,6)-glycosidic linkage with α - as well as β -constitution were present.

Patterns suggestive of diet-related quantitative effects could not be reliably determined. To ensure stable and reproducible results, the UHPLC-IM-MS method should be enhanced by testing various additives in the mobile phase. Moreover, the UHPLC-IM-MS method should also be improved by, first, optimisation of monosaccharide identification, second, enhancing resolution by the utilisation of higher ion mobility resolution modes in certain mobility ranges. Finally, usage of automated

data analyses to ensure a fast, reliable and independent application may be beneficial. Additionally, the library could be expanded by further oligosaccharides as well as putative saccharides of plant and insect metabolomes. An excellent goal is to make the method as well as the ion mobility library accessible for colleagues to raise utility and promote further development.

References

- [1] P. Bruice, *Organic chemistry*, ch. Carbohydrates, pp. pp. 878 – 911. Upper Saddle River, N.J: Prentice Hall, 2001.
- [2] C. Schmidt, “Über Pflanzenschleim und Bassorin,” *Justus Liebigs Annalen der Chemie*, vol. 51, no. 1, pp. 29–62, 1844.
- [3] B. Kohaupt, *Praxiswissen Chemie für Techniker und Ingenieure*. Springer Fachmedien, 1996.
- [4] A. Varki, “Biological roles of oligosaccharides: all of the theories are correct,” *Glycobiology*, vol. 3, pp. 97–130, apr 1993.
- [5] Y. Huang, A. Gelb, and E. Dodds, “Carbohydrate and glycoconjugate analysis by ion mobility mass spectrometry: Opportunities and challenges,” *Current Metabolomics*, vol. 1, pp. 291–305, jan 2014.
- [6] J. Hofmann and K. Pagel, “Glycan analysis by ion mobility–mass spectrometry,” *Angewandte Chemie International Edition*, vol. 56, pp. 8342–8349, jun 2017.
- [7] F. Brouns, “Saccharide characteristics and their potential health effects in perspective,” *Frontiers in Nutrition*, vol. 7, jul 2020.
- [8] D. M. D. L. Navarro, J. J. Abelilla, and H. H. Stein, “Structures and characteristics of carbohydrates in diets fed to pigs: A review,” vol. 10, apr 2019.
- [9] M. Asif, M. Akram, T. Saeed, I. Khan, A. Naveed, M. Riaz Ur Rehman, D. S. Ali Shah, K. Nazish, and G. Shaheen, “Review paper carbohydrates 1,” vol. 1, pp. 1–5, feb 2011.
- [10] M. J. P. Canny, *Transport in plants*. Berlin New York: Springer-Verlag, 1975.
- [11] H. F. Emden, *Aphids as crop pests*. Wallingford, Oxfordshire, UK Boston, MA: CABI, 2017.
- [12] T. Will and A. J. E. van Bel, “Physical and chemical interactions between aphids and plants,” *Journal of Experimental Botany*, vol. 57, pp. 729–737, feb 2006.

-
- [13] D. Ashford, W. Smith, and A. Douglas, "Living on a high sugar diet: The fate of sucrose ingested by a phloem-feeding insect, the pea aphid *Acyrtosiphon pisum*," *Journal of Insect Physiology*, vol. 46, pp. 335–341, mar 2000.
- [14] D. Price, A. Karley, D. Ashford, H. Isaacs, M. Pownall, H. Wilkinson, J. Gatehouse, and A. Douglas, "Molecular characterisation of a candidate gut sucrose in the pea aphid, *Acyrtosiphon pisum*," *Insect Biochemistry and Molecular Biology*, vol. 37, pp. 307–317, apr 2007.
- [15] T. Wilkinson, D. Ashford, J. Pritchard, and A. Douglas, "Honeydew sugars and osmoregulation in the pea aphid *Acyrtosiphon pisum*," *The Journal of experimental biology*, vol. 200, pp. 2137–43, aug 1997.
- [16] P. T. Cristofolletti, A. F. Ribeiro, C. Deraison, Y. Rahbé, and W. R. Terra, "Midgut adaptation and digestive enzyme distribution in a phloem feeding insect, the pea aphid *Acyrtosiphon pisum*," *Journal of Insect Physiology*, vol. 49, pp. 11–24, jan 2003.
- [17] J. D. Rhodes, P. C. Croghan, and A. F. G. Dixon, "Dietary sucrose and oligosaccharide synthesis in relation to osmoregulation in the pea aphid *Acyrtosiphon pisum*," vol. 22, pp. 373–379, Wiley, dec 1997.
- [18] D. Wool, D. L. Hendrix, and O. Shukry, "Seasonal variation in honeydew sugar content of galling aphids (*Aphidoidea: Pemphigidae: Fordinae*) feeding on *Pistacia*: Host ecology and aphid physiology," *Basic and Applied Ecology*, vol. 7, pp. 141–151, mar 2006.
- [19] F. S. Walters and C. A. Mullin, "Sucrose-dependent increase and in and oligosaccharide production and associated and glycosidase activities and in the potato and aphid and *Macrosiphum euphorbiae* (Thomas)," *Archives of Insect Biochemistry and Physiology*, vol. 9, pp. 35–46, 1988.
- [20] A. E. Douglas, "Phloem-sap feeding by animals: Problems and solutions," *Journal of Experimental Botany*, vol. 57, pp. 747–754, jan 2006.
- [21] W. Völkl, J. Woodring, M. Fischer, M. W. Lorenz, and K. H. Hoffmann, "Ant-aphid mutualisms: the impact of honeydew production and honeydew sugar composition on ant preferences," *Oecologia*, vol. 118, pp. 483–491, mar 1999.

- [22] D. N. Byrne and W. B. Miller, “Carbohydrate and amino acid composition of phloem sap and honeydew produced by *Bemisia tabaci*,” *Journal of Insect Physiology*, vol. 36, pp. 433–439, jan 1990.
- [23] D. L. Hendrix, Y. an Wei, and J. E. Leggett, “Homopteran honeydew sugar composition is determined by both the insect and plant species,” *Comparative Biochemistry and Physiology Part B: Comparative Biochemistry*, vol. 101, pp. 23–27, jan 1992.
- [24] M. E. Salvucci, “Sorbitol accumulation in whiteflies: evidence for a role in protecting proteins during heat stress,” *Journal of Thermal Biology*, vol. 25, pp. 353–361, oct 2000.
- [25] D. L. Hendrix and Y. an Wei, “Bemisiose: an unusual trisaccharide in *Bemisia* honeydew,” *Carbohydrate Research*, vol. 253, pp. 329–334, feb 1994.
- [26] M. K. Fischer, W. Völkl, and K. H. Hoffmann, “Honeydew production and honeydew sugar composition of polyphagous black bean aphid, *Aphis fabae* (hemiptera: Aphididae) on various host plants and implications for ant-attendance,” *European Journal of Entomology*, vol. 102, pp. 155–160, may 2005.
- [27] P. K. Nguyen, J. E. Owens, L. E. Lowe, and E. H. Mooney, “Analysis of sugars and amino acids in aphid honeydew by hydrophilic interaction liquid chromatography – Mass spectrometry,” *MethodsX*, vol. 7, p. 101050, 2020.
- [28] K. A. Wyckhuys, J. E. Strange-George, C. A. Kulhanek, F. L. Wäckers, and G. E. Heimpel, “Sugar feeding by the aphid parasitoid *Binodoxys communis*: How does honeydew compare with other sugar sources?,” *Journal of Insect Physiology*, vol. 54, pp. 481–491, feb 2008.
- [29] M. K. Fischer, W. Völkl, R. Schopf, and K. H. Hoffmann, “Age-specific patterns in honeydew production and honeydew composition in the aphid *Metopeurum fuscoviride*: implications for ant-attendance,” *Journal of Insect Physiology*, vol. 48, pp. 319–326, mar 2002.
- [30] M. Fischer and A. Shingleton, “Host plant and ants influence the honeydew sugar composition of aphids,” *Functional Ecology*, vol. 15, no. 4, pp. 544–550, 2001.

-
- [31] H. E. Gray and G. Fraenkel, “Fructomaltose, a recently discovered trisaccharide isolated from honeydew,” *Science*, vol. 118, pp. 304–305, sep 1953.
- [32] D. B. Fisher, J. P. Wright, and T. E. Mittler, “Osmoregulation by the aphid *Myzus persicae*: a physiological role for honeydew oligosaccharides,” *Journal of Insect Physiology*, vol. 30, pp. 387–393, jan 1984.
- [33] M. S. Moon, “Phagostimulation of a monophagous aphid,” *Oikos*, vol. 18, no. 1, p. 96, 1967.
- [34] L. W. Doner, “The sugars of honey— a review,” *Journal of the Science of Food and Agriculture*, vol. 28, pp. 443–456, may 1977.
- [35] G. C. Daily, P. R. Ehrlich, and N. M. Haddad, “Double keystone bird in a keystone species complex,” *Proceedings of the National Academy of Sciences*, vol. 90, pp. 592–594, jan 1993.
- [36] D. Peach, R. Gries, N. Young, R. Lakes, E. Galloway, S. Alamsetti, E. Ko, A. Ly, and G. Gries, “Attraction of female *Aedes aegypti* (L.) to aphid honeydew,” *Insects*, vol. 10, p. 43, feb 2019.
- [37] C. Przybylski and V. Bonnet, “Discrimination of isomeric trisaccharides and their relative quantification in honeys using trapped ion mobility spectrometry,” *Food Chemistry*, vol. 341, p. 128182, mar 2021.
- [38] A. M. Zhou, B. Q. Kuang, Y. R. Gao, and G. W. Liang, “Sucrose triggers honeydew preference in the ghost ant, *Tapinoma melanocephalum* (hymenoptera: Formicidae),” *Florida Entomologist*, vol. 98, pp. 1217–1222, dec 2015.
- [39] J. Woodring, R. Wiedemann, W. Völkl, and K. H. Hoffmann, “Oligosaccharide synthesis regulates gut osmolality in the ant-attended aphid *Metopeurum fuscoviride* but not in the unattended aphid *Macrosiphoniella tanacetaria*,” *Journal of Applied Entomology*, vol. 131, pp. 1–7, feb 2007.
- [40] R. D. Fell, “The qualitative and quantitative analysis of insect hemolymph sugars by high performance thin-layer chromatography,” *Comparative Biochemistry and Physiology Part A: Physiology*, vol. 95, pp. 539–544, jan 1990.
- [41] D. A. Rhodes J, Croghan P, “Uptake, excretion and respiration of sucrose and amino acids in the pea aphid *Acyrtosiphon pisum*,” *The Journal of Experimental Biology*, vol. 199, p. 1269–1276, 1996.

- [42] A. Dell, “Glycoprotein structure determination by mass spectrometry,” *Science*, vol. 291, pp. 2351–2356, mar 2001.
- [43] B. Shaaban, V. Seeburger, A. Schroeder, and G. Lohaus, “Sugar, amino acid and inorganic ion profiling of the honeydew from different hemipteran species feeding on *Abies alba* and *Picea abies*,” *PLOS ONE*, vol. 15, jan 2020.
- [44] C. J. Gray, B. Schindler, L. G. Migas, M. Pičmanová, A. R. Allouche, A. P. Green, S. Mandal, M. S. Motawia, R. Sánchez-Pérez, N. Bjarnholt, B. L. Møller, A. M. Rijs, P. E. Barran, I. Compagnon, C. E. Eyers, and S. L. Flitsch, “Bottom-up elucidation of glycosidic bond stereochemistry,” *Analytical Chemistry*, vol. 89, pp. 4540–4549, apr 2017.
- [45] J. Zeleny, “VI. On the ratio of the velocities of the two ions produced in gases by Röntgen radiation; and on some related phenomena,” *The London, Edinburgh, and Dublin Philosophical Magazine and Journal of Science*, vol. 46, pp. 120–154, jul 1898.
- [46] J. Thomson, “XIX. Further experiments on positive rays,” *The London, Edinburgh, and Dublin Philosophical Magazine and Journal of Science*, vol. 24, pp. 209–253, aug 1912.
- [47] D. L. Albritton, T. M. Miller, D. W. Martin, and E. W. McDaniel, “Mobilities of mass-identified H_3^+ and H^+ ions in hydrogen,” *Physical Review*, vol. 171, pp. 94–102, jul 1968.
- [48] M. J. Cohen and F. W. Karasek, “Plasma chromatography - a new dimension for gas chromatography and mass spectrometry,” *Journal of Chromatographic Science*, vol. 8, pp. 330–337, jun 1970.
- [49] J. C. May and J. A. McLean, “Ion mobility-mass spectrometry: Time-dispersive instrumentation,” *Analytical Chemistry*, vol. 87, pp. 1422–1436, jan 2015.
- [50] “timstofTM flexibility to empower your ideas,” 2017.
- [51] K. Giles, J. L. Wildgoose, D. J. Langridge, and I. Campuzano, “A method for direct measurement of ion mobilities using a travelling wave ion guide,” *International Journal of Mass Spectrometry*, vol. 298, no. 1-3, pp. 10–16, 2010.

- [52] V. Gabelica, A. A. Shvartsburg, C. Afonso, P. Barran, J. L. Benesch, C. Bleiholder, M. T. Bowers, A. Bilbao, M. F. Bush, J. L. Campbell, I. D. Campuzano, T. Causon, B. H. Clowers, C. S. Creaser, E. D. Pauw, J. Far, F. Fernandez-Lima, J. C. Fjeldsted, K. Giles, M. Groessl, C. J. Hogan, S. Hann, H. I. Kim, R. T. Kurulugama, J. C. May, J. A. McLean, K. Pagel, K. Richardson, M. E. Ridgeway, F. Rosu, F. Sobott, K. Thalassinos, S. J. Valentine, and T. Wyttenbach, "Recommendations for reporting ion mobility mass spectrometry measurements," *Mass Spectrometry Reviews*, vol. 38, pp. 291–320, feb 2019.
- [53] Bruker, *otofControl 6.0 - User Manual*. Bruker Daltonik GmbH, Bruker Daltonik GmbH, Bremen (Germany), revision a ed., Apr. 2019.
- [54] R. Cumeras, E. Figueras, C. E. Davis, J. I. Baumbach, and I. Gràcia, "Review on ion mobility spectrometry. part 1: Current instrumentation," *The Analyst*, vol. 140, no. 5, pp. 1376–1390, 2015.
- [55] M. Schroeder, S. W. Meyer, H. M. Heyman, A. Barsch, and L. W. Sumner, "Generation of a collision cross section library for multi-dimensional plant metabolomics using UHPLC-trapped ion mobility-MS/MS," *Metabolites*, vol. 10, p. 13, dec 2019.
- [56] H. E. Revercomb and E. A. Mason, "Theory of plasma chromatography/-gaseous electrophoresis. Review," *Analytical Chemistry*, vol. 47, pp. 970–983, jun 1975.
- [57] S. M. Stow, N. M. Lareau, K. M. Hines, C. R. McNees, C. R. Goodwin, B. O. Bachmann, and J. A. Mclean, "Structural separations for natural product characterization by ion mobility-mass spectrometry," in *Natural Products Analysis*, pp. 397–431, John Wiley & Sons, Inc, sep 2014.
- [58] K. J. Pacholarz and P. E. Barran, "Distinguishing loss of structure from subunit dissociation for protein complexes with variable temperature ion mobility mass spectrometry," *Analytical Chemistry*, vol. 87, pp. 6271–6279, jun 2015.
- [59] W. Gabryelski and K. L. Froese, "Rapid and sensitive differentiation of anomers, linkage, and position isomers of disaccharides using high-field asymmetric waveform ion mobility spectrometry (FAIMS)," *Journal of the American Society for Mass Spectrometry*, vol. 14, pp. 265–277, mar 2003.

- [60] G. Paglia, J. P. Williams, L. Menikarachchi, J. W. Thompson, R. Tyldesley-Worster, S. Halldórsson, O. Rolfsson, A. Moseley, D. Grant, J. Langridge, B. O. Palsson, and G. Astarita, “Ion mobility derived collision cross sections to support metabolomics applications,” *Analytical Chemistry*, vol. 86, pp. 3985–3993, mar 2014.
- [61] C. M. Nichols, J. N. Dodds, B. S. Rose, J. A. Picache, C. B. Morris, S. G. Codreanu, J. C. May, S. D. Sherrod, and J. A. McLean, “Untargeted molecular discovery in primary metabolism: Collision cross section as a molecular descriptor in ion mobility-mass spectrometry,” *Analytical Chemistry*, vol. 90, pp. 14484–14492, nov 2018.
- [62] B. H. Clowers, P. Dwivedi, W. E. Steiner, H. H. Hill, and B. Bendiak, “Separation of sodiated isobaric disaccharides and trisaccharides using electrospray ionization-atmospheric pressure ion mobility-time of flight mass spectrometry,” *Journal of the American Society for Mass Spectrometry*, vol. 16, pp. 660–669, may 2005.
- [63] J. Hofmann, H. S. Hahm, P. H. Seeberger, and K. Pagel, “Identification of carbohydrate anomers using ion mobility–mass spectrometry,” *Nature*, vol. 526, pp. 241–244, sep 2015.
- [64] M. Zhu, B. Bendiak, B. Clowers, and H. H. Hill, “Ion mobility-mass spectrometry analysis of isomeric carbohydrate precursor ions,” *Analytical and Bioanalytical Chemistry*, vol. 394, pp. 1853–1867, jun 2009.
- [65] S. M. Munisamy, C. K. Chambliss, and C. Becker, “Direct infusion electrospray ionization – ion mobility – high resolution mass spectrometry (DIESI-IM-HRMS) for rapid characterization of potential bioprocess streams,” *Journal of The American Society for Mass Spectrometry*, vol. 23, pp. 1250–1259, may 2012.
- [66] K. Pagel and D. J. Harvey, “Ion mobility–mass spectrometry of complex carbohydrates: Collision cross sections of sodiated N-linked glycans,” *Analytical Chemistry*, vol. 85, pp. 5138–5145, may 2013.
- [67] J. Wei, J. Wu, Y. Tang, M. E. Ridgeway, M. A. Park, C. E. Costello, J. Zaia, and C. Lin, “Characterization and quantification of highly sulfated

- glycosaminoglycan isomers by gated-trapped ion mobility spectrometry negative electron transfer dissociation MS/MS,” *Analytical Chemistry*, vol. 91, pp. 2994–3001, jan 2019.
- [68] J. Hofmann, A. Stuckmann, M. Crispin, D. J. Harvey, K. Pagel, and W. B. Struwe, “Identification of lewis and blood group carbohydrate epitopes by ion mobility-tandem-mass spectrometry fingerprinting,” *Analytical Chemistry*, vol. 89, pp. 2318–2325, feb 2017.
- [69] P. Both, A. P. Green, C. J. Gray, R. Šardžik, J. Voglmeir, C. Fontana, M. Austeri, M. Rejzek, D. Richardson, R. A. Field, G. Widmalm, S. L. Flitsch, and C. E. Eyers, “Discrimination of epimeric glycans and glycopeptides using IM-MS and its potential for carbohydrate sequencing,” *Nature Chemistry*, vol. 6, pp. 65–74, dec 2013.
- [70] G. Nagy, I. K. Attah, S. V. B. Garimella, K. Tang, Y. M. Ibrahim, E. S. Baker, and R. D. Smith, “Unraveling the isomeric heterogeneity of glycans: Ion mobility separations in structures for lossless ion manipulations,” *Chemical Communications*, vol. 54, no. 83, pp. 11701–11704, 2018.
- [71] X. Zheng, X. Zhang, N. S. Schocker, R. S. Renslow, D. J. Orton, J. Khamsi, R. A. Ashmus, I. C. Almeida, K. Tang, C. E. Costello, R. D. Smith, K. Michael, and E. S. Baker, “Enhancing glycan isomer separations with metal ions and positive and negative polarity ion mobility spectrometry-mass spectrometry analyses,” *Analytical and Bioanalytical Chemistry*, vol. 409, pp. 467–476, sep 2016.
- [72] C. Xie, Q. Wu, S. Zhang, C. Wang, W. Gao, J. Yu, and K. Tang, “Improving glycan isomeric separation via metal ion incorporation for drift tube ion mobility-mass spectrometry,” *Talanta*, vol. 211, p. 120719, may 2020.
- [73] L. S. Fenn and J. A. McLean, “Structural resolution of carbohydrate positional and structural isomers based on gas-phase ion mobility-mass spectrometry,” *Phys. Chem. Chem. Phys.*, vol. 13, no. 6, pp. 2196–2205, 2011.
- [74] H. Li, B. Bendiak, W. F. Siems, D. R. Gang, and H. H. Hill, “Ion mobility mass spectrometry analysis of isomeric disaccharide precursor, product and cluster ions,” *Rapid Communications in Mass Spectrometry*, vol. 27, no. 23, pp. 2699–2709, 2013.

- [75] T. Yamagaki and A. Sato, "Isomeric oligosaccharides analyses using negative-ion electrospray ionization ion mobility spectrometry combined with collision-induced dissociation MS/MS," *Analytical Sciences*, vol. 25, no. 8, pp. 985–988, 2009.
- [76] M. D. Leavell, S. P. Gaucher, J. A. Leary, J. A. Taraszka, and D. E. Clemmer, "Conformational studies of Zn-ligand-hexose diastereomers using ion mobility measurements and density functional theory calculations," *Journal of the American Society for Mass Spectrometry*, vol. 13, pp. 284–293, mar 2002.
- [77] B. C. Bohrer and D. E. Clemmer, "Biologically-inspired peptide reagents for enhancing IMS-MS analysis of carbohydrates," *Journal of The American Society for Mass Spectrometry*, vol. 22, pp. 1602–1609, jun 2011.
- [78] X. Zheng, N. A. Aly, Y. Zhou, K. T. Dupuis, A. Bilbao, V. L. Paurus, D. J. Orton, R. Wilson, S. H. Payne, R. D. Smith, and E. S. Baker, "A structural examination and collision cross section database for over 500 metabolites and xenobiotics using drift tube ion mobility spectrometry," *Chemical Science*, vol. 8, no. 11, pp. 7724–7736, 2017.
- [79] P. Dwivedi, B. Bendiak, B. H. Clowers, and H. H. Hill, "Rapid resolution of carbohydrate isomers by electrospray ionization ambient pressure ion mobility spectrometry-time-of-flight mass spectrometry (ESI-APIMS-TOFMS)," *Journal of the American Society for Mass Spectrometry*, vol. 18, pp. 1163–1175, jul 2007.
- [80] Y. Liu and D. E. Clemmer, "Characterizing oligosaccharides using injected-ion mobility/mass spectrometry," *Analytical Chemistry*, vol. 69, pp. 2504–2509, jul 1997.
- [81] J. P. Williams, M. Grabenauer, R. J. Holland, C. J. Carpenter, M. R. Wormald, K. Giles, D. J. Harvey, R. H. Bateman, J. H. Scrivens, and M. T. Bowers, "Characterization of simple isomeric oligosaccharides and the rapid separation of glycan mixtures by ion mobility mass spectrometry," *International Journal of Mass Spectrometry*, vol. 298, pp. 119–127, dec 2010.
- [82] Y. Pu, M. E. Ridgeway, R. S. Glaskin, M. A. Park, C. E. Costello, and C. Lin, "Separation and identification of isomeric glycans by selected accumulation-

- trapped ion mobility spectrometry-electron activated dissociation tandem mass spectrometry,” *Analytical Chemistry*, vol. 88, pp. 3440–3443, mar 2016.
- [83] S. L. Koeniger, S. I. Merenbloom, S. J. Valentine, M. F. Jarrold, H. R. Udseth, R. D. Smith, and D. E. Clemmer, “An IMS-IMS analogue of MS-MS,” *Analytical Chemistry*, vol. 78, pp. 4161–4174, jun 2006.
- [84] S. I. Merenbloom, R. S. Glaskin, Z. B. Henson, and D. E. Clemmer, “High-resolution ion cyclotron mobility spectrometry,” *Analytical Chemistry*, vol. 81, pp. 1482–1487, jan 2009.
- [85] K. R. McKenna, L. Li, A. G. Baker, J. Ujma, R. Krishnamurthy, C. L. Liotta, and F. M. Fernández, “Carbohydrate isomer resolution via multi-site derivatization cyclic ion mobility-mass spectrometry,” *The Analyst*, vol. 144, no. 24, pp. 7220–7226, 2019.
- [86] H. Li, B. Bendiak, W. F. Siems, D. R. Gang, and H. H. Hill, “Carbohydrate structure characterization by tandem ion mobility mass spectrometry (*IMMS*²),” *Analytical Chemistry*, vol. 85, pp. 2760–2769, feb 2013.
- [87] J. A. Picache, B. S. Rose, A. Balinski, K. L. Leaptrot, S. D. Sherrod, J. C. May, and J. A. McLean, “Collision cross section compendium to annotate and predict multi-omic compound identities,” *Journal of Chemical Sciences*, vol. 10, no. 4, pp. 983–993, 2019.
- [88] D. H. Ross, J. H. Cho, and L. Xu, “Breaking down structural diversity for comprehensive prediction of ion-neutral collision cross sections,” *American Chemical Society*, vol. 92, pp. 4548–4557, feb 2020.
- [89] Z. Zhou, M. Luo, X. Chen, Y. Yin, X. Xiong, R. Wang, and Z.-J. Zhu, “Ion mobility collision cross-section atlas for known and unknown metabolite annotation in untargeted metabolomics,” *Nature Communications*, vol. 11, aug 2020.
- [90] G. Febvay, B. Delobel, and Y. Rahbé, “Influence of the amino acid balance on the improvement of an artificial diet for a biotype of *Acyrtosiphon pisum* (homoptera: Aphididae),” *Canadian Journal of Zoology*, vol. 66, pp. 2449–2453, nov 1988.

- [91] M. R. Zimmermann, T. Knauer, and A. C. U. Furch, *Collection of Phloem Sap in Phytoplasma-Infected Plants*, pp. 291–299. New York, NY: Springer New York, 2019.
- [92] “Application notebook thermo scientific hypercarb columns,” https://assets.thermofisher.com/TFS-Assets/CMD/Application-Notes/ANGSCHYPERCARB0609-hypercarb_appnotebook.pdf, 2009.
- [93] C. D. Nelson, “The translocation of organic compounds in plants,” *Canadian Journal of Botany*, vol. 40, pp. 757–770, may 1962.
- [94] F. A. C. Neerbos, J. G. Boer, L. Salis, W. Tollenaar, M. Kos, L. E. M. Vet, and J. A. Harvey, “Honeydew composition and its effect on life-history parameters of hyperparasitoids,” *Ecological Entomology*, vol. 45, pp. 278–289, sep 2019.
- [95] A. Bogo, “New group of oligosaccharides excreted in honeydew from scale insects *Stigmacoccus sp.* and *Coccus hesperidum L.*,” *Ciência Rural*, vol. 33, pp. 593–599, aug 2003.
- [96] A. Bogo and P. Mantle, “Oligosaccharides in the honeydew of *Coccoidea scale* insects: *Coccus hesperidum L.* and a new *Stigmacoccus sp.* in brazil,” *Anais da Sociedade Entomológica do Brasil*, vol. 29, pp. 589–595, sep 2000.
- [97] A. E. Douglas, D. R. G. Price, L. B. Minto, E. Jones, K. V. Pescod, C. L. M. J. François, J. Pritchard, and N. Boonham, “Sweet problems: Insect traits defining the limits to dietary sugar utilisation by the pea aphid, *Acyrtosiphon pisum*,” *Journal of Experimental Biology*, vol. 209, pp. 1395–1403, apr 2006.
- [98] A. Balvasi, G. Rassoulilian, A. Bandani, and J. Khalghani, “Suitability of an artificial diet for rape aphid, *Brevicoryne brassicae*, using life table parameters,” *African Journal of Biotechnology*, vol. 8, pp. 4663–4666, 2009.
- [99] J. Gruhn, S. Karolak, and R. Schweiger, “Tolerance of an aphid species towards dietary sucrose-to-amino acid ratios and recovery from suboptimal nutrition,” *Entomologia Experimentalis et Applicata*, vol. 169, pp. 732–742, may 2021.
- [100] T. E. Mittler and T. Meikle, “Effects of dietary sucrose concentration on aphid honeydew carbohydrate levels and rates of excretion,” *Entomologia Experimentalis et Applicata*, vol. 59, pp. 1–7, apr 1991.

- [101] K. Lamb, "Composition of the honeydew of the aphid *Brevicoryne brassicae* (L.) feeding on swedes (*Brassica napobrassica* DC.)," *Journal of Insect Physiology*, vol. 3, pp. 1–13, feb 1959.
- [102] R. Isaacs, D. N. Byrne, and D. L. Hendrix, "Feeding rates and carbohydrate metabolism by *Bemisia tabaci* (homoptera: Aleyrodidae) on different quality phloem saps," *Physiological Entomology*, vol. 23, pp. 241–248, sep 1998.
- [103] D. N. Byrne, D. L. Hendrix, and L. H. Williams, "Presence of trehalulose and other oligosaccharides in hemipteran honeydew, particularly *Aleyrodidae*," *Physiological Entomology*, vol. 28, pp. 144–149, jun 2003.
- [104] M. E. Salvucci, G. R. Wolfe, and D. L. Hendrix, "Effect of sucrose concentration on carbohydrate metabolism in *Bemisia argentifolii*: Biochemical mechanism and physiological role for trehalulose synthesis in the silverleaf whitefly," *Journal of Insect Physiology*, vol. 43, pp. 457–464, may 1997.
- [105] D. L. Hendrix and M. E. Salvucci, "Isobemisiolose: an unusual trisaccharide abundant in the silverleaf whitefly, *Bemisia argentifolii*," *Journal of Insect Physiology*, vol. 47, pp. 423–432, apr 2001.
- [106] M. E. Salvucci, "Distinct sucrose isomerases catalyze trehalulose synthesis in whiteflies, *Bemisia argentifolii*, and *Erwinia rhapsodica*," *Comparative Biochemistry and Physiology Part B: Biochemistry and Molecular Biology*, vol. 135, pp. 385–395, jun 2003.
- [107] D. L. Hendrix and M. E. Salvucci, "Polyol metabolism in homopterans at high temperatures: Accumulation of mannitol in aphids (*Aphididae: Homoptera*) and sorbitol in whiteflies (*Aleyrodidae: Homoptera*)," *Comparative Biochemistry and Physiology Part A: Molecular & Integrative Physiology*, vol. 120, pp. 487–494, jul 1998.
- [108] Y. Huang and E. D. Dodds, "Ion mobility studies of carbohydrates as group i adducts: Isomer specific collisional cross section dependence on metal ion radius," *Analytical Chemistry*, vol. 85, pp. 9728–9735, sep 2013.
- [109] A. Krueve and K. Kaupmees, "Adduct formation in ESI/MS by mobile phase additives," *Journal of The American Society for Mass Spectrometry*, vol. 28, pp. 887–894, mar 2017.

-
- [110] B. A. Cerda and C. Wesdemiotis, “Thermochemistry and structures of Na⁺ coordinated mono- and disaccharide stereoisomers,” *International Journal of Mass Spectrometry*, vol. 189, pp. 189–204, aug 1999.
- [111] S. M. Stow, T. J. Causon, X. Zheng, R. T. Kurulugama, T. Mairinger, J. C. May, E. E. Rennie, E. S. Baker, R. D. Smith, J. A. McLean, S. Hann, and J. C. Fjeldsted, “An interlaboratory evaluation of drift tube ion mobility–mass spectrometry collision cross section measurements,” *Analytical Chemistry*, vol. 89, pp. 9048–9055, aug 2017.

A. Appendix

A.1. Saccharide Standards

A.1.1. InChiKey

Table I: List of all observed saccharide standards. Composition, CAS and InChi-Key are according to <https://pubchem.ncbi.nlm.nih.gov/> (2021/02/26).

MW [g/mol]	Compound name	Neutral formula	Reducing sugar	CAS	InChi-Key
150,13	Arabinose	C ₅ H ₁₀ O ₅	yes	5328-37-0	SRBFZHDQGSBBOR-QMKXCQHVSA-N
150,13	Xylose	C ₅ H ₁₀ O ₅	yes	58-86-6	SRBFZHDQGSBBOR-IOVATXLUSA-N
180,16	Allose	C ₆ H ₁₂ O ₆	yes	2595-97-3	GZCGUPFRVQUAUEE-OB00ZECYSA-N
180,16	Fructose	C ₆ H ₁₂ O ₆	yes	57-48-7	RFSUNEUAIZKAJO-ARQDHWQXSA-N
164,16	Fucose	C ₆ H ₁₂ O ₅	yes	2438-80-4	SHZGCJCMOBCKMK-DHVFOXMCESA-N
180,16	Galactose	C ₆ H ₁₂ O ₆	yes	59-23-4	WQZGKKKJIFFOK-PHYPRBDBSA-N
180,16	Glucose	C ₆ H ₁₂ O ₆	yes	50-99-7	WQZGKKKJIFFOK-GASJEMHNSA-N
180,16	Mannose	C ₆ H ₁₂ O ₆	yes	3458-28-4	WQZGKKKJIFFOK-QTVWNMPRSA-N
180,16	Psicose/Allulose	C ₆ H ₁₂ O ₆	no	551-68-8	BJHIKXHVCFQLS-PUFIMZNGSA-N
164,16	Rhamnose	C ₆ H ₁₂ O ₅	yes	3615-41-6	PNNNRSQAQSRJVS-BXKVDMCESA-N
180,16	Sorbose	C ₆ H ₁₂ O ₆	no	87-79-6	BJHIKXHVCFQLS-OTWZMJISA-N
180,16	Tagatose	C ₆ H ₁₂ O ₆	no	87-81-0	BJHIKXHVCFQLS-PQLUHF TBSA-N
182,17	Galactitol	C ₆ H ₁₄ O ₆	no	608-66-2	FBPFZTCFMRRESA-GUCUJZJISA-N
180,16	myo-Inositol	C ₆ H ₁₂ O ₆	no	87-89-8	CDAISMWEOUEBRE-UHFFFAOYSA-N
182,17	Mannitol	C ₆ H ₁₄ O ₆	no	69-65-8	FBPFZTCFMRRESA-KVTDHHQDSA-N
182,17	Sorbitol	C ₆ H ₁₄ O ₆	no	50-70-4	FBPFZTCFMRRESA-JGWLITMVSA-N
326,3	Rutinose	C ₁₂ H ₂₂ O ₁₀	yes	90-74-4	OVVGHNDPYGTYIT-BNXXONSGSA-N
342,30	Cellobiose	C ₁₂ H ₂₂ O ₁₁	yes	528-50-7	GUBGYTABKSRVRQ-QRZGKKJRSA-N
342,30	Gentiobiose (beta)	C ₁₂ H ₂₂ O ₁₁	yes	554-91-6	DLRVVLDZNNYCBX-LIZSDCNHSA-N
342,30	Isomaltose	C ₁₂ H ₂₂ O ₁₁	yes	499-40-1	DLRVVLDZNNYCBX-RTPHMHGBSA-N
342,30	Isomaltulose/Pallatinose	C ₁₂ H ₂₂ O ₁₁	no	13718-94-0	RJPPRBMGVWEZRR-WTZPKTTFSA-N
342,30	Lactose	C ₁₂ H ₂₂ O ₁₁	yes	63-42-3	GUBGYTABKSRVRQ-XLOQQCPSA-N
342,30	Leucrose	C ₁₂ H ₂₂ O ₁₁	no	7158-70-5	DXALOGXSFZLLN-WTZPKTTFSA-N
342,30	Maltose	C ₁₂ H ₂₂ O ₁₁	yes	69-79-4	GUBGYTABKSRVRQ-PICCSMPSSA-N
342,30	Maltulose	C ₁₂ H ₂₂ O ₁₁	yes	17606-72-3	IHNLNTEFVNSVIFH-OEFDZIMQSA-N
342,30	Melibiose	C ₁₂ H ₂₂ O ₁₁	yes	585-99-9	DLRVVLDZNNYCBX-ABXHMFFYSA-N
342,30	Nigerose	C ₁₂ H ₂₂ O ₁₁	yes	497-48-3	QIGJYVCQYDKYDW-NSYYTRPSSA-N
342,30	Sophorose	C ₁₂ H ₂₂ O ₁₁	no	534-46-3	HIWPGCMGAMJNRG-NCFXGAEVSA-N
342,30	Sucrose	C ₁₂ H ₂₂ O ₁₁	no	57-50-1	CZMRCDWAGMRECN-UGDNZRGBSA-N
342,30	Trehalose	C ₁₂ H ₂₂ O ₁₁	no	99-20-7	HDTRYLNUVZCQOY-LIZSDCNHSA-N
342,30	a,b-Trehalose	C ₁₂ H ₂₂ O ₁₁	no	585-91-1	HDTRYLNUVZCQOY-BTLHAWITSA-N
342,30	Trehalulose	C ₁₂ H ₂₂ O ₁₁	yes	51411-23-5	NMELTECMHKXLF-DGQJZECASA-N
342,30	Turanose	C ₁₂ H ₂₂ O ₁₁	no	547-25-1	RULSWEULPANCDV-PIXUTMIVSA-N
342,30	Galactinol	C ₁₂ H ₂₂ O ₁₁	no	3687-64-7	VCWMRQDBPZKXKG-UHFFFAOYSA-N
504,44	Erllose	C ₁₈ H ₃₂ O ₁₆	no	13101-54-7	FVVCFHXLWDDRHG-KKNDGLDKSA-N
504,44	Isomaltotriose	C ₁₈ H ₃₂ O ₁₆	yes	3371-50-4	FBJQEBRMDXPWNX-FYHZNSTMSA-N
504,44	1-Kestose	C ₁₈ H ₃₂ O ₁₆	no	562-68-5	ODEHMIGXGLNAKK-OESPXITSA-N
504,44	Maltotriose	C ₁₈ H ₃₂ O ₁₆	yes	1109-28-0	FYGDTMLNYKFZSV-DZOUCCHMSA-N
504,44	Melezitose	C ₁₈ H ₃₂ O ₁₆	no	597-12-6	QWIZNVHXZRPDR-WSCXOGSTSA-N
504,44	Panose	C ₁₈ H ₃₂ O ₁₆	yes	33401-87-5	ZCLAHAZPPEVDX-MQHGYCBSA-N
504,44	Raffinose	C ₁₈ H ₃₂ O ₁₆	no	512-69-6	MUPFKEGTMRGPLJ-ZQSKZDJDSA-N
666,58	Maltotetraose	C ₂₄ H ₄₂ O ₂₁	yes	34612-38-9	LUWUZLMQUOBSB-ZLBHSGTGSA-N
666,58	Nystose	C ₂₄ H ₄₂ O ₂₁	no	13133-07-8	FLDFNEBHEXLZRX-DLQNOBSRSA-N
666,58	Stachyose	C ₂₄ H ₄₂ O ₂₁	no	470-55-3	UQZIYBXSHAGNOE-XNSRJBNSA-N
828,72	Maltopentaose	C ₃₀ H ₅₂ O ₂₆	yes	34620-76-3	FTNIPWXXIGNQQF-HZWIHCTQSA-N
990,86	Maltohexaose	C ₃₆ H ₆₂ O ₃₁	yes	34620-77-4	OCIBBXPLUVYKCH-LIGGPISVSA-N
1153,00	Maltoheptaose	C ₄₂ H ₇₂ O ₃₆	yes	34620-78-5	BNABBHGYMZMOA-QJBBZCPBSA-N

A.1.2. Chemical Structures

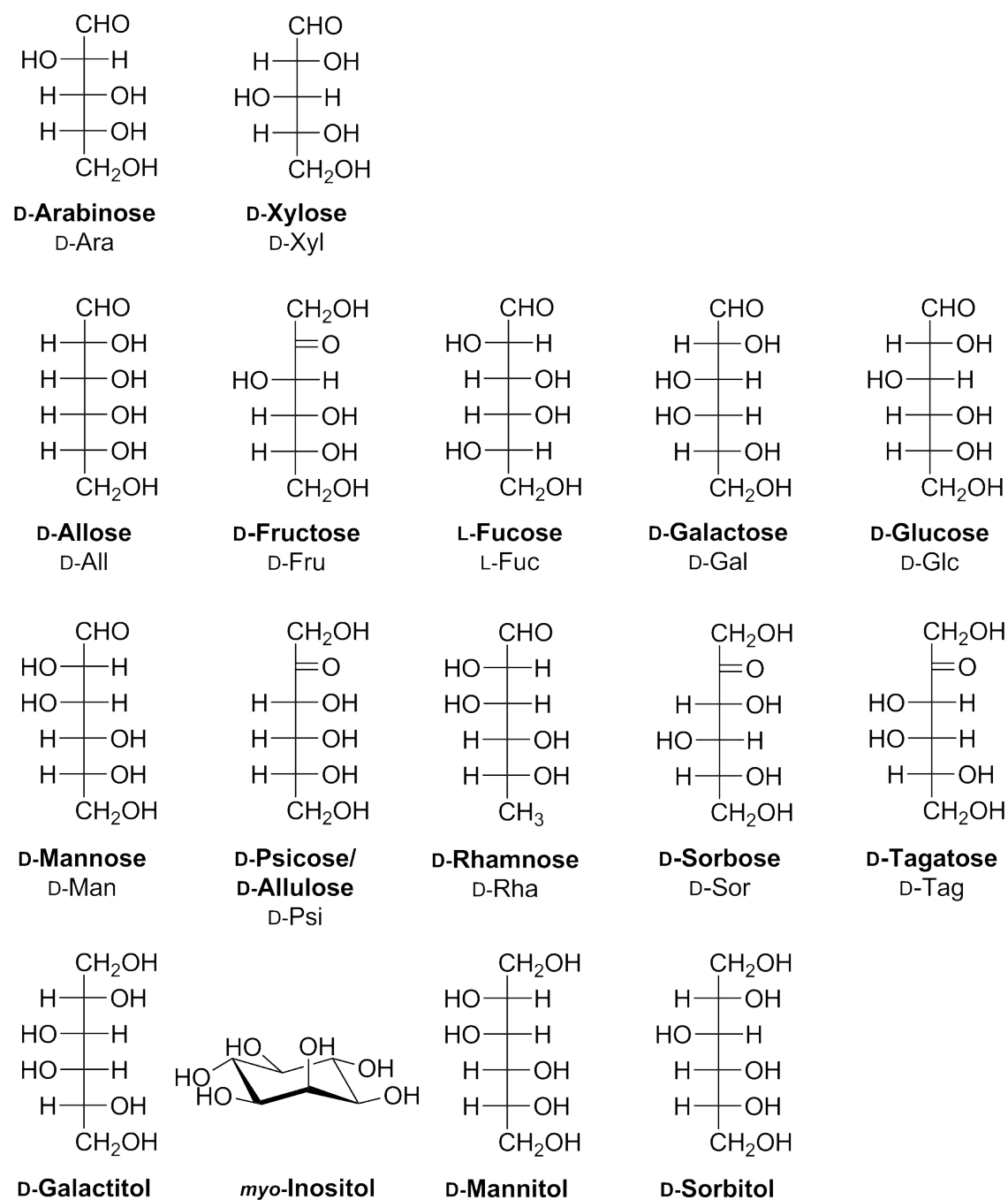


Figure I: Monosaccharides and monosaccharide alcohols included into the UHPLC-ion mobility-MS library.

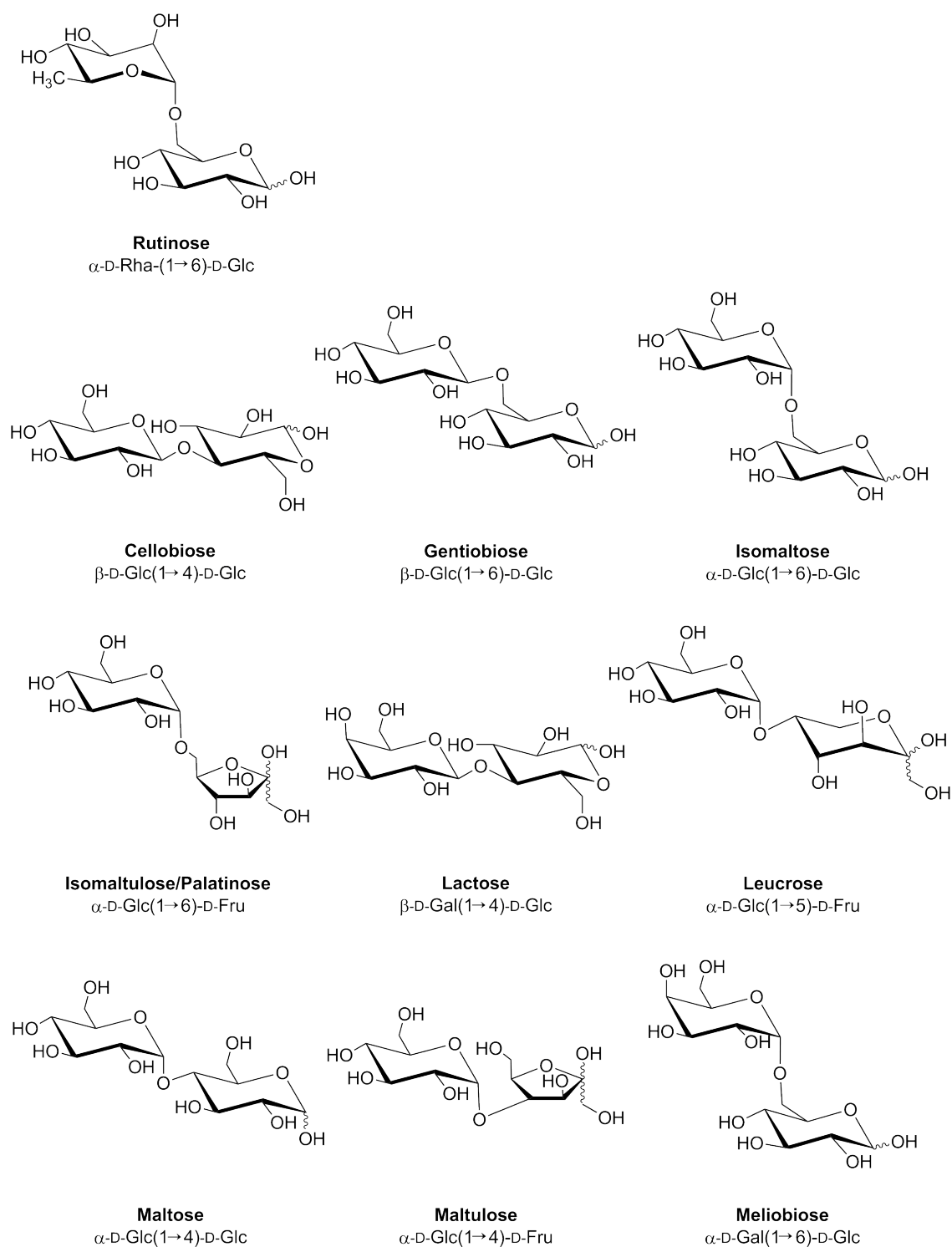


Figure II: Disaccharides included into the UHPLC-ion mobility-MS library.

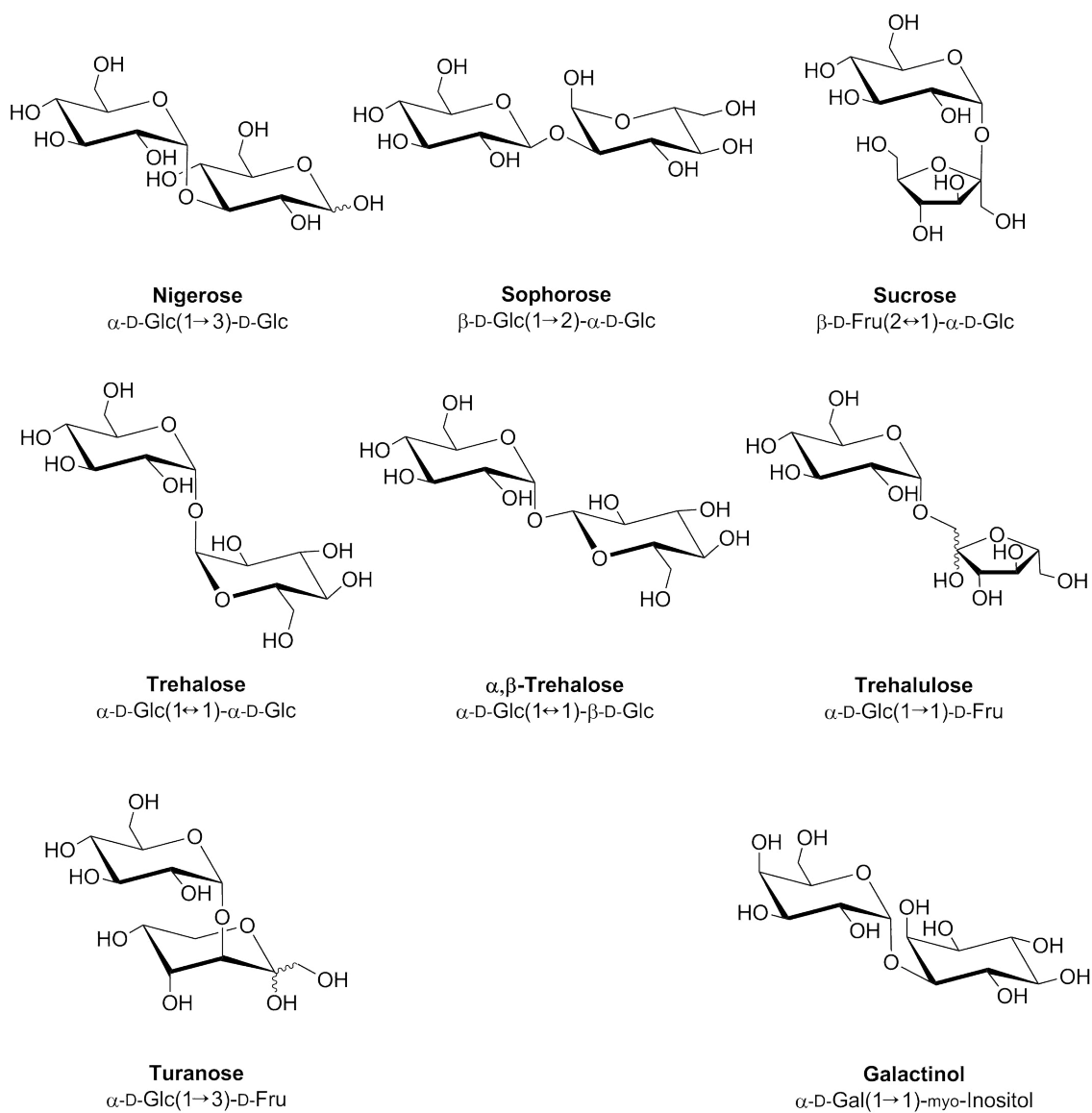


Figure III: Disaccharides and disaccharide alcohol included into the UHPLC-ion mobility-MS library (continued).

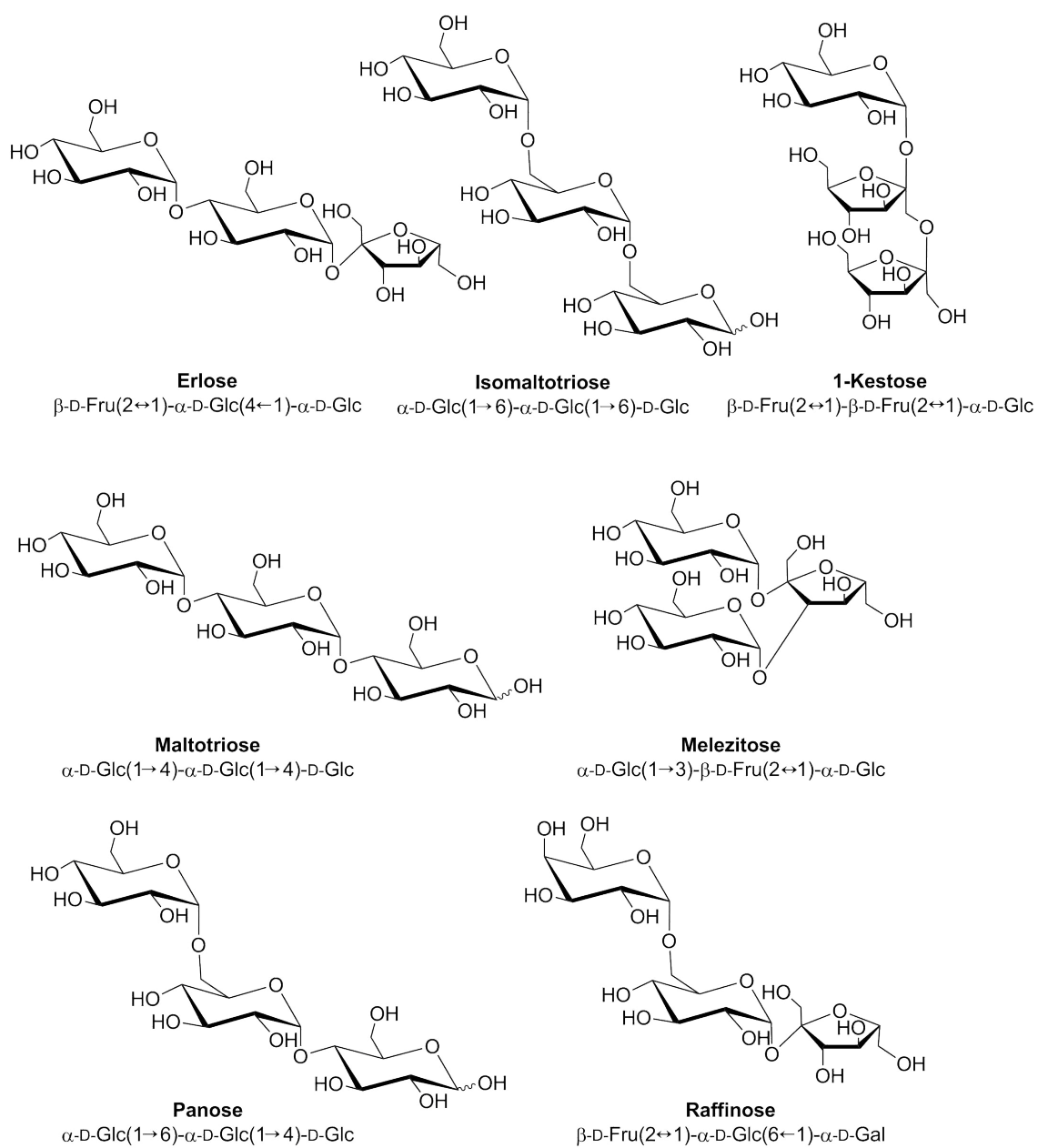


Figure IV: Trisaccharides included into the UHPLC-ion mobility-MS library.

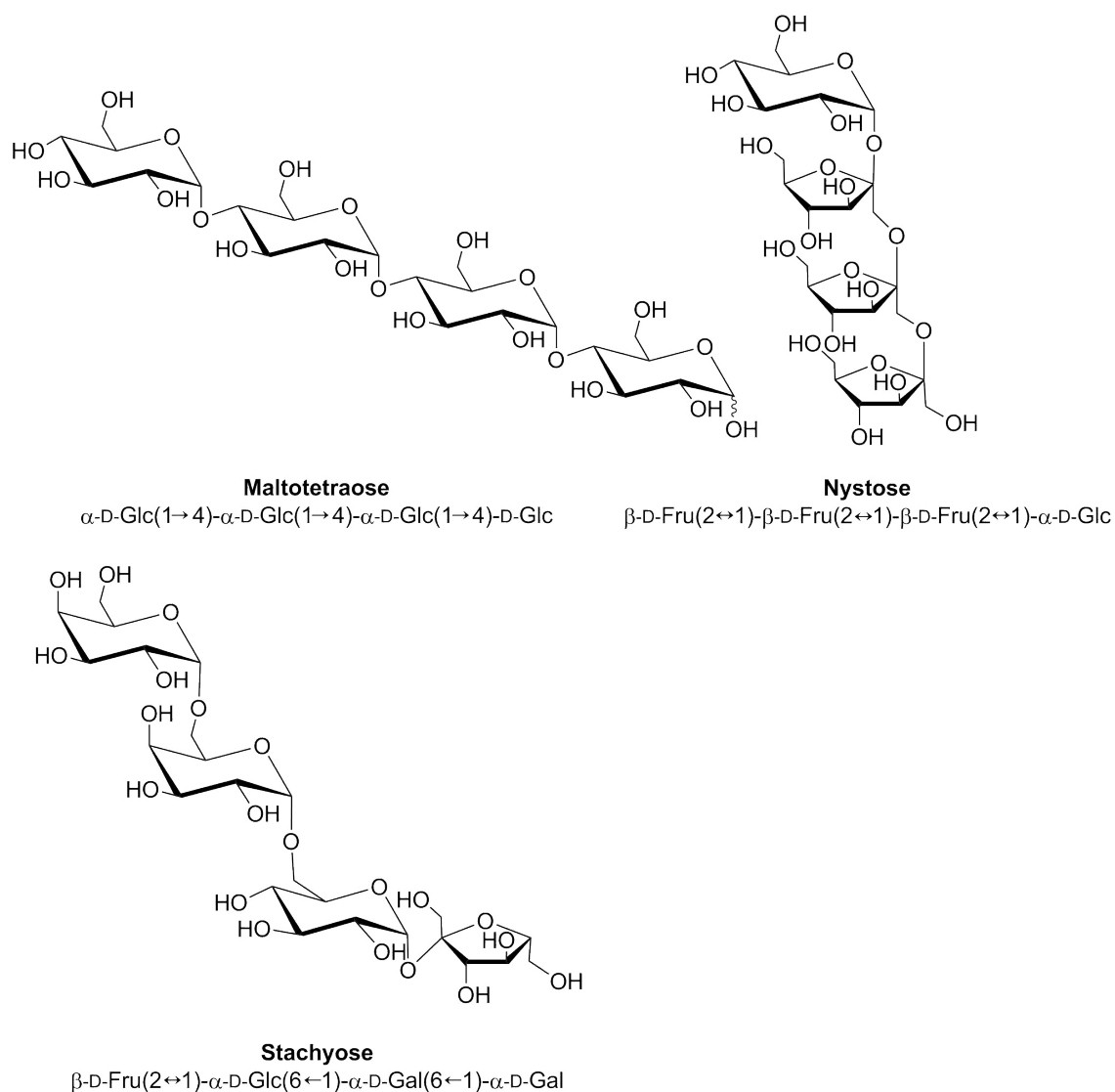


Figure V: Tetrasaccharides included into the UHPLC-ion mobility-MS library.

A.2. Material and Method Details

Table II: Supplier sugar standards.

Substance	Supplier
Allose, D-	Aldrich, Steinheim, Germany
Arabinose, L-(+)	Sigma Life Science, Steinheim, Germany
Cellobiose, D-(+)	Fluka, Buchs, Germany
Erllose	Sigma-Aldrich, Steinheim, Germany
Fructose, D(-)	Sigma-Aldrich, Steinheim, Germany
Fucose, L(-)-	TCl, Tokyo, Japan
Galactinol dihydrate	Sigma-Aldrich, Steinheim, Germany
Galactitol	TCl, Tokyo, Japan
Galactose, D-(+)	Carl Roth, Karlsruhe, Germany
Gentiobiose, beta-D-	Carl Roth, Karlsruhe, Germany
Glucose, D-(+), wasserfrei	Sigma Life Science, Steinheim, Germany
Inositol, myo-	Sigma Life Science, Steinheim, Germany
Isomaltose	Sigma Life Science, Steinheim, Germany
Isomaltotriose	Supelco, Steinheim, Germany
Isomaltulose monohydrate	Carl Roth, Karlsruhe, Germany
Kestose, 1-	Sigma-Aldrich, Steinheim, Germany
Lactose monohydrate	Duchefa Biochemie B.V, Haarlem, Netherlands
Leucrose	Combi-Blocks, San Diego, CA, USA
Maltoheptaose	Sigma Life Science, Steinheim, Germany
Maltohexaose	Sigma Life Science, Steinheim, Germany
Maltopentaose	Carbosynth Ltd., Berkshire, UK
Maltose monohydrate, D-(+)	Alfa Aesar, Kandel, Germany
Maltotetraose	Carbosynth Ltd., Berkshire, UK
Maltotriose	Serva, Heidelberg, Germany
Maltulose monohydrate	Sigma Life Science, Steinheim, Germany
Mannitol	Alfa Aesar, Kandel, Germany
Mannose, D-(+)	Carl Roth, Karlsruhe, Germany
Melezitose monohydrate, D-(+)	Fluka, Buchs, Germany
Melibiose, D-(+)	Sigma-Aldrich, Steinheim, Germany
Nigerose	Sigma-Aldrich, Steinheim, Germany
Nystose	Sigma-Aldrich, Steinheim, Germany
Panose	Biosynth. Carbosynth., Berkshire, UK
Psicose, D-	Sigma Life Science, Steinheim, Germany
Raffinose pentahydrate, D-(+)	Fluka, Buchs, Germany
Rhamnose monohydrate, L-(+)	Carl Roth, Karlsruhe, Germany
Rutinose	Sigma-Aldrich, Steinheim, Germany
Saccharose, D-(+)	Carl Roth, Karlsruhe, Germany
Sophorose monohydrate, alpha-	Serva, Heidelberg, Germany
Sorbitol, D-	Aldrich, Steinheim, Germany
Sorbose, L(-)	Acrose Organics, Fair Lawn, NJ, USA
Stachyose	Sigma Life Science, Steinheim, Germany
Tagatose, D(-)-	Sigma-Aldrich, Steinheim, Germany
Trehalose dihydrate, D-(+)	Sigma Life Science, Steinheim, Germany
Trehalose, alpha-,beta-	Sigma Life Science, Steinheim, Germany
Trehalulose	BOC Sciences, Shirley, NY, USA
Turanose, D-	Alfa Aesar, Kandel, Germany
Xylose, D-(+)	Sigma Life Science, Steinheim, Germany

Table III: Supplier ingredients of artificial diet for *Brevicoryne brassicae*.

Substance	Supplier
Alanine	Duchefa Biochemie B.V, Haarlem, Netherlands
Arginine	Duchefa Biochemie B.V, Haarlem, Netherlands
Asparagine.H ₂ O	Duchefa Biochemie B.V, Haarlem, Netherlands
Aspartic acid	Sigma Life Science, Steinheim, Germany
Beta-alanine	Aldrich, Steinheim, Germany
Calcium citrate	Aldrich, Steinheim, Germany
Calcium panthothenate	Carl Roth, Karlsruhe, Germany
Cholesteryl benzoate	Sigma-Aldrich, Steinheim, Germany
Choline chloride	Duchefa Biochemie B.V, Haarlem, Netherlands
CuSO ₄ .5H ₂ O	ICN Biomedical, Mesa, CA, USA
Cysteine	Fluka, Buchs, Germany
FeCl ₃ .6H ₂ O	Carl Roth, Karlsruhe, Germany
Folic acid	TCl, Tokyo, Japan
Glutamic acid	Sigma Life Science, Steinheim, Germany
Glutamine	Fluka, Buchs, Germany
Glycine	Carl Roth, Karlsruhe, Germany
Histidine	Sigma Life Science, Steinheim, Germany
i-Inositol anhydrous	Sigma-Aldrich, Steinheim, Germany
Isoleucine	Carl Roth, Karlsruhe, Germany
KH ₂ PO ₄	Carl Roth, Karlsruhe, Germany
KOH	Fluka, Buchs, Germany
L-Ascorbic acid	Carl Roth, Karlsruhe, Germany
Leucine	Duchefa Biochemie B.V, Haarlem, Netherlands
Lysine HCl	Duchefa Biochemie B.V, Haarlem, Netherlands
Methionine	Sigma Life Science, Steinheim, Germany
MgSO ₄ .7H ₂ O	Carl Roth, Karlsruhe, Germany
MnCl ₂ .4H ₂ O	Merck, Darmstadt, Germany
NaCl	Carl Roth, Karlsruhe, Germany
Nicotinamide	Sigma-Aldrich, Steinheim, Germany
Ornithine HCl	Duchefa Biochemie B.V, Haarlem, Netherlands
p-Amino benzoic acid	Aldrich, Steinheim, Germany
Phenylalanine	Duchefa Biochemie B.V, Haarlem, Netherlands
Proline	Duchefa Biochemie B.V, Haarlem, Netherlands
Pyridoxine HCl	Duchefa Biochemie B.V, Haarlem, Netherlands
Riboflavin	Carl Roth, Karlsruhe, Germany
Serine	Carl Roth, Karlsruhe, Germany
Sucrose	Carl Roth, Karlsruhe, Germany
Thiamine HCl	Carl Roth, Karlsruhe, Germany
Threonine	Carl Roth, Karlsruhe, Germany
Tryptophan	Carl Roth, Karlsruhe, Germany
Tyrosine	Duchefa Biochemie B.V, Haarlem, Netherlands
Valine	Sigma-Aldrich, Steinheim, Germany
ZnCl ₂	Fluka, Buchs, Germany

Table IV: Recipe artificial diet. The artificial diet for *Brevicoryne brassicae* was adapted from A_0 by Febvay et al., the ingredients are listed in the order of addition⁹⁰.

Ingredient	Amount for 200 ml [mg]
Tyrosine	77,26
Glutamine	891,22
KH ₂ PO ₄	500
MgSO ₄ .7H ₂ O	484
Asparagine.H ₂ O	597,1
Aspartic acid	176,5
Tryptophan	85,5
Alanine	357,42
Beta-alanine	12,44
Arginine	489,8
Cysteine	59,18
Glutamic acid	298,72
Glycine	333,12
Histidine	201,3
Isoleucine	329,5
Leucine	463,12
Lysine HCl	702,18
Methionine	144,7
Phenylalanine	589,06
Proline	258,66
Serine	248,56
Threonine	254,32
Valine	381,7
L-Ascorbic acid	200
Ornithine HCl	18,82
Calcium citrate	20
Cholesteryl benzoate	5
p-Amino benzoic acid	20
Pyridoxine HCl	5
Riboflavin	1
Thiamine HCl	5
Nicotinamide	20
Folic acid	2
Calcium panthothenate	10
i-Inositol anhydrous	100
Choline chloride	100
CuSO ₄ .5H ₂ O	0,94
FeCl ₃ .6H ₂ O	8,9
MnCl ₂ .4H ₂ O	1,3
NaCl	5,08
ZnCl ₂	1,66
Sucrose (20%)	40g
adjust pH with KOH to pH 7,5	

Table V: Parameters of multi reaction monitoring (MRM), with Q1, m/z of quadrupole one; Q3, m/z of quadrupole three; DP, declustering potential; EP, entrance potential; CE, collision energy; CXP, collision cell exit potential.

Q1 Mass [Da]	Q3 Mass [Da]	Time [min]	ID	DP [volts]	EP [volts]	CE [volts]	CXP [volts]
178,8	89	6,2	Glucose-neg	-50	-9,5	-10	0
178,801	89	6,2	Fructose-neg	-50	-9	-12	-2
340,9	59	8,5	Saccharose-neg	-65	-10	-46	0
503,1	179	10,5	Raffinose-neg	-95	-10	-28	-4
665,2	179	11,5	Stachyose-neg	-100	-10	-48	-4
827,3	179	12,5	Verbascose-neg-2	-125	-10	-58	-4
341,031	160,898	8,5	Maltose-1	-50	-4	-10	-4
341,036	101	8,5	Lactose-2	-50	-3	-24	-2
341,03	88,924	8,5	Trehalose-2	-65	-11	-30	-2
219,932	118,81	3	NAcGlucosamine-1	-50	-4,5	-10	-4
148,892	88,92	5,5	Arabinose-1	-50	-8,5	-10	-2
989,4	179	14	Gly6-neg	-145	-10	-70	-3
1151,5	179	14	Gly7-neg	-155	-10	-80	-3
148,8	74	2,5	Xylose-1	-50	-9,5	-10	0
148,8	75	2,5	Xylose-2	-50	-9,5	-10	0

A.2.1. Calibration

Table VI: Script automated calibration. The mass and mobility calibration in DataAnalysis were done automatically using this mini script.

```
Analysis.RecalibrateAutomatically
```

```
Analysis.RecalibrateMobilityAutomatically
```

```
Analysis.Save
```

```
Form.Close
```

Table VII: Parameters of automated calibration. The mass and mobility calibration in DataAnalysis were done automatically using listed parameters.

Analysis Info		Acquisition Date 4/13/2021 3:55:27 PM	
Analysis Name	D:\Data\johanna_jore6814\210413 neg nNH2 calibr Mannitol\21041300-jr-negtims-NH2-blank_GA1_1_5686_4-13-2021.d	Operator	Demo User
Method	jr_negtims_sugars_200804_win10.m	Instrument	timsTOF
Sample Name	21041300-jr-negtims-NH2-blank		1844426.19
Comment			

Acquisition Parameter

Source Type	ESI	Ion Polarity	Negative	Set Nebulizer	1.8 Bar
Focus	Not active			Set Dry Heater	230 °C
Scan Begin	50 m/z	Set Capillary	4500 V	Set Dry Gas	10.0 l/min
Scan End	1500 m/z	Set End Plate Offset	-500 V	Set Divert Valve	Waste

DataAnalysis Method Part Parameter

Delete previously found compounds in selected range: yes

Sensitivity (SE1):	99
Sensitivity (SE2):	99
Area threshold:	off
Intensity threshold, absolute:	1000
Baseline smooth, minutes:	12
Baseline smooth, force:	0.1
Start end slope:	10
Valley filter:	10
Baseline noise correction:	off
Algorithm Version:	3.0
Spectrum type (Line/Profile):	Auto
Additional background subtraction (except MSn):	Peak (Start and end spectra)
Add UV spectrum, resp. mass spectrum:	no

Sensitivity:	100
Area threshold, relative:	5
Intensity threshold, absolute:	100
Valley filter:	off
Resolution:	250
Spectrum type (Line/Profile):	Line spectra only

Intensity threshold, positive:	1000
Intensity threshold, negative:	1000
Maximum number of compounds:	100000
Use retention time window:	no
m/z window:	0.5000
Use mobility window:	no
Fragments qualified by:	<no>
Filter for detected neutral losses only:	no
Spectrum type (Line/Profile):	Auto
Background subtraction (except MSn):	None
Add UV spectra if available	no
Advanced precursor determination:	no
Determine alternate precursor:	no
Separate by collision energy:	no

Internal signal to noise threshold:	3
Maximum number of overlapping compounds:	5
Apply base peak intensity:	no
Spectrum type (Line/Profile):	Auto
Cut-off intensity:	0.1
Add UV spectrum:	no

Internal signal to noise threshold:	1
Maximum number of overlapping compounds:	10
Apply base peak intensity:	yes
Spectrum type (Line/Profile):	Auto
Cut-off intensity:	0.1
Add UV spectrum:	no

Signal to noise threshold:	3
Correlation coefficient threshold:	0.7

Minimum compound length: 20 spectra
Smoothing width: 10
Additional smoothing: yes
Proteomics: yes
Spectrum type (Line/Profile): Line spectra only
Background subtraction: None
Delete peaks in range: yes

Mode: Proteomics
Load Fragments: yes

Include chromatogram: no
Spectrum type (Line/Profile): Line spectra only

Instrument type: <unknown>
Peak finder: Sum Peak
Use same sum width as used in acquisition: yes
Peak width (FWHM): 3 points
Signal to noise threshold: 1
Relative intensity threshold: 0.1
Absolute intensity threshold: 100
Filter exclusion masses: no
Use peak finder to calculate peak position: yes

Clear previous results: yes
Create neutral spectrum: no

Adduct ion, positive: +H
Adduct ion, negative: -H
MS Full Scan, Abundance cutoff: 2
MS Full Scan, Maximum charge: 5
MS MaxRes Scan, Abundance cutoff: 2
MS(n), Abundance cutoff: 0.5
MS(n), Maximum charge: 4
Allow precursor deconvolution from fragment spectra: no
Related ion deconvolution: no

Extend reconstructed mass envelope: no
Include shifted spectrum: no
Retain residual: no
Set precursor to mono-isotopic mass: yes
Auto apply: no

Delta rt: 1.5
Threshold sigma: 0.050
Detection tolerance: 0.005
Identification tolerance: 10.000
Use relative tolerances: no
relative Detection tolerance: 5.000
relative Identification tolerance: 5.000
Database name: C:\BDALSystemData\BuildingBlocks\TargetScreeningDataBase.csv
Use sample info XML: no
Retention time range start: 0.00
Retention time range end: 0.00
Retention time window half width: 45.00
Create chromatogram time slices: yes
Enable base peak chromatograms: yes
Evaluate qualifier ions: yes
Qualifier ion intensity threshold: 0
Use Dabase: no
GroupId: :
LCMethodId: :
MSMethodId: :
MatrixId: :
Sort Analytes: 4
Create Chromatograms Qual/Quan: no

Clear previous results: yes

<No libraries defined>

Search all libraries parallel	no	
Retention time database enabled	no	
Cross-match to all compound spectra	no	
Desired score	900	
Minimum score	400	
Minimum parameter match score	250	
Maximum number of spectra	10	
Sort results by	Purity	
Include precursor spectra for effective score calculation	yes	
Include UV spectra for effective score calculation	no	
Exclude precursor signals from fragment spectra	no	
Skip fragment spectra with low signals only	yes	
Minimum effective score	500	
Relative effective score difference	50	
Ignore library spectrum masses below measured mass range	no	
Ignore library spectrum masses above measured mass range	no	
Apply retention time matching	no	
Accepted retention time deviation	0.000	
Maximum retention time deviation	0.000	
Apply CCS matching	no	
Accepted CCS deviation	1.0	
Maximum CCS deviation	20.0	
Instrument Type	medium	
Ionization Method	low	
Polarity	forbidden	
MS vs. MS/MS	forbidden	
MS/MS Stage	medium	
Last Precursor Ion	none	
All Precursor Ions	none	
Product Ion	none	
Trap Drive	low	
Fragmentation Amplitude	low	
Isolation Width	none	
Collision Gas	none	
Collision Gas Pressure	none	
Reagent Ion	none	
Reagent Gas Pressure	none	
Collision Energy	none	
Peak Width	none	
Reflector	none	
Post Source Decay	none	
Charge Deconvoluted	none	
Add to existing compound:		If compound exists, add spectra without confirmation
Maximum number of (most abundant) masses	250	
Include retention time:	no	
Lower boundary formula:		
Upper boundary formula:		
Tolerance:	5 ppm	
Tolerance (MSn):	2 mDa	
Charge	1	
Maximum number of formulas:	500	
Relative intensity threshold:	10 %	
Filter H/C ratio, minimum	0	
Filter H/C ratio, maximum	3	
Electron configuration, MS:	Even	
Electron configuration, MS(n):	Both	
Sigma limit, MS:	0.02	
Sigma limit, MS(n):	0.05	
Automatically locate monoisotopic peak:	no	
Estimate carbon count:	yes	
Delete previously found results:	yes	
Include exclusion masses:	no	
Isotopic fine structure:	no	
Neutral loss tolerance:	2	

Intensity threshold, MS: 100
Intensity threshold, MS(n): 100
Filter abundant peaks automatically: no
Number of peaks to be explained: 5
Highlight unexplained intense peaks: no
Processing range left: 3
Processing range right: 5

<none>

Calibration group: ESI
Calibration list: Tuning Mix ES-TOF (ESI)

Name	m/z
C5H12NO2	118.0863
C6H19N3O6P3	322.0481
C12H19F12N3O6P3	622.0290
C18H19F24N3O6P3	922.0098
C24H19F36N3O6P3	1221.9906
C30H19F48N3O6P3	1521.9715
C36H19F60N3O6P3	1821.9523
C42H19F72N3O6P3	2121.9331
C48H19F84N3O6P3	2421.9140
C54H19F96N3O6P3	2721.8948
C2F3O2	112.9856
C6HF9N3O	301.9981
C12HF21N3O	601.9790
C20H18F27N3O8P3	1033.9881
C26H18F39N3O8P3	1333.9689
C32H18F51N3O8P3	1633.9498
C38H18F63N3O8P3	1933.9306
C44H18F75N3O8P3	2233.9115
C50H18F87N3O8P3	2533.8923
C56H18F99N3O8P3	2833.8731

Mode: Quadratic
Search range (m/z): 0.05
Intensity threshold: 1000

Use calibration segment: no
Start: 0.1
End: 0.3
Fall-back calibration mode: yes
Use spectrum type: 0
Retain calibration data: yes
Perform lock mass calibration: no

Calibration group: ESI
Calibration list: Tuning Mix ES-TOF (ESI)

Name	m/z
C5H12NO2	118.0863
C6H19N3O6P3	322.0481
C12H19F12N3O6P3	622.0290
C18H19F24N3O6P3	922.0098
C24H19F36N3O6P3	1221.9906
C30H19F48N3O6P3	1521.9715
C36H19F60N3O6P3	1821.9523
C42H19F72N3O6P3	2121.9331
C48H19F84N3O6P3	2421.9140
C54H19F96N3O6P3	2721.8948
C2F3O2	112.9856
C6HF9N3O	301.9981
C12HF21N3O	601.9790
C20H18F27N3O8P3	1033.9881
C26H18F39N3O8P3	1333.9689
C32H18F51N3O8P3	1633.9498
C38H18F63N3O8P3	1933.9306
C44H18F75N3O8P3	2233.9115
C50H18F87N3O8P3	2533.8923

C56H18F99N3O8P3 2833.8731

Mode: Linear
Search range (m/z): 0.1
Intensity threshold: 0

Use calibration segment: no
Start: 0.1
End: 0.3
Fall-back calibration mode: yes
Use spectrum type: 0
Retain calibration data: yes
Perform lock mass calibration: no

Compound Number
Retention Time (apex)
Peak: Area
Integration Type
Peak: Intensity
Peak: Signal-to-Noise Ratio
Related Trace
Maximum Mass-to-Charge Ratio
Peak: Full Width at Half Maximum
Mobility, 1/KO
Mob.Peak: Resolution, 1/KO
Collision Cross Section [\AA^2]

Compound Number
Mass-to-Charge Ratio
Resolving Power
Signal-to-Noise Ratio
Intensity
Relative Intensity [%]
Full Width at Half Maximum

Measured m/z
Index
Ion Formula
m/z
Error [ppm]
mSigma
mSigma Rank
Score
Rings and Double Bonds
Electron Configuration
Nitrogen Rule

Mass precision: 4
Retention time precision: 2
Mobility precision: 3
CCS precision: 2
Wavelength precision: 1
Intensity precision: 0
Area precision: -1
Signal-to-noise precision: 1
Percent precision: -1
Size of largest structure: 30
Label trace peaks with: Index, Mobility

Smoothing
Smoothing algorithm: 1
Smoothing width (sec): 0.1
Cycles: 1
Replace original: no
Disable original: no
Use same color as original: yes
Baseline subtraction
Flatness: 0.8
Replace original: no
Disable original: no

Use same color as original: yes

Smoothing

Smoothing algorithm: 0
Smoothing width (V·s/cm²): 0.005
Cycles: 1
Replace original: no
Disable original: yes
Use same color as original: yes
Baseline subtraction
Flatness: 0.8
Replace original: no
Disable original: yes
Use same color as original: yes

Smoothing

Smoothing algorithm: 1
Smoothing width (Da): 0.2
Cycles: 1
Replace original: no
Disable original: no
Use same color as original: yes
Baseline subtraction
Flatness: 0.8
Replace original: no
Disable original: no
Use same color as original: yes

Mode: Xpose
Ratio: 5
Retention time window: 0.5
Inherit traces: yes

XML, Include detailed information: no
XML, Include peptide database query information: yes
XML, Include full peptide database query information: yes
Mascot, Include peptide database query information: yes
Protein Analysis, Export MGF: yes
Protein Analysis, Export XML: yes

Global charge limitation: 1+, 2+ and 3+
Export: Mixed list
Include S/N ratio and FWHM: no
Normalize MS(n) data: no
Export deconvoluted peaks as single-charged ion: no
Prefer Full Scan spectrum deconvolution results: yes
Export N most abundant non-deconvoluted MS/MS signals: 50
Intensity threshold for non-deconvoluted MS/MS signals: 100
Export N most abundant deconvoluted MS signals: 2
Export N most abundant non-deconvoluted MS signals: 20

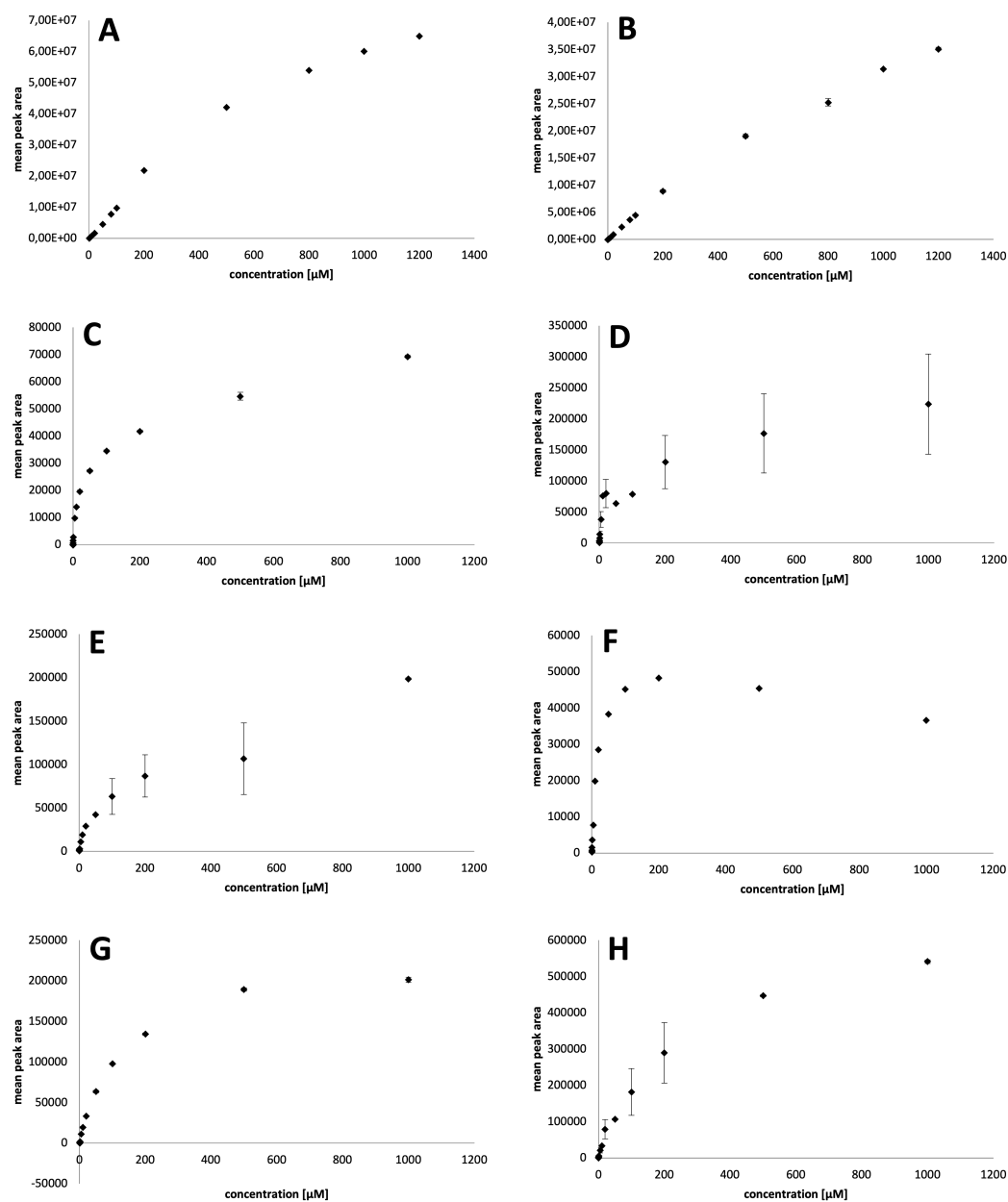


Figure VI: Calibration curves. For quantitative analysis calibration curves of saccharide standards were created of glucose (A) and fructose (B) via API5000 and mannitol (C), sucrose (extracted ion mobility) (D), trehalose (extracted ion mobility) (E), maltose (extracted ion mobility) (F), gentiobiose (G) and melezitose (extracted ion mobility) (H) via timsTOF.

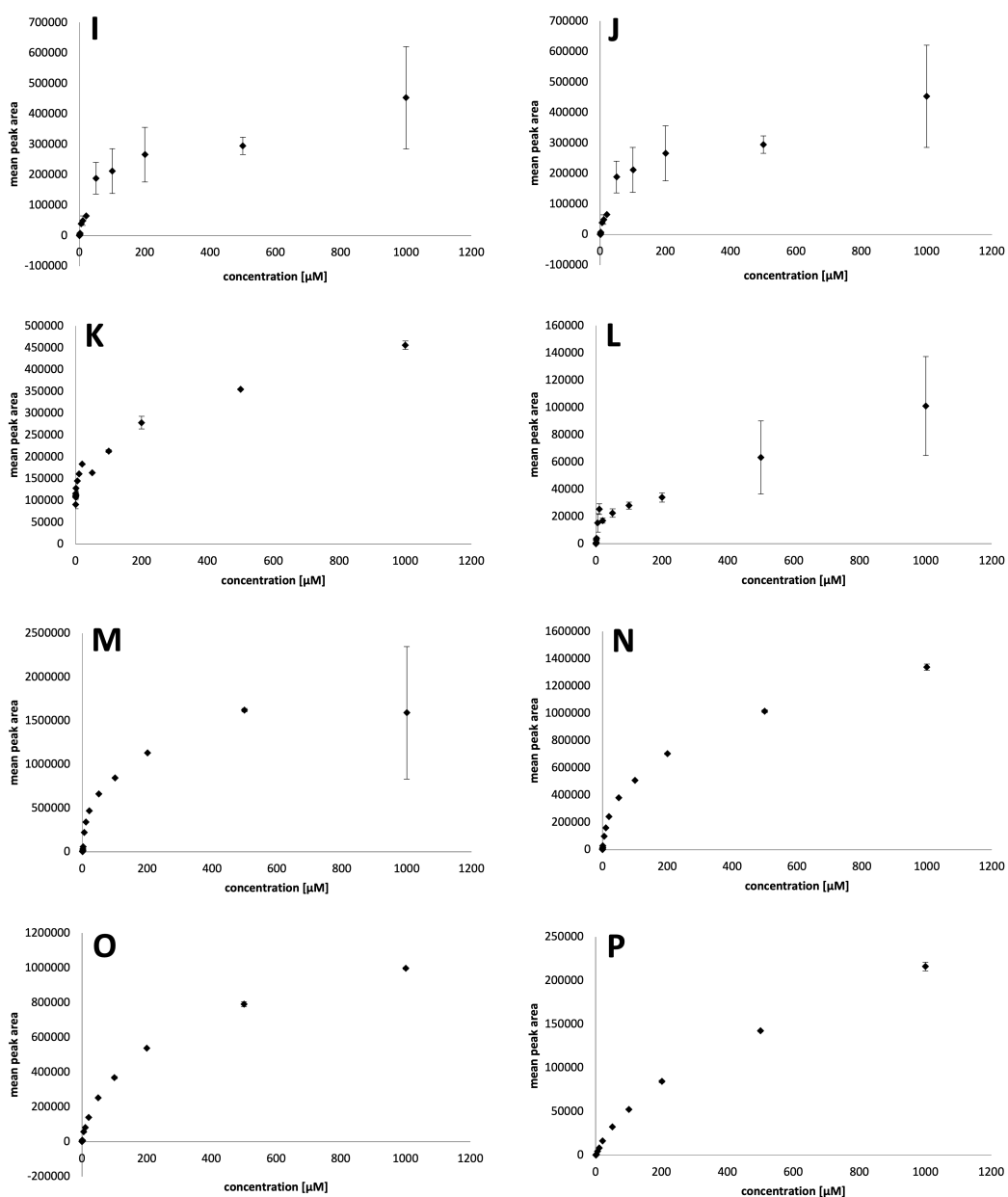


Figure VII: Calibration curves (continued). For quantitative analysis calibration curves of saccharide standards were created of kestose (extracted ion mobility) (I), raffinose (J) maltotriose (K), panose (extracted ion mobility) (L), maltotetraose (M), maltopentaose (N), maltohexaose (O) and maltoheptaose (P) via timsTOF.

A.2.2. R Code

R Code supporting quantitative analysis. The custom R script (created by Andreas Neudecker) was used to transform peak areas into concentration according to the calibration curves.

```
library(readxl)

# Input file
df <- read_excel("calibration.xlsx", skip = 11, sheet = "Maltose")

# Supplementary functions
lossFun <- function(basis, df) {
  df <- na.omit(df[c("concentration", "areatarget")])
  conc <- unique(df$concentration)
  area <- unlist(lapply(conc, function(i)
    mean(df$areatarget[df$concentration == i])))

  function(a) {
    vals <- mapply(function(coef, fun) {
      coef*fun(conc)
    }, coef = a, fun = basis)

    sqrt(mean((apply(vals, 1, sum) - area)^2))
  }
}

solution <- function(basis, df) {
  ff <- lossFun(basis, df)
  res <- optim(rep(1, length(basis)), ff)
  res$par
}

buildFun <- function(coef, basis) {
  function(x) {
    vals <- mapply(function(c, f) {
      c*f(x)
    }, coef, basis)
  }
}
```

```
    if (is.null(dim(vals))) sum(vals)
    else apply(vals, 1, sum)
  }
}

## Define base
basis <- list(sqrt, function(x) log(x + 1))
s <- solution(basis, calibration)

## Build fitted function
fun <- buildFun(s, basis)

# Plot function
plot(df$concentration, df$areatarget)
lines(0:1000, fun(0:1000), col = "orange", lwd = 2)

## Inverse
inverse <- function(y) {
  uniroot(function(x) fun(x) - y, lower = 0.0, upper = 40000)[[1]]
}

# Inverse for table
ra <- read_excel("quant-sap_HD-maize.xlsx", sheet= "Tabelle4")

for (col in 2:3){
  column =ra[[col]]
  for (value in 1:length(column)){
    column[value]=inverse(column[value])
  }
  ra[[col]]=column
  print("Done")}

# Inverse for one point
inverse(1338281.208)
```

Table VIII: Constants used for CCS calculation. Following constants were used to transform mobility into CCS values using the Mason-Schamp-Equation⁵⁶.

Name	Symbol	Value	Unit
Mass of the ion	m_i	28,0134	Da
Da in kg		1,6605E-27	
Temperature	T	305	K
Pressure	p	1	atm
Absolute integer charge state of the ion	z	1	
Loschmidt's number	N_0	2,6868E+25	1/m ³
Boltzmann constant	k_B	1,3806E-23	J*kg
Charge of electron	e	1,6022E-19	A*s

A.3. Results

A.3.1. Ion Mobility and CCS Library

Table IX: Ion mobility and CCS library of saccharide standards. Utilising UHPLC-IM-MS a comprehensive library of 47 commercially available standards was generated including molecular weight (MW), retention times of both amine (NH₂) and graphite column (PGC), mass-to-charge ratios (m/z) of observed ion species in negative (black) and positive (blue) ionisation mode and according mean values of inverse standard mobilities 1/K₀, standard deviations (SD) and collision cross sections (CCS) calculated by using the Mason-Schamp-equation.

Compound name	MW [g/mol]	RT (Average ± SD) [min]			m/z	Mobility 1/K ₀ (Average ± SD) [V·s·cm ⁻²] Ion species	Mobility 1/K ₀ (Average ± SD) [V·s·cm ⁻²]		TM _{CCS} (Average ± SD) [Å ²]	
		NH ₂	NH ₂ (API5000)	PGC			NH ₂	PGC	NH ₂	PGC
Arabinose	150,13	1,24 ± 0,02	5,54 ± 0	1,63 ± 0	149,008	[M-H] ⁻	0,577 ± 0,002		126,01 ± 0,448	
Xylose	150,13	1,23 ± 0	5,57 ± 0,01	1,8 ± 0,01	149,009	[M-H] ⁻	0,578 ± 0,002	0,841 ± 0,002	126,228 ± 0,544	183,628 ± 0,544
Allose	180,16	6,11 ± 0,05	6,52 ± 0,04	2,25 ± 0,01	179,056	[M-H] ⁻	0,847 ± 0	0,848 ± 0	182,469 ± 0,102	182,54 ± 0,102
					359,120	[2M-H] ⁻	0,846 ± 0	0,845 ± 0,001	175,963 ± 0,098	175,686 ± 0,17
Fructose	180,16	5,8 ± 0,06	6,15 ± 0,04	1,74 ± 0,04	179,056	[M-H] ⁻		0,838 ± 0,002		180,531 ± 0,537
					359,121	[2M-H] ⁻		0,896 ± 0,032		186,29 ± 6,653
Fucose	164,16	4,77 ± 0,01		3,42 ± 0	163,062	[M-H] ⁻				
				4,05 ± 0,01						
Galactose	180,16	6,75 ± 0,08	7,2 ± 0,03	2,47 ± 0,03	179,056	[M-H] ⁻		0,84 ± 0		180,961 ± 0,102
				2,79 ± 0,03						
Glucose	180,16	6,78 ± 0,09	7,23 ± 0,05	2,21 ± 0,04	179,056	[M-H] ⁻		0,848 ± 0,002	190,171 ± 9,659	182,54 ± 0,406
					359,120	[2M-H] ⁻	0,915 ± 0,046	0,869 ± 0,015		180,607 ± 3,038
Mannose	180,16	6,32 ± 0,06	6,7 ± 0,05	2,24 ± 0,03	179,056	[M-H] ⁻		0,851 ± 0,001		183,258 ± 0,176
				2,59 ± 0,04						
Psicose/Allulose	180,16	4,97 ± 0,01	5,15 ± 0,03	2,34 ± 0,02	179,056	[M-H] ⁻		0,794 ± 0,006		170,912 ± 1,366
		8,07 ± 0,01								
Rhamnose	164,16	4,42 ± 0		2,65 ± 0,01	163,062	[M-H] ⁻				
				3,1 ± 0,01						
Sorbitol	180,16	6,15 ± 0,07	6,51 ± 0,04	2 ± 0	179,056	[M-H] ⁻		0,844 ± 0,002		181,679 ± 0,442
					359,121	[2M-H] ⁻	0,866 ± 0,011	180,122 ± 2,261		
Tagatose	180,16	5,78 ± 0,05	6,08 ± 0,04	1,87 ± 0,02	179,056	[M-H] ⁻	1,055 ± 0	0,838 ± 0,002	227,189 ± 0	180,53 ± 0,508
Galactitol	182,17	6,59 ± 0,04		1,78 ± 0,01	181,072	[M-H] ⁻	0,606 ± 0	0,608 ± 0	130,4 ± 0	130,831 ± 0
myo-Inositol	180,16	8,42 ± 0,03		1,48 ± 0,04	179,056	[M-H] ⁻	0,607 ± 0,001	0,607 ± 0	130,642 ± 0,203	130,714 ± 0
					359,121	[2M-H] ⁻	0,848 ± 0,001	0,847 ± 0,001	176,31 ± 0,17	176,102 ± 0,17
					203,052	[M+Na] ⁺	0,812 ± 0		173,459 ± 0	
							0,901 ± 0,001		192,471 ± 0,214	
		0,955 ± 0,04		203,9 ± 8,438						
Mannitol	182,17	6,55 ± 0,02		1,97 ± 0,01	181,072	[M-H] ⁻	0,608 ± 0,001	0,609 ± 0	130,903 ± 0,268	131,046 ± 0
Sorbitol	182,17	6,36 ± 0,06		2,14 ± 0,02	181,072	[M-H] ⁻	0,609 ± 0	0,609 ± 0	130,974 ± 0,101	131,046 ± 0

Rutinose	326,30	7,82 ± 0,05	7,11 ± 0 7,78 ± 0	325,114	[M-H] ⁻		0,841 ± 0		175,585 ± 0,098
				361,090	[M+Cl] ⁻	0,834 ± 0,001	0,834 ± 0	173,434 ± 0,196	173,296 ± 0,098
				371,119	[M+HCOO] ⁻	0,841 ± 0	0,839 ± 0	174,581 ± 0,098	174,304 ± 0,098
				651,235	[2M-H] ⁻	1,14 ± 0	1,141 ± 0,001	233,21 ± 0,096	233,347 ± 0,167
				349,110	[M+Na] ⁺	0,842 ± 0,001		175,14 ± 0,104	
						1,16 ± 0		241,325 ± 0,104	
Cellobiose	342,30	8,7 ± 0,04	9,67 ± 0 9,85 ± 0	365,105	[M+K] ⁺	0,836 ± 0,001		173,712 ± 0,208	
						1,16 ± 0,002		240,932 ± 0,312	
				341,109	[M-H] ⁻		0,602 ± 0,365		125,34 ± 75,946
				377,085	[M+Cl] ⁻	0,855 ± 0,001	0,853 ± 0	177,389 ± 0,196	177,113 ± 0,098
				387,114	[M+HCOO] ⁻	0,859 ± 0	0,859 ± 0,001	178,129 ± 0	178,198 ± 0,259
				683,225	[2M-H] ⁻	1,126 ± 0	1,127 ± 0,001	230,125 ± 0,096	230,329 ± 0,193
				365,105	[M+Na] ⁺	0,85 ± 0		176,621 ± 0	
						1,127 ± 0		234,248 ± 0,098	
						1,152 ± 0		239,304 ± 0,098	
						0,886 ± 0		183,974 ± 0	
Gentiobiose	342,30	9,37 ± 0,06	8,58 ± 0,01 9,22 ± 0,02	372,308	pos	0,86 ± 0		178,501 ± 0,098	
				381,079	[M+K] ⁺	1,105 ± 0		229,264 ± 0	
				707,221	[2M+Na] ⁺	1,127 ± 0,002		230,039 ± 0,347	
						1,151 ± 0,001		235,007 ± 0,289	
				341,109	[M-H] ⁻		0,859 ± 0		179,007 ± 0,098
							0,83 ± 0		172,897 ± 0
Isomaltose	342,30	9,19 ± 0,03	7,01 ± 0,01 7,57 ± 0	377,085	[M+Cl] ⁻	0,847 ± 0,001		175,798 ± 0,169	
				387,114	[M+HCOO] ⁻		0,858 ± 0,001		177,922 ± 0,169
				683,225	[2M-H] ⁻	1,166 ± 0,001	1,166 ± 0,001	238,297 ± 0,193	238,161 ± 0,193
				365,105	[M+Na] ⁺	0,847 ± 0		175,998 ± 0	
						1,158 ± 0		240,689 ± 0,098	
				381,079	[M+K] ⁺	0,861 ± 0,001		178,57 ± 0,196	
Isomaltulose	342,30	9,19 ± 0,03	7,01 ± 0,01 7,57 ± 0	377,085	[M+Cl] ⁻	0,837 ± 0		173,723 ± 0	
				387,114	[M+HCOO] ⁻		0,85 ± 0		176,194 ± 0,098
				683,225	[2M-H] ⁻	1,133 ± 0,001	1,134 ± 0,001	231,487 ± 0,167	231,691 ± 0,167
				365,105	[M+Na] ⁺	0,846 ± 0		175,72 ± 0,098	
						1,138 ± 0,001		236,464 ± 0,17	
				381,079	[M+K] ⁺	0,853 ± 0,001		176,979 ± 0,169	
Isomaltulose/ Pallatinose	342,30	8,25 ± 0,06	7,06 ± 0,02	707,221	[2M+Na] ⁺	1,144 ± 0,001		237,287 ± 0,196	
						1,137 ± 0		232,081 ± 0,096	
				341,109	[M-H] ⁻		0,807 ± 0,002		168,106 ± 0,34
							0,851 ± 0		177,271 ± 0
				377,085	[M+Cl] ⁻	0,836 ± 0,002	0,835 ± 0	173,515 ± 0,339	173,238 ± 0,098
				683,225	[2M-H] ⁻	1,126 ± 0	1,126 ± 0	230,056 ± 0	230,125 ± 0,096
Lactose	342,30	8,72 ± 0,05	7,91 ± 0,01 8,45 ± 0,02	365,105	[M+Na] ⁺	0,836 ± 0		173,781 ± 0,098	
				381,100	[M+K] ⁺	0,856 ± 0,001		177,601 ± 0,169	
				341,109	[M-H] ⁻		0,805 ± 0,001		167,897 ± 0
				377,085	[M+Cl] ⁻		0,847 ± 0		176,352 ± 0,098
				387,114	[M+HCOO] ⁻		0,849 ± 0		176,125 ± 0,098
				683,225	[2M-H] ⁻	1,117 ± 0		228,15 ± 0,096	231,555 ± 0,255
Leucrose	342,30	8,17 ± 0,03	6,92 ± 0,01 -7,54 ± 0,03 -7,66 ± 0,02	365,105	[M+Na] ⁺	0,837 ± 0,001		173,85 ± 0,196	
						1,125 ± 0		233,763 ± 0	
				381,079	[M+K] ⁺	0,852 ± 0,001		176,703 ± 0,196	
						1,099 ± 0		228,019 ± 0	
						1,125 ± 0		233,414 ± 0	
				707,221	[2M+Na] ⁺	1,123 ± 0		229,29 ± 0	
				341,109	[M-H] ⁻	0,807 ± 0,001	0,806 ± 0	168,002 ± 0,104	167,828 ± 0,098
							0,843 ± 0		175,605 ± 0
				377,085	[M+Cl] ⁻	0,837 ± 0	0,835 ± 0	173,792 ± 0,098	173,238 ± 0,098
				387,114	[M+HCOO] ⁻		0,84 ± 0,001		174,258 ± 0,196
683,225	[2M-H] ⁻	1,143 ± 0,001	1,145 ± 0,001	233,462 ± 0,193	233,87 ± 0,255				
Maltose	342,30	8,79 ± 0,06	7,96 ± 0,01 8,11 ± 0,02	365,105	[M+Na] ⁺	0,826 ± 0,001		171,565 ± 0,196	
						1,109 ± 0		230,369 ± 0,098	
				381,100	[M+K] ⁺	0,86 ± 0,001		178,431 ± 0,169	
						1,125 ± 0,001		233,413 ± 0,169	
				341,109	[M-H] ⁻		0,804 ± 0		179,563 ± 0
							0,862 ± 0		
377,085	[M+Cl] ⁻	0,857 ± 0	0,856 ± 0	177,874 ± 0	177,666 ± 0				
			0,861 ± 0,001		178,613 ± 0,196				

				683,225	[2M-H] ⁻	1,164 ± 0	1,164 ± 0,001	237,752 ± 0,096	237,82 ± 0,167
				365,105	[M+Na] ⁺	0,85 ± 0		176,552 ± 0,098	
						1,168 ± 0		242,698 ± 0	
				707,221	[2M+Na] ⁺	1,163 ± 0,001		237,457 ± 0,289	
Maltulose	342,30	8,22 ± 0,06	-6,86 ± 0,03						
			7,45 ± 0,02	341,109	[M-H] ⁻	0,805 ± 0,001	0,806 ± 0	167,62 ± 0,26	167,828 ± 0,098
				377,085	[M+Cl] ⁻	0,846 ± 0	0,846 ± 0	201,852 ± 0	178,174 ± 0,098
				387,114	[M+HCOO] ⁻	0,855 ± 0,001	0,855 ± 0,001	175,66 ± 0,098	175,66 ± 0,098
				683,225	[2M-H] ⁻	1,134 ± 0	1,134 ± 0,001	231,623 ± 0,096	231,691 ± 0,167
						1,162 ± 0	1,163 ± 0,001	237,616 ± 0,167	
				365,105	[M+Na] ⁺	0,848 ± 0		176,275 ± 0,098	
Melibiose	342,30	9,26 ± 0,05	7,36 ± 0,01						
			8,32 ± 0,01	341,109	[M-H] ⁻		0,806 ± 0,002		167,828 ± 0,491
							0,853 ± 0		177,619 ± 0,098
				377,085	[M+Cl] ⁻	0,839 ± 0	0,839 ± 0,001	174,207 ± 0,098	174,069 ± 0,196
				387,114	[M+HCOO] ⁻		0,851 ± 0	176,885 ± 0	176,401 ± 0,098
				683,225	[2M-H] ⁻	1,147 ± 0	1,147 ± 0,001	234,347 ± 0	234,347 ± 0,167
						0,843 ± 0		175,166 ± 0	
				365,105	[M+Na] ⁺	1,163 ± 0		241,659 ± 0	
				381,079	[M+K] ⁺	0,856 ± 0		177,533 ± 0,098	
						1,175 ± 0,001		243,718 ± 0,196	
				707,221	[2M+Na] ⁺	1,161 ± 0		237,049 ± 0	
Nigerose	342,30	8,61 ± 0,03	8,3 ± 0,01						
			8,85 ± 0,01	341,109	[M-H] ⁻		0,856 ± 0		178,382 ± 0,098
							0,992 ± 0,002		206,574 ± 0,354
				377,085	[M+Cl] ⁻	0,848 ± 0,001	0,847 ± 0	176,006 ± 0,169	175,867 ± 0,098
				387,114	[M+HCOO] ⁻	0,857 ± 0,001	0,856 ± 0	177,611 ± 0,104	177,576 ± 0,098
				683,225	[2M-H] ⁻	1,153 ± 0	1,154 ± 0,001	235,573 ± 0	235,777 ± 0,167
						0,836 ± 0		173,781 ± 0,098	
				365,105	[M+Na] ⁺	1,121 ± 0,001		232,863 ± 0,196	
						1,141 ± 0		237,157 ± 0,098	
Sophorose	342,30	8,82 ± 0,05	9,17 ± 0						
				341,109	[M-H] ⁻	0,805 ± 0			167,481 ± 0
							0,88 ± 0		183,382 ± 0,098
				377,085	[M+Cl] ⁻	0,871 ± 0	0,871 ± 0	180,849 ± 0,098	180,71 ± 0,098
				387,114	[M+HCOO] ⁻		0,88 ± 0		182,553 ± 0,098
				683,225	[2M-H] ⁻	1,142 ± 0,001	1,142 ± 0,001	233,394 ± 0,193	233,257 ± 0,255
						1,183 ± 0,001	1,183 ± 0,001	241,702 ± 0,167	241,702 ± 0,167
				365,105	[M+Na] ⁺	0,851 ± 0		176,759 ± 0,098	
						1,193 ± 0,003		247,962 ± 0,686	
				381,079	[M+K] ⁺	0,861 ± 0		178,708 ± 0,098	
						1,172 ± 0,003		243,234 ± 0,641	
				707,221	[2M+Na] ⁺	1,183 ± 0		241,609 ± 0,096	
Sucrose	342,30	8,02 ± 0,04	7,67 ± 0,01						
				341,109	[M-H] ⁻	0,805 ± 0	0,806 ± 0	167,759 ± 0,098	167,828 ± 0,098
				377,085	[M+Cl] ⁻	0,828 ± 0,001	0,828 ± 0	171,855 ± 0,169	171,855 ± 0
				387,114	[M+HCOO] ⁻	0,837 ± 0,001	0,838 ± 0,001	173,463 ± 0,104	173,705 ± 0,196
				683,225	[2M-H] ⁻	1,115 ± 0,001	1,116 ± 0	227,877 ± 0,255	227,945 ± 0,096
						0,826 ± 0		171,634 ± 0	
				365,105	[M+Na] ⁺	1,112 ± 0,001		231,131 ± 0,259	
Trehalose	342,30	8,72 ± 0,06	6,91 ± 0,01						
				341,109	[M-H] ⁻	0,813 ± 0	0,813 ± 0,001	169,425 ± 0,098	169,286 ± 0,26
				377,085	[M+Cl] ⁻	0,834 ± 0	0,835 ± 0,001	173,169 ± 0,098	173,308 ± 0,169
				387,114	[M+HCOO] ⁻	0,848 ± 0,001	0,847 ± 0	175,848 ± 0,169	175,71 ± 0,098
				683,225	[2M-H] ⁻	1,127 ± 0,001	1,128 ± 0,001	230,329 ± 0,255	230,465 ± 0,167
						0,835 ± 0,001		173,504 ± 0,17	
				365,105	[M+Na] ⁺	1,137 ± 0		236,256 ± 0	
a,b-Trehalose	342,30	8,68 ± 0,05	8,25 ± 0						
				341,109	[M-H] ⁻	0,826 ± 0,001	0,827 ± 0	172,133 ± 0,196	172,202 ± 0,098
							0,862 ± 0		179,493 ± 0,098
				377,085	[M+Cl] ⁻	0,853 ± 0,001	0,853 ± 0	176,974 ± 0,196	177,044 ± 0
				387,114	[M+HCOO] ⁻	0,861 ± 0	0,861 ± 0	178,475 ± 0,098	178,475 ± 0,098
				683,225	[2M-H] ⁻	1,181 ± 0,001	1,182 ± 0,001	241,294 ± 0,289	241,498 ± 0,167
						0,841 ± 0,001		174,751 ± 0,17	
				365,105	[M+Na] ⁺				
Trehalulose	342,30	-8,05 ± 0,01	5,99 ± 0,02						
		8,29 ± 0,02	7,07 ± 0,01	341,109	[M-H] ⁻	0,806 ± 0,001	0,844 ± 0,001	167,897 ± 0,17	175,883 ± 0,196
			7,74 ± 0,07			0,83 ± 0	0,829 ± 0	172,201 ± 0,098	172,131 ± 0,098
				377,085	[M+Cl] ⁻		0,845 ± 0		175,295 ± 0,098
				387,114	[M+HCOO] ⁻				
				683,225	[2M-H] ⁻	1,134 ± 0,001	1,136 ± 0	231,759 ± 0,255	232,032 ± 0,096
						0,837 ± 0		173,989 ± 0,098	
				365,105	[M+Na] ⁺	1,131 ± 0		234,94 ± 0,098	
						0,843 ± 0		174,835 ± 0,098	
				381,079	[M+K] ⁺	1,119 ± 0,002		232,1 ± 0,391	
Turanose	342,30	8,01 ± 0,05	6,83 ± 0,01						
				341,109	[M-H] ⁻		0,846 ± 0	167,897 ± 0	176,23 ± 0

				377,085	[M+Cl] ⁻	0,976 ± 0,002		203,379 ± 0,354	
				387,114	[M+HCOO] ⁻	0,838 ± 0	0,836 ± 0,001	173,999 ± 0,098	173,515 ± 0,169
				683,225	[2M-H] ⁻	1,122 ± 0	0,846 ± 0		175,433 ± 0
				365,105	[M+Na] ⁺	0,829 ± 0	1,122 ± 0	229,307 ± 0,096	229,239 ± 0
						1,138 ± 0		172,257 ± 0	
								236,533 ± 0,098	
Galactinol	342,30	10,34 ± 0,08	6,51 ± 0,01	341,109	[M-H] ⁻	0,806 ± 0,001	0,806 ± 0	167,897 ± 0,17	
				377,085	[M+Cl] ⁻	0,845 ± 0	0,845 ± 0,001	175,383 ± 0	167,219 ± 0,098
				387,114	[M+HCOO] ⁻	0,855 ± 0,001	0,855 ± 0	177,23 ± 0,259	175,226 ± 0,169
				683,225	[2M-H] ⁻	1,165 ± 0	1,165 ± 0	238,093 ± 0,096	174,62 ± 0,096
				365,105	[M+Na] ⁺	0,844 ± 0		175,374 ± 0	
Erlöse	504,44	9,77 ± 0,05	10,25 ± 0	503,162	[M-H] ⁻	0,985 ± 0,001	0,985 ± 0	202,73 ± 0,194	202,593 ± 0,097
				539,138	[M+Cl] ⁻	0,998 ± 0		204,906 ± 0,097	
				549,167	[M+HCOO] ⁻	1,013 ± 0	1,011 ± 0,001	207,893 ± 0,097	207,483 ± 0,194
				1007,331	[2M-H] ⁻	1,292 ± 0,001	1,291 ± 0	262,295 ± 0,166	262,159 ± 0,096
				527,157	[M+Na] ⁺	0,991 ± 0		203,651 ± 0	
				543,131	[M+K] ⁺	0,984 ± 0		202,063 ± 0	
				1031,330	[2M+Na] ⁺	1,29 ± 0,006		261,738 ± 1,287	
Isomaltotriose	504,44	11,05 ± 0,07	9,19 ± 0	503,162	[M-H] ⁻	0,982 ± 0	0,982 ± 0	202,044 ± 0	202,113 ± 0,097
			9,78 ± 0,01	539,138	[M+Cl] ⁻	1,01 ± 0,001	1,01 ± 0	207,439 ± 0,168	207,371 ± 0,097
				549,167	[M+HCOO] ⁻	1,025 ± 0,001	1,025 ± 0	210,425 ± 0,168	210,425 ± 0
				1007,331	[2M-H] ⁻	1,37 ± 0	1,367 ± 0,006	278,197 ± 0,096	277,419 ± 1,117
				527,157	[M+Na] ⁺	1,012 ± 0,001		208,035 ± 0,194	
				543,131	[M+K] ⁺	1,01 ± 0,001		207,333 ± 0,194	
				1031,330	[2M+Na] ⁺	1,377 ± 0,002		279,53 ± 0,506	
Kestose	504,44	9,75 ± 0,05	9,95 ± 0	503,162	[M-H] ⁻	0,983 ± 0,001	0,983 ± 0,001	202,25 ± 0,168	202,182 ± 0,194
				539,138	[M+Cl] ⁻	1,002 ± 0,001	0,997 ± 0,002	205,728 ± 0,194	204,838 ± 0,422
				549,167	[M+HCOO] ⁻	1,009 ± 0,001	1,009 ± 0,001	207,072 ± 0,256	207,141 ± 0,29
				1007,331	[2M-H] ⁻	1,313 ± 0,001	1,314 ± 0	266,558 ± 0,166	266,828 ± 0,096
				505,175	[M+H] ⁺	0,811 ± 0,001		166,775 ± 0,257	
						0,922 ± 0		189,611 ± 0,097	
				527,157	[M+Na] ⁺	0,982 ± 0,001		201,87 ± 0,256	
				543,131	[M+K] ⁺	0,989 ± 0,001		203,158 ± 0,194	
				1031,330	[2M+Na] ⁺	1,334 ± 0,002		270,668 ± 0,345	
Maltotriose	504,44	10,49 ± 0,07	9,8 ± 0	503,161	[M-H] ⁻		1,008 ± 0,001	212,881 ± 0,097	207,462 ± 0,194
			10,19 ± 0	539,138	[M+Cl] ⁻	1,016 ± 0,001	1,018 ± 0	208,74 ± 0,256	209,014 ± 0,097
				549,167	[M+HCOO] ⁻	1,035 ± 0	1,034 ± 0	212,41 ± 0,097	212,204 ± 0,097
				1007,331	[2M-H] ⁻	1,286 ± 0,004	1,284 ± 0	261,144 ± 0,818	260,738 ± 0,096
				527,157	[M+Na] ⁺	1,019 ± 0,001		209,474 ± 0,256	
				543,131	[M+K] ⁺	1,03 ± 0,002		211,44 ± 0,422	
				1031,330	[2M+Na] ⁺	1,334 ± 0,004		270,803 ± 0,747	
Melezitose	504,44	9,65 ± 0,05	8,41 ± 0	503,162	[M-H] ⁻	0,948 ± 0	0,948 ± 0,001	195,118 ± 0,097	194,98 ± 0,194
				539,138	[M+Cl] ⁻	0,974 ± 0	0,97 ± 0,001	199,977 ± 0,097	199,156 ± 0,194
				549,167	[M+HCOO] ⁻	0,982 ± 0	0,98 ± 0,001	201,598 ± 0	201,119 ± 0,194
				1007,331	[2M-H] ⁻	1,325 ± 0,001	1,326 ± 0	268,994 ± 0,166	269,197 ± 0
				527,157	[M+Na] ⁺	0,965 ± 0,001		198,377 ± 0,194	
						1,326 ± 0,001		272,563 ± 0,256	
				543,131	[M+K] ⁺	0,969 ± 0,001		199,051 ± 0,194	
						1,334 ± 0,002		273,935 ± 0,335	
				1031,330	[2M+Na] ⁺	1,329 ± 0,001		269,721 ± 0,287	
Panose	504,44	10,74 ± 0,04	9,69 ± 0	503,162	[M-H] ⁻	0,967 ± 0	0,968 ± 0,001	198,89 ± 0,097	199,164 ± 0,168
				539,138	[M+Cl] ⁻	0,996 ± 0,001	0,997 ± 0	204,564 ± 0,168	204,701 ± 0,097
				549,167	[M+HCOO] ⁻	1,016 ± 0	1,017 ± 0	208,646 ± 0,097	208,714 ± 0,097
				1007,331	[2M-H] ⁻	1,331 ± 0,002	1,331 ± 0,001	270,212 ± 0,332	270,212 ± 0,166
				527,157	[M+Na] ⁺	1,003 ± 0		206,049 ± 0,097	
				543,131	[M+K] ⁺	0,986 ± 0		202,405 ± 0,097	
						1,013 ± 0		208,086 ± 0,097	
				1031,330	[2M+Na] ⁺	1,375 ± 0		279,124 ± 0,096	
Raffinose	504,44	10,08 ± 0,06	11,86 ± 0	503,162	[M-H] ⁻	0,963 ± 0	0,961 ± 0	198,135 ± 0	197,792 ± 0,097
				539,138	[M+Cl] ⁻	0,994 ± 0	0,993 ± 0,001	204,222 ± 0,097	203,948 ± 0,168
				549,167	[M+HCOO] ⁻	1,005 ± 0,001	1,004 ± 0	206,319 ± 0,168	206,183 ± 0,097
				1007,331	[2M-H] ⁻	1,357 ± 0	1,356 ± 0,001	275,423 ± 0,096	275,22 ± 0,191
				527,157	[M+Na] ⁺	1,001 ± 0,001		205,775 ± 0,194	
				543,133	[M+K] ⁺	1,011 ± 0		207,607 ± 0	
				1031,330	[2M+Na] ⁺	1,352 ± 0,002		274,321 ± 0,345	
Maltotetraose	666,58	11,89 ± 0,07	11,47 ± 0,01						

			11,68 ± 0	665,215 701,191 711,220 1331,433 689,210 705,000	[M-H] ⁻ [M+Cl] ⁻ [M+HCOO] ⁻ [2M-H] ⁻ [M+Na] ⁺ [M+K] ⁺	1,092 ± 0 1,156 ± 0,002 1,194 ± 0,001 1,512 ± 0,001 1,12 ± 0 1,127 ± 0,001	1,092 ± 0 1,193 ± 0 1,508 ± 0,002	223,161 ± 0,096 235,999 ± 0,481 243,761 ± 0,167 305,945 ± 0,165 228,723 ± 0,096 230,121 ± 0,167	223,161 ± 0,096 243,488 ± 0,096 305,136 ± 0,33
Nystose	666,58	10,88 ± 0,07	10,95 ± 0,02	665,215 701,191 711,220 1331,439 689,210 705,184	[M-H] ⁻ [M+Cl] ⁻ [M+HCOO] ⁻ [2M-H] ⁻ [M+Na] ⁺ [M+K] ⁺	1,135 ± 0,001 1,15 ± 0,001 1,151 ± 0,002 1,505 ± 0,002 1,126 ± 0,001 1,144 ± 0,001	1,134 ± 0 1,153 ± 0,001 1,509 ± 0,003	232,019 ± 0,167 234,841 ± 0,289 234,982 ± 0,333 304,596 ± 0,382 230,017 ± 0,167 233,659 ± 0,255	231,883 ± 0,096 235,322 ± 0,255
Stachyose	666,58	11,8 ± 0,07	11,83 ± 0,01	665,215 701,191 711,220 1331,433 689,210 705,000	[M-H] ⁻ [M+Cl] ⁻ [M+HCOO] ⁻ [2M-H] ⁻ [M+Na] ⁺ [M+K] ⁺	1,091 ± 0,001 1,147 ± 0 1,16 ± 0,001 1,581 ± 0,001 1,132 ± 0 1,153 ± 0,001	1,092 ± 0 1,159 ± 0,001 1,576 ± 0,002	223,024 ± 0,167 234,297 ± 0,096 236,819 ± 0,167 319,907 ± 0,202 231,243 ± 0 235,498 ± 0,193	223,297 ± 0,096 236,547 ± 0,192 318,895 ± 0,33
Maltopentaose	828,72	13,07 ± 0,08	12,64 ± 0,02	827,267 873,256 829,283 851,264 867,240	[M-H] ⁻ [M+HCOO] ⁻ [M+H] ⁺ [M+Na] ⁺ [M+K] ⁺	1,24 ± 0 1,237 ± 0,002 1,244 ± 0,002 1,247 ± 0,003	1,244 ± 0,002 1,266 ± 0	252,546 ± 0,096 251,925 ± 0,346 253,175 ± 0,44 253,644 ± 0,583	253,36 ± 0,48 257,549 ± 0
Maltohexaose	990,86	13,96 ± 0,09 0 ± 1,35 0 ± 1,39	13,35 ± 0	989,320 1013,860	[M-H] ⁻ [M+Na] ⁺	1,019 ± 0,001 1,337 ± 0,002 1,376 ± 0,001 1,347 ± 0,001	1,019 ± 0,001 1,337 ± 0,001 1,375 ± 0,002	206,923 ± 0,166 271,565 ± 0,417 279,417 ± 0,287 273,436 ± 0,287	206,923 ± 0,166 271,565 ± 0,191 279,281 ± 0,417
Maltoheptaose	1153,00	-14,05 ± 0,1 14,4 ± 0,04	13,84 ± 0,03	1151,373	[M-H] ⁻	1,467 ± 0,008 1,485 ± 0	1,086 ± 0 1,482 ± 0,007 1,376 ± 0	297,385 ± 1,564 300,966 ± 0	220,1 ± 0 300,425 ± 1,327

Table X: Comparison of CCS values with literature. The table shows for matching compounds the molecular weight (MW), mass-to-charge-ratio (m/z), ion species, calculated collision cross section values (CCS) and standard deviation (SD) recorded in this study and CCS values published in the Pacific Northwest National Library (PNNL), Przybylski and Bonnet or the database of the McLean Research Group^{78,87,37}.

Compound name	MW [g/mol]	m/z	Ion species	TM CCS _{N₂} [Å ²] (Average ± SD)		CCS [Å ²] (Literature)		
				NH ₂	PGC	PNNL	Przybylski	McLean
Cellobiose	342,30	365,105	[M+Na] ⁺	176,621 ± 0		178,66		178,4
			[M+K] ⁺	178,501 ± 0,098			180,6	
Gentiobiose	342,30	341,109	[M-H] ⁻		179,007 ± 0,098	180,8		180,2
			[M+Na] ⁺	175,998 ± 0		180,53	179,4	
Isomaltose	342,30	341,109	[M-H] ⁻	168,036 ± 0,196	167,897 ± 0,34	180,77		180,1
			[M+Na] ⁺	175,72 ± 0,098		178,02		
Isomaltulose/ Pallatinose	342,30	341,109	[M-H] ⁻		168,106 ± 0,34			175,4
			[M+Na] ⁺	173,781 ± 0,098			176,2	
			[M+K] ⁺	177,601 ± 0,169			177,7	
Lactose	342,30	341,109	[M-H] ⁻	167,897 ± 0	167,689 ± 0,208	170,23		176,8
			[M+Na] ⁺	173,85 ± 0,196		178,83		
Maltose	342,30	341,109	[M-H] ⁻		179,563 ± 0	205,9		190,9
			[M+Na] ⁺	176,552 ± 0,098		179,19	178,4	
Maltulose	342,30	341,109	[M-H] ⁻	167,62 ± 0,26	167,828 ± 0,098	180,6		
			[M+Na] ⁺	176,275 ± 0,098		181,27		
Melibiose	342,30	341,109	[M-H] ⁻		167,828 ± 0,491	172,63		178
			[M+Na] ⁺	175,166 ± 0		181,14	177,1	
			[M+K] ⁺	177,533 ± 0,098			179,8	
Sophorose	342,30	341,109	[M-H] ⁻		183,382 ± 0,098	187,07		
			[M+Na] ⁺	176,759 ± 0,098		183,57		
Sucrose	342,30	341,109	[M-H] ⁻	167,759 ± 0,098	167,828 ± 0,098	168,47		168,2
			[M+Na] ⁺	171,634 ± 0		173,93	173,9	
Trehalose	342,30	341,109	[M-H] ⁻	169,425 ± 0,098	169,286 ± 0,26			169,9
			[M+Na] ⁺	173,504 ± 0,17			176,1	
Turanose	342,30	341,109	[M-H] ⁻	167,897 ± 0	176,23 ± 0	178,97		
			[M+Na] ⁺	172,257 ± 0		177		
Eriose	504,44	527,157	[M+Na] ⁺	203,651 ± 0			206,9	
			[M+K] ⁺	202,063 ± 0			203,3	
Isomaltotriose	504,44	503,162	[M-H] ⁻	202,044 ± 0	202,113 ± 0,097	202,92		
			[M+Na] ⁺	208,035 ± 0,194		210,83	212,3/202,1	
			[M+K] ⁺	207,333 ± 0,194			213,5/203,0	
Kestose	504,44	503,162	[M-H] ⁻	202,25 ± 0,168	202,182 ± 0,194	202,78		204,1
			[M+Na] ⁺	201,87 ± 0,256		205,43	205,5	204,2
			[M+K] ⁺	203,158 ± 0,194			207,1	
Maltotriose	504,44	503,161	[M-H] ⁻	212,881 ± 0,097	207,462 ± 0,194	213,01		
			[M+Na] ⁺	209,474 ± 0,256		212,54	213,3	211,1
			[M+K] ⁺	211,44 ± 0,422			216,0/213,8	212,1
			[2M+Na] ⁺	270,803 ± 0,747				
Melezitose	504,44	503,162	[M-H] ⁻	195,118 ± 0,097	194,98 ± 0,194	203,52		202,8
			[M+Na] ⁺	198,377 ± 0,194		203,23	201,8	
			[M+K] ⁺	199,051 ± 0,194			202,6	

Panose	504,44	527,157 [M+Na] ⁺	206,049 ± 0,097		209,2	
		543,131 [M+K] ⁺	202,405 ± 0,097		206,3	
			208,086 ± 0,097		211,9	
Raffinose	504,44	503,162 [M-H] ⁻	198,135 ± 0	197,792 ± 0,097	197,59	197
		527,157 [M+Na] ⁺	205,775 ± 0,194		208,72	209,5
		543,133 [M+K] ⁺	207,607 ± 0			211
Maltotetraose	666,58	665,215 [M-H] ⁻	223,161 ± 0,096	223,161 ± 0,096	221,08	
		689,210 [M+Na] ⁺	228,723 ± 0,096		230,47	231,3
Stachyose	666,58	665,215 [M-H] ⁻	223,024 ± 0,167	223,297 ± 0,096	226,67	223,8
		689,210 [M+Na] ⁺	231,243 ± 0		236,4	235,2
Maltopentaose	828,72	827,267 [M-H] ⁻	252,546 ± 0,096	253,36 ± 0,48	254,9	256,4
		851,264 [M+Na] ⁺	253,175 ± 0,44		257,04	257,2
		867,240 [M+K] ⁺	253,644 ± 0,583			258,2
Maltohexaose	990,86	989,320 [M-H] ⁻	279,417 ± 0,287	279,281 ± 0,417	279,97	
		1013,860 [M+Na] ⁺	273,436 ± 0,287		279,7	281,5

A.3.2. Application on Biological Samples

Table XI: Saccharide composition of maize phloem sap (amine column). The phloem sap of *Zea mays* was analysed via UHPLC-IM-MS (timsTOF, Bruker) in negative (black) and positive ionisation mode (blue) utilising the amine column. Displayed are identified compounds, retention times (RT), mass-to-charge ratios (m/z), mean values of inverse standard mobilities $1/K_0$, standard deviations (SD) and calculated collision cross sections (CCS).

Compound	RT [min]	m/z	Mobility $1/K_0$ (Average \pm SD) [V·s·cm ⁻²]	^{TIM} CCS _{N₂} [Å ²]
Sucrose	7,75	341,109	0,805 \pm 167,749	167,75
		377,085	0,829 \pm 172,033	172,03
		387,114	0,838 \pm 173,745	173,74
		387,114	0,901 \pm 186,927	186,93
		387,114	0,954 \pm 197,859	197,86
		683,225	1,115 \pm 227,867	227,87
		365,102	0,83 \pm 172,465	172,47
		381,076	0,841 \pm 174,386	174,39
Trehalose	8,43	341,109	0,814 \pm 169,564	169,56
		387,114	0,847 \pm 175,641	175,64
		683,222	1,13 \pm 230,874	230,87

Table XII: Saccharide composition of maize phloem sap (graphite column). The phloem sap of *Zea mays* was analysed via UHPLC-IM-MS (timsTOF, Bruker) in negative ionisation mode utilising the graphite column. Displayed are identified compounds, retention times (RT), mass-to-charge ratios (m/z), mean values of inverse standard mobilities $1/K_0$, standard deviations (SD) and calculated collision cross sections (CCS).

Compound	RT [min]	m/z	Mobility $1/K_0$ (Average \pm SD) [V·s·cm ⁻²]	^{TIM} CCS _{N₂} [Å ²]
Sucrose	7,6	341,109	0,806 \pm 167,897	167,90
		377,085	0,831 \pm 172,388	172,39
		387,114	0,837 \pm 173,656	173,66
		683,225	1,116 \pm 228,043	228,04

Table XIII: Saccharide composition of maize phloem sap (dark, amine column). The phloem sap of *Zea mays*, being in the dark for 48 h before measurement, was analysed via UHPLC-IM-MS (timsTOF, Bruker) in negative (black) and positive ionisation mode (blue) utilising the amine column. Displayed are identified compounds, retention times (RT), mass-to-charge ratios (m/z), mean values of inverse standard mobilities $1/K_0$, standard deviations (SD) and calculated collision cross sections (CCS).

Compound	RT [min]	m/z	Mobility $1/K_0$ (Average \pm SD) [$V\cdot s\cdot cm^{-2}$]	$^{TIM}CCS_{N_2}$ [\AA^2]
Sucrose	7,76	341,109	0,805 \pm 167,654	167,65
		377,090	0,827 \pm 171,73	171,73
		387,115	0,836 \pm 173,429	173,43
		387,115	0,901 \pm 186,908	186,91
		387,115	0,954 \pm 197,864	197,86
		683,225	1,115 \pm 227,877	227,88
		365,105	0,829 \pm 172,257	172,26
		381,079	0,838 \pm 173,867	173,87
Trehalose	8,41	341,109	0,812 \pm 169,147	169,15
		387,114	0,848 \pm 175,848	175,85
		683,229	1,125 \pm 229,852	229,85
		683,229	1,155 \pm 235,982	235,98
Kestose	9,49	503,161	0,985 \pm 202,662	202,66
		549,167	1,008 \pm 206,935	206,94
	9,99	503,161	0,964 \pm 198,341	198,34
		549,167	1,025 \pm 210,425	210,43
	10,95	665,214	1,096 \pm 224,046	224,05
		711,220	1,14 \pm 232,736	232,74

Table XIV: Saccharide composition of maize phloem sap (dark). The phloem sap of *Zea mays*, being in the dark for 48 h before measurement, was analysed via UHPLC-IM-MS (timsTOF, Bruker) in negative ionisation mode utilising the pgc column. Displayed are identified compounds, retention times (RT), mass-to-charge ratios (m/z), mean values of inverse standard mobilities $1/K_0$, standard deviations (SD) and calculated collision cross sections (CCS).

Compound	RT [min]	m/z	Mobility $1/K_0$ (Average \pm SD) [V·s·cm ⁻²]	^{TIM} CCS _{N₂} [Å ²]
Trehalose	6,8	341,109	0,813 \pm 169,356	169,36
		377,085	0,832 \pm 172,685	172,68
		387,114	0,847 \pm 175,641	175,64
		683,225	1,131 \pm 231,078	231,08
Sucrose	7,58	341,109	0,805 \pm 167,759	167,76
		377,085	0,827 \pm 171,647	171,65
		387,114	0,837 \pm 173,463	173,46
		683,225	1,114 \pm 227,503	227,50
	9,43	503,161	0,963 \pm 198,135	198,14
		539,137	1,005 \pm 206,412	206,41
		549,167	1,024 \pm 210,22	210,22
	9,69	503,161	0,961 \pm 197,724	197,72
		549,167	1,03 \pm 211,452	211,45
	9,89	503,161	0,982 \pm 202,044	202,04
		549,167	1,007 \pm 206,73	206,73
	(Kestose)	10,12	503,161	0,984 \pm 202,456
539,137			0,995 \pm 204,359	204,36
549,167			1,007 \pm 206,73	206,73
549,167			1,296 \pm 266,06	266,06
10,93		665,214	1,117 \pm 228,339	228,34
		711,224	1,138 \pm 232,328	232,33
11,11		665,214	1,123 \pm 229,566	229,57
		711,224	1,167 \pm 238,248	238,25
11,75		665,214	1,096 \pm 224,046	224,05
		711,224	1,138 \pm 232,328	232,33
12,69		827,2676	1,203 \pm 244,944	244,94
		873,2722	1,239 \pm 252,057	252,06
13,3	989,32	1,348 \pm 273,731	273,73	
13,64	989,32	1,342 \pm 272,512	272,51	
	1151,379	1,479 \pm 299,75	299,75	

Table XV: Saccharide composition of maize feeding aphids (amine column). The honeydew of *Rhopalosiphum padi* and *Sitobion avenae* was analysed via UHPLC-IM-MS (timsTOF, Bruker) in negative (black) and positive ionisation mode (blue) utilising the amine column. Displayed are identified compounds, retention times (RT), mass-to-charge ratios (m/z), mean values of inverse standard mobilities $1/K_0$, standard deviations (SD) and calculated collision cross sections (CCS).

Compound	RT [min]	m/z	Mobility $1/K_0$ (Average \pm SD) [V·s·cm ⁻²]	TM CCS _{N2} [Å ²]
	5,49	179,056	0,984 \pm 0,052	211,791
		255,233	0,802 \pm 0	169,099
		367,106	0,831 \pm 0,001	172,722
Fructose	5,61	179,056	1,019 \pm 0,053	219,393
		359,119	0,952 \pm 0,01	197,974
		367,105	0,831 \pm 0,001	172,722
Mannitol	6,26	181,072	0,609 \pm 0	131,046
		271,044	0,691 \pm 0,001	145,347
		371,136	0,84 \pm 0,001	174,494
Glucose	6,55	179,056	0,977 \pm 0,054	210,435
		359,119	0,938 \pm 0,003	195,105
		367,105	0,833 \pm 0,001	172,972
Sucrose	7,78	341,109	0,806 \pm 0,001	167,814
		377,085	0,83 \pm 0,001	172,187
		387,114	0,837 \pm 0,001	173,484
		387,114	0,901 \pm 0,001	186,797
		683,225	1,116 \pm 0	227,932
		365,105	0,83 \pm 0	172,465
		381,079	0,84 \pm 0	174,282
Trehalose/ Maltose	8,51	341,109	0,812 \pm 0	169,147
		377,085	0,833 \pm 0	172,892
		377,085	0,859 \pm 0,001	178,247
		387,114	0,846 \pm 0,001	175,433
		683,225	1,162 \pm 0	237,493
		365,105	0,851 \pm 0	176,829
		381,079	0,866 \pm 0	179,677
		381,079	1,156 \pm 0	239,845
Melezitose/ Erlöse	9,53	503,161	0,947 \pm 0,001	194,884
		503,161	0,988 \pm 0	203,197
		539,138	0,969 \pm 0,001	198,936
		539,138	1,002 \pm 0,002	205,755
		549,167	0,977 \pm 0,001	200,530
		549,167	1,012 \pm 0,001	207,715
		1007,330	1,296 \pm 0,012	263,188
		527,157	0,995 \pm 0	204,473
		543,131	0,986 \pm 0	202,473

(Raffinose)	10,03	503,161	0,965 ± 0	198,506	
		539,138	1,008 ± 0,001	207,111	
		549,167	1,024 ± 0	210,302	
		1007,330	1,294 ± 0,004	262,633	
		1007,330	1,306 ± 0,002	265,137	
		1007,330	1,321 ± 0,002	268,182	
		527,157	0,997 ± 0	204,884	
		527,157	1,019 ± 0	209,405	
		543,131	1,012 ± 0	207,812	
		11,00	665,214	1,097 ± 0,001	224,292
701,199	1,147 ± 0,002			234,229	
711,220	1,141 ± 0,001			233,022	
1331,439	1,514 ± 0,001			306,431	
689,210	1,109 ± 0			226,544	
705,183	1,12 ± 0			228,690	
11,17	827,267			1,246 ± 0	253,618
		705,183	1,117 ± 0	228,078	
		867,236	1,203 ± 0	244,759	
11,41	665,214	1,121 ± 0,002	229,239		
		701,182	1,169 ± 0,004	238,762	
		711,220	1,171 ± 0	239,147	
		827,267	1,247 ± 0,002	253,822	
		689,210	1,111 ± 0	226,953	
		705,183	1,122 ± 0	229,099	
		Maltotetraose	11,66	665,214	1,092 ± 0,001
665,214	1,126 ± 0,002			230,128	
711,220	1,192 ± 0,002			243,434	
705,183	1,124 ± 0			229,507	
12,08	827,267		1,204 ± 0,001	245,229	
			873,272	1,24 ± 0,001	252,301
			989,320	1,352 ± 0,001	274,624
			989,320	1,387 ± 0,002	281,610
			867,238	1,244 ± 0	253,101
12,24	827,267		0,952 ± 0,001	193,919	
		827,267	1,204 ± 0,001	245,148	
		873,273	1,239 ± 0,001	252,138	
		989,320	1,353 ± 0,001	274,705	
		989,320	1,385 ± 0,001	281,285	
		867,238	1,246 ± 0	253,508	
12,54	827,267	1,269 ± 0,001	258,342		
		873,272	1,238 ± 0,001	251,812	
		873,272	1,284 ± 0,001	261,252	

		867,238	1,25 ± 0	254,322
Maltopentaose	12,82	827,267	1,24 ± 0,001	252,519
		1151,372	1,424 ± 0,001	288,603
		1151,372	1,461 ± 0,001	296,020
		867,238	1,244 ± 0	253,101
Maltohexaose	13,05	827,267	1,241 ± 0,001	252,600
		989,320	1,019 ± 0,001	206,841
		989,320	1,344 ± 0,001	273,000
		1151,373	1,424 ± 0,002	288,643
		1151,373	1,473 ± 0,002	298,452
	13,22	989,320	1,018 ± 0,001	206,719
		989,320	1,344 ± 0,002	272,878
		1035,326	1,353 ± 0,002	274,578
		1151,373	1,425 ± 0,002	288,765
		1151,373	1,475 ± 0,004	298,939
		829,282	1,229 ± 0	250,228
		829,282	1,33 ± 0	270,792
	13,47	989,320	1,392 ± 0,002	282,747
1035,324		1,363 ± 0,005	276,607	
1029,292		1,285 ± 0	260,798	
1029,292		1,343 ± 0	272,570	
13,72	989,320	1,38 ± 0,003	280,269	
14,06	1151,372	1,458 ± 0,012	295,575	
14,27	1151,372	1,435 ± 0,004	290,792	
	1151,372	1,467 ± 0,002	297,216	
14,42	1151,372	1,47 ± 0,004	297,885	

Table XVI: Saccharide composition of maize feeding aphids (graphite column). The honeydew of *Rhopalosiphum padi* and *Sitobion avenae* was analysed via UHPLC-IM-MS (tim-sTOF, Bruker) in negative ionisation mode utilising the graphite column. Displayed are identified compounds, retention times (RT), mass-to-charge ratios (m/z), mean values of inverse standard mobilities $1/K_0$, standard deviations (SD) and calculated collision cross sections (CCS).

Compound	RT [min]	m/z	Mobility $1/K_0$ (Average \pm SD) [V \cdot s \cdot cm $^{-2}$]	$^{TIM}CCS_{N_2}$ [Å 2]	
Fructose	1,66	367,106	0,832 \pm 0,002	172,89	
		5,76	179,056	0,822 \pm 0,001	177,01
	6,42			0,845 \pm 0,001	181,92
			341,109	0,844 \pm 0,001	175,77
			377,085	0,829 \pm 0,001	172,06
			387,115	0,847 \pm 0,004	175,64
			683,225	1,135 \pm 0,001	231,98
	Trehalose	6,80	341,109	0,813 \pm 0	169,27
			387,115	0,848 \pm 0,001	175,77
683,225			1,129 \pm 0,001	230,71	
Maltulose	7,36	341,109	0,805 \pm 0,001	167,61	
			0,853 \pm 0,001	177,77	
		387,115	0,847 \pm 0,001	175,59	
		683,225	1,131 \pm 0,001	231,16	
Sucrose	7,58		1,161 \pm 0,003	237,25	
		341,109	0,806 \pm 0,001	167,94	
		377,085	0,83 \pm 0	172,23	
		387,115	0,838 \pm 0,001	173,69	
Maltose	8,05	683,225	1,117 \pm 0,001	228,18	
		341,109	0,805 \pm 0,001	167,69	
			0,838 \pm 0,001	174,56	
			0,863 \pm 0,001	179,73	
		377,085	0,855 \pm 0	177,50	
		387,115	0,838 \pm 0,001	173,86	
			0,862 \pm 0,001	178,67	
Melezitose	8,30	683,225	1,163 \pm 0,001	237,66	
		503,161	0,948 \pm 0,001	194,97	
		539,137	0,97 \pm 0,001	199,22	
		549,167	0,98 \pm 0	201,27	
(Maltotriose)	8,71	1007,332	1,326 \pm 0,001	269,28	
		503,161	1,009 \pm 0,002	207,64	
		549,167	0,976 \pm 0,001	200,45	
		1,034 \pm 0	212,27		

	8,93	503,161	1,011 ± 0,001	207,97
		549,167	1,005 ± 0,001	206,40
		1007,330	1,315 ± 0,002	266,88
			1,325 ± 0	268,99
	9,44	503,161	0,965 ± 0,002	198,63
		549,167	1,026 ± 0,001	210,55
		1007,332	1,314 ± 0,002	266,80
Erlose	10,13	503,161	0,988 ± 0,003	203,20
		549,167	1,013 ± 0,001	208,00
		1007,332	1,287 ± 0,007	261,28
			1,314 ± 0,014	266,66
	10,56	665,214	1,092 ± 0,003	223,27
		711,220	1,098 ± 0,001	224,12
			1,144 ± 0,001	233,60
	10,88	665,214	1,116 ± 0,002	228,22
		701,191	1,165 ± 0,002	237,95
		711,220	1,147 ± 0,001	234,25
		711,220	1,173 ± 0,002	239,47
	11,07	665,214	1,105 ± 0,01	225,78
		701,191	1,145 ± 0,001	233,89
		711,220	1,143 ± 0,001	233,42
		827,267	1,246 ± 0,002	253,70
		827,267	1,271 ± 0	258,79
Maltotetraose/ (Stachyose)	11,47	665,214	1,092 ± 0,001	223,23
		701,191	1,142 ± 0,002	233,17
		711,220	1,167 ± 0,002	238,25
			1,194 ± 0,002	243,76
		827,267	1,245 ± 0,002	253,58
Maltotetraose	11,61	665,214	1,092 ± 0,001	223,27
		711,220	1,142 ± 0	233,10
		827,267	1,244 ± 0,001	253,25
	11,77	665,214	1,1 ± 0,002	224,76
		711,220	1,143 ± 0,001	233,27
		827,267	1,246 ± 0,002	253,62
		827,267	1,27 ± 0	258,59
	11,92	665,214	1,095 ± 0,001	223,84
		711,220	1,14 ± 0,001	232,70
		827,267	1,268 ± 0,001	258,22

	873,272	1,232 ± 0,004	250,55
	873,272	1,291 ± 0,002	262,64
12,21	827,267	1,242 ± 0,001	252,97
	827,267	1,279 ± 0,002	260,42
	873,272	1,281 ± 0,002	260,60
	989,320	1,387 ± 0,001	281,69
12,61	827,267	0,951 ± 0,008	193,63
	827,267	1,213 ± 0,014	246,98
	873,272	1,24 ± 0,001	252,34
	989,320	1,353 ± 0,001	274,83
	989,320	1,395 ± 0,004	283,36
13,03	989,320	1,019 ± 0,001	206,88
	989,320	1,352 ± 0,003	274,46
	989,320	1,383 ± 0,002	280,92
	1151,373	1,461 ± 0,002	296,18
13,36	989,320	1,016 ± 0,001	206,31
	989,320	1,344 ± 0,002	272,84
	989,320	1,383 ± 0,002	280,92
	1151,373	1,436 ± 0,019	290,93
	1151,373	1,477 ± 0,003	299,41
13,62	989,320	1,02 ± 0,005	207,21
	989,320	1,349 ± 0	273,97
	989,320	1,386 ± 0,003	281,45
	1151,373	1,084 ± 0,001	219,61
	1151,373	1,421 ± 0,002	287,99
	1151,373	1,467 ± 0,003	297,40
14,02	1151,373	1,423 ± 0,002	288,36
	1151,373	1,466 ± 0,002	297,11

Table XVII: Saccharide composition of *Brevicoryne brassicae* (amine column). The honeydew of was analysed via UHPLC-IM-MS (timsTOF, Bruker) in negative (black) and positive ionisation mode (blue) utilising the amine column. Displayed are identified compounds, retention times (RT), mass-to-charge ratios (m/z), mean values of inverse standard mobilities $1/K_0$, standard deviations (SD) and calculated collision cross sections (CCS).

Compound	RT [min]	m/z	Mobility $1/K_0$ (Average \pm SD) [V \cdot s \cdot cm $^{-2}$]	$^{TIM}CCS_{N_2}$ [Å 2]
	2,59	145,098	0,608 \pm 0	132,99
		189,056	0,648 \pm 0,001	139,04
		397,114	0,949 \pm 0	196,62
	3,39	179,056	0,794 \pm 0,005	170,98
		322,093	0,827 \pm 0,001	172,66
	4,46	128,960	0,692 \pm 0	152,88
		179,054	0,865 \pm 0	186,27
		275,057	0,742 \pm 0,001	155,86
		402,141	0,874 \pm 0,001	181,06
Fructose	5,79	179,058	0,821 \pm 0,001	176,80
		299,138	0,867 \pm 0,001	181,46
Mannitol	6,31	181,072	0,61 \pm 0,001	131,22
		369,140	0,888 \pm 0,001	184,34
Glucose	6,74	145,098	0,606 \pm 0	132,55
		179,056	0,843 \pm 0,003	181,43
		179,056	0,849 \pm 0,005	182,72
		357,166	0,908 \pm 0,006	188,82
		357,166	0,919 \pm 0,001	191,11
	6,73	325,160	0,847 \pm 0,001	176,66
		359,120	0,99 \pm 0	205,83
Sucrose	7,91	341,109	0,804 \pm 0	167,56
		377,085	0,829 \pm 0,001	172,02
		683,225	1,116 \pm 0,001	227,97
		343,194	0,85 \pm 0,001	176,94
		365,105	0,828 \pm 0,001	171,97
		381,079	0,839 \pm 0,001	174,03
Trehalulose	8,13	341,109	0,804 \pm 0	167,40
		367,107	0,947 \pm 0	196,74
		377,085	0,831 \pm 0,001	172,52
		506,188	1,004 \pm 0	206,54
		683,225	1,132 \pm 0,003	231,33
		343,194	0,849 \pm 0,001	176,73
		365,105	0,837 \pm 0,001	174,00
		381,079	0,846 \pm 0,002	175,53

Trehalulose	8,25	341,109	0,804 ± 0	167,53		
		367,106	0,946 ± 0,001	196,53		
		377,086	0,829 ± 0,001	172,11		
		377,086	0,846 ± 0,002	175,54		
		683,225	1,116 ± 0	228,01		
		365,105	0,84 ± 0	174,58		
		381,079	0,856 ± 0,001	177,60		
	8,45	341,109	0,804 ± 0	167,41		
		377,085	0,852 ± 0	176,77		
		683,225	1,159 ± 0,003	236,87		
		365,105	0,842 ± 0,002	175,04		
		381,079	0,856 ± 0,001	177,64		
Maltose/ Trehalose	8,57	341,109	0,804 ± 0	167,41		
		341,109	0,811 ± 0	168,94		
		367,106	0,947 ± 0	196,70		
		377,085	0,833 ± 0,001	172,89		
		377,085	0,856 ± 0,001	177,62		
		387,150	0,845 ± 0	175,23		
		506,188	1,001 ± 0,003	205,88		
		506,188	1,023 ± 0	210,45		
		683,225	1,162 ± 0,001	237,33		
		343,193	0,847 ± 0,001	176,40		
		365,105	0,85 ± 0,001	176,70		
		381,079	0,863 ± 0,004	179,10		
			8,71	343,125	0,835 ± 0	173,90
				377,085	0,858 ± 0	178,08
683,225	1,163 ± 0			237,62		
365,106	0,827 ± 0			171,84		
381,079	0,838 ± 0			173,87		
(Melibiose/ Isomaltose)	8,94	341,109	0,804 ± 0,001	167,48		
		343,125	0,834 ± 0,001	173,61		
		377,085	0,839 ± 0,001	174,09		
		377,085	0,85 ± 0	176,42		
Gentiobiose	9,19	341,109	0,804 ± 0,001	167,40		
		377,086	0,847 ± 0,002	175,72		
		382,136	0,866 ± 0,002	179,56		
		683,234	1,135 ± 0	231,90		
		683,234	1,165 ± 0,002	237,96		
		343,194	0,847 ± 0,001	176,31		
		365,105	0,848 ± 0,001	176,29		
		381,079	0,862 ± 0,001	178,85		
			9,36	503,162	0,944 ± 0,002	194,28
503,162	0,977 ± 0,002			200,91		

		539,138	0,964 ± 0,002	198,04		
		539,138	0,998 ± 0	205,03		
		549,168	0,978 ± 0,002	200,83		
		549,168	1,007 ± 0,002	206,73		
		1007,326	1,366 ± 0,032	277,22		
		527,158	0,971 ± 0,007	199,54		
		527,158	1,006 ± 0,002	206,63		
		543,132	0,978 ± 0,007	200,83		
		543,132	1,015 ± 0,001	208,38		
Melezitose/ Erlose	9,59	503,162	0,946 ± 0,001	194,64		
		503,162	0,985 ± 0,001	202,66		
		539,138	0,968 ± 0,001	198,73		
		539,138	0,997 ± 0,002	204,85		
		549,168	0,98 ± 0,001	201,19		
		549,168	1,013 ± 0,003	207,96		
		1007,328	1,302 ± 0,002	264,32		
		325,113	0,987 ± 0	205,98		
		325,113	1,038 ± 0	216,63		
		325,113	1,13 ± 0	235,83		
		505,236	0,986 ± 0,003	202,91		
		505,236	1,025 ± 0,011	210,87		
		505,236	1,141 ± 0	234,73		
		527,158	0,969 ± 0,001	199,08		
		527,158	0,995 ± 0,004	204,43		
		543,132	0,969 ± 0,004	198,91		
		543,132	0,986 ± 0,001	202,56		
543,132	1,019 ± 0,002	209,25				
Raffinose	9,93	503,161	0,962 ± 0,001	197,85		
		539,138	0,994 ± 0,001	204,07		
		539,138	1,019 ± 0,002	209,29		
		549,167	1,005 ± 0,002	206,28		
		549,167	1,044 ± 0	214,39		
		1007,334	1,363 ± 0,012	276,61		
		505,272	1,008 ± 0,001	207,37		
		527,158	1,001 ± 0,002	205,65		
		543,132	1,008 ± 0,001	207,03		
		543,132	1,037 ± 0,001	212,91		
			10,14	503,161	0,964 ± 0	198,34
				539,138	1,007 ± 0,001	206,82
				549,167	1,028 ± 0,001	210,94
1007,334	1,311 ± 0,001			266,15		
505,272	1,009 ± 0			207,58		
527,158	0,998 ± 0,001			204,99		
527,158	1,02 ± 0			209,61		
543,132	1,013 ± 0,002			207,92		
543,132	1,035 ± 0			212,54		

Table XVIII: Saccharide composition of *Brevicoryne brassicae* (graphite column). The honeydew of was analysed via UHPLC-IM-MS (timsTOF, Bruker) in negative ionisation mode utilising the graphite column. Displayed are identified compounds, retention times (RT), mass-to-charge ratios (m/z), mean values of inverse standard mobilities $1/K_0$, standard deviations (SD) and calculated collision cross sections (CCS).

Compound	RT [min]	m/z	Mobility $1/K_0$ (Average \pm SD) [V \cdot s \cdot cm $^{-2}$]	^{TIM} CCS _{N₂} [Å ²]
Trehalose	6,75	179,054	0,809 \pm 0,004	174,21
		179,054	0,821 \pm 0	176,80
		341,109	0,812 \pm 0,002	169,15
		377,085	0,837 \pm 0,002	173,81
		387,081	0,848 \pm 0,002	175,89
	6,99	341,109	0,804 \pm 0	167,48
		341,109	0,814 \pm 0,001	169,46
		377,085	0,835 \pm 0,001	173,22
		683,225	1,131 \pm 0,004	231,04
	Sucrose	7,57	341,109	0,805 \pm 0
377,085			0,828 \pm 0,001	171,90
387,112			0,838 \pm 0,001	173,73
683,225			1,114 \pm 0,002	227,69
Maltose	7,88	341,109	0,806 \pm 0,002	167,79
		341,109	0,813 \pm 0	169,36
		377,085	0,858 \pm 0,001	178,16
		387,112	0,862 \pm 0,001	178,75
		387,112	0,871 \pm 0	180,62
		683,225	1,165 \pm 0,001	238,07
Maltose	8,02	341,109	0,808 \pm 0,002	168,21
		341,109	0,813 \pm 0	169,36
		377,085	0,857 \pm 0,001	177,92
		683,225	1,164 \pm 0,002	237,90
Melezitose	3,19); 8,25	343,125	0,834 \pm 0	173,73
		503,161	0,947 \pm 0,001	194,76
		539,138	0,97 \pm 0	199,14
		549,167	0,978 \pm 0,001	200,78
Gentiobiose	8,54	341,110	0,806 \pm 0,001	167,90
		357,104	0,807 \pm 0	167,82
		357,104	0,828 \pm 0,003	172,26
		377,085	0,847 \pm 0,001	175,85
		683,225	1,163 \pm 0,002	237,51
	8,67	341,110	0,805 \pm 0,001	167,69
		357,104	0,807 \pm 0,001	167,82
		357,104	0,828 \pm 0	172,19
		683,225	1,159 \pm 0,003	236,80

	9,36	341,109	0,805 ± 0,003	167,69
		357,104	0,806 ± 0,001	167,57
		357,104	0,83 ± 0	172,60
		503,162	0,963 ± 0,001	198,18
		539,138	1,006 ± 0,002	206,62
		549,163	1,023 ± 0,002	210,10
		683,224	1,165 ± 0,001	238,02
		1007,331	1,316 ± 0,001	267,07
		1007,331	1,33 ± 0,001	270,01
	9,61	341,109	0,949 ± 0,04	197,73
		357,104	0,807 ± 0,003	167,72
		383,225	0,876 ± 0	181,72
		503,161	0,967 ± 0,001	198,92
		539,138	1,001 ± 0,002	205,49
		549,166	1,028 ± 0,007	210,96
		1007,331	1,285 ± 0,003	260,87
		1007,331	1,328 ± 0,001	269,55
		1007,331	1,365 ± 0,003	277,01
	9,86	341,109	0,805 ± 0,001	167,69
		341,109	0,901 ± 0,046	187,69
		357,104	0,808 ± 0,002	168,03
		503,162	0,967 ± 0	198,96
		503,162	0,994 ± 0,003	204,56
		539,138	1,004 ± 0,003	206,21
		549,160	1,01 ± 0,003	207,30
		549,160	1,032 ± 0,002	211,86
		1007,331	1,323 ± 0,002	268,59
		1007,331	1,333 ± 0	270,52
Erlöse	10,10	357,104	0,809 ± 0	168,24
		503,162	0,985 ± 0,001	202,70
		539,138	0,994 ± 0,002	204,15
		549,160	1,011 ± 0,001	207,47
		549,160	1,034 ± 0,002	212,36
		1007,332	1,291 ± 0,001	262,09
	10,27	503,162	0,974 ± 0	200,35
		549,160	1,007 ± 0,003	206,63
		549,160	1,037 ± 0,002	212,89
		1007,316	1,349 ± 0,003	273,92
		665,215	1,099 ± 0,004	224,56
		665,215	1,115 ± 0,006	228,00
	10,47	503,162	0,962 ± 0	197,93
		539,138	0,988 ± 0,001	202,92
		549,168	1 ± 0,001	205,29

		549,168	1,045 ± 0,002	214,46
		665,215	1,091 ± 0,002	223,02
		665,215	1,12 ± 0	228,95
		1007,326	1,335 ± 0	271,02
	10,56	503,162	0,962 ± 0,001	197,83
		503,162	0,999 ± 0,002	205,44
		539,138	1,018 ± 0,001	208,98
		549,168	1,042 ± 0,002	213,92
		665,214	1,102 ± 0,009	225,17
		665,214	1,119 ± 0	228,75
		1007,327	1,331 ± 0	270,21
	10,97	665,215	1,107 ± 0,001	226,38
		701,193	1,143 ± 0,003	233,34
		711,221	1,171 ± 0,002	238,98
	11,09	665,215	1,092 ± 0,001	223,13
		665,215	1,13 ± 0,001	231,00
		711,221	1,164 ± 0	237,64
		711,221	1,193 ± 0,001	243,45
	11,25	665,215	1,09 ± 0,001	222,78
		665,215	1,13 ± 0,002	230,89
		711,221	1,157 ± 0,001	236,26
		711,221	1,189 ± 0,002	242,82
		711,221	1,229 ± 0,002	250,87
	11,46	665,215	1,091 ± 0	223,02
		701,193	1,133 ± 0	231,37
		711,221	1,166 ± 0	238,04
	11,55	665,215	1,087 ± 0	222,21
		665,215	1,115 ± 0,001	227,97
		701,193	1,125 ± 0,002	229,69
		711,221	1,164 ± 0,002	237,64
	11,72	665,215	1,098 ± 0,002	224,51
		665,215	1,127 ± 0,002	230,34
		701,193	1,127 ± 0,013	230,19
		711,221	1,143 ± 0,004	233,31
Raffinose	11,85	503,162	0,961 ± 0,001	197,76
		539,138	0,992 ± 0,001	203,66
		539,138	1,017 ± 0,002	208,79
		549,160	1,003 ± 0,001	205,95
		549,160	1,045 ± 0,003	214,45
		1007,332	1,331 ± 0,002	270,14
		1007,332	1,351 ± 0,007	274,27

Selbstständigkeitserklärung

Hiermit erkläre ich, Johanna Rettner, dass ich die vorliegende Arbeit selbstständig verfasst und keine anderen als die angegebenen Quellen und Hilfsmittel verwendet habe. Insbesondere versichere ich, dass ich alle wörtlichen und sinngemäßen Übernahmen aus anderen Werken als solche kenntlich gemacht habe und die Arbeit in gleicher oder ähnlicher Fassung noch nicht Bestandteil einer Studien- oder Prüfungsleistung war.

Ort und Datum

Unterschrift